Master's thesis

NTNU
Norwegian University of Science and Technology
Faculty of Information Technology and Electrical Engineering
Department of Energy and Process Engineering

Marius Aaslund Berge
Ola Eriksen

Power Sizing Procedures for Highly-Insulated Office Buildings

Master's thesis in Energy and Environmental Engineering
Supervisor: Laurent Georges
June 2019

NTNU
Norwegian University of Science and Technology

Marius Aaslund Berge
Ola Eriksen

Power Sizing Procedures for Highly-Insulated Office Buildings

Master's thesis in Energy and Environmental Engineering
Supervisor: Laurent Georges
June 2019

Norwegian University of Science and Technology
Faculty of Information Technology and Electrical Engineering
Department of Energy and Process Engineering

NTNU
Norwegian University of
Science and Technology

Preface

This work is the Master's thesis of Marius Aaslund Berge and Ola Eriksen, and a continuation of the Specialization Project completed December 2018. We would like to thank Associate Professor Laurent Georges (NTNU) for helping us realize this thesis through valuable guidance and advises. In addition, special thanks to Finn Volla Karlsen (Erichsen & Horgen) who, as a co-supervisor, has provided valuable insights in the HVAC industry.

Further, thanks to: Erik Aune (GK), for providing access to GKBT's and HENT's building management systems (BMS); Henrik Larsen (NCC), for project files on STG; Herdis Maribu (HENT AS), for project files on HENT; Jørn Stene (NTNU/Cowi), for guidance on heat pump technology and ONV12E; Lucas Lundström (Ph.D. at Mälardalen University), for providing radiation data for weather files; Mathias Metlid (M.Sc. student at NTNU), for building energy model and introduction to ONV12E's BMS; Mika Vuolle (Equa), for guidance in IDA ICE regarding thermal mass; Mohammed Hamdy (NTNU), for input on building time constant calculations; Ole Morten Småøyen (Schneider Electrics), for providing ONV12E's BMS; Per Arne Severinsen (Multiconsult), for HVAC consulting on STG; Tony Øyen (Kieldsberggruppen), for providing STG's BMS.

Trondheim, June 2019

Marius Aaslund Berge

Ola Eriksen

Abstract

As of 2018-01-01 there are 4.2 million buildings in Norway, which together account for approximately 36 % of Norway's total energy consumption. At the same time, sustainability issues are high on the agenda. Political and socioeconomic drivers are causing energy efficiency requirements to continuously get stricter. New, smart electricity meters and an undersized power grid make it relevant to study power consumption. Unfortunately, it is a known problem in the industry that HVAC systems are oversized as a result of discrepancies between calculated and measured energy consumption and peak loads. This can lead to poor system efficiency, increased resource usage, poor regulation, and that environmentally friendly solutions are eliminated because the potential savings are underestimated.

The overall goal of this Master's thesis is to improve today's method for calculating space heating loads. This is done by reviewing relevant literature regarding the subject, and testing out different methods on four case buildings. Measured heating loads are extracted from the buildings' building management systems and are compared to the installed heating capacities. The buildings are also simulated in IDA ICE, where different methods are tested.

The four case buildings used in this thesis are Baard Iversens veg 7 (GKBT), Otto Nielsens veg 12E (ONV12E), Sluppenvegen 17B (STG), and Vestre Rosten 69 (HENT). All of the case buildings are modern highly-insulated office buildings located in Trondheim. Heat pump and district heating is used as base load and peak load respectively in all the buildings.

In GKBT, occupancy in single offices, meeting rooms, and total occupancy are studied. For HENT, only the total occupancy is studied. Total occupancy from GKBT is compared to several relevant standards, and one relevant study. The results showed that NS 3031 and TS 3031 are within the range of the standard deviation of the measured occupancy. Electricity to lighting in GKBT and ONV12E is measured and compared; the results showing that the intensity at GKBT is somewhat higher, and starts earlier in the day. Lighting from GKBT is also compared to relevant standards; the results showing that the standards exaggerate the intensity compared to the measurements from GKBT. The intensity from NS 3701 fits best, while the duration is somewhere between TS 3031 and NS 3701. Electrical consumption to technical equipment is also measured at GKBT and ONV12E. As for lighting, the technical equipment in GKBT starts earlier in the day compared to ONV12E. Also, both of the buildings consume electricity outside operating hours. Comparing the measurements from GKBT to standards showed that all the standards exaggerate the intensity, and assumes zero intensity outside of the operating hours. NS 3701 matches the intensity from GKBT the best, while TS 3031 matches the duration the best.

The measured occupancy do not give any new insights in occupancy patterns, but supports the findings in the literature review. For both lighting and technical equipment, it can be suggested that the intensity in the standards are exaggerated. Additionally, the measurements present consumption outside operating

hours. Internal gains are recommended to be include in sizing of heat pumps, but further studies are needed before it is included in design of the peak load system, as internal gains can vary significantly from building to building and tenant to tenant.

Comparison between measured heating load and installed heating capacities suggest that three of the four case buildings have oversized peak load systems, while two out of four have oversized heat pumps. This can lead to poor regulation, higher investment costs, higher operating costs, and shorter lifetime.

This thesis suggests using the building time constant when choosing the design outdoor temperature, to account for thermal mass. This method is tested by simulating a step response to find the time constant for each building. The heating system is then sized by a steady state heat load simulation, using the design outdoor temperature based on the time constant. Then, several dynamic simulations are run with measured weather data from 2005-2018 to investigate how the heating system perform by using this method. Unmet hours are logged when the heating system is not able to ensure set-point temperature. The results showed that there are only a few unmet hours during the year of 2010. This is to be expected as 2010 was the coldest year in Trondheim the last 50 years. With this method, the calculated peak heat load was reduced by 11.9 % on average, compared to sizing with -19 °C. It is concluded that this method can reduce oversizing of peak load systems.

Dynamic simulations with weather data from 2010, and internal loads, are run to investigate the resulting heat load. Two sets of simulations are conducted; with and without solar radiation. Occupancy from TS 3031 is used, while lighting and technical equipment are gotten from NS 3701. By including 100 % internal gains, the results showed an average reduction in the calculated space heating load by 24.1 % and 23.5 % with and without solar radiation respectively, compared to excluding internal gains entirely.

A simple validation of the GKBT model is also conducted. Measured and simulated space heating load are compared. Measured internal gains and weather data from 2018 is used in the simulation to give the best basis for comparison possible. The results showed that the simulated space heating load was 10.9 % higher than measured. This suggest that it is possible to achieve relatively accurate results from simple building energy models when correct input values are used.

Sammendrag

Per 2018-01-01 er det 4,2 millioner bygninger i Norge, som til sammen står for cirka 36 % av Norges totale energiforbruk. Samtidig står bærekraftsspørsmål høyt på dagsordenen. Politiske og sosioøkonomiske drivere sørger for stadige innstramminger i krav til energieffektivitet. Nye smartmålere og et underdimensjonert strømnett gjør at også effektforbruk er viktig. Dessverre er det et kjent problem i byggebransjen at VVS-tekniske anlegg overdimensjoneres som et resultat av avvik mellom prosjektert og målt energibruk og topplast. Dette kan føre til lavere systemvirkningsgrader, økt ressursbruk, dårlig regulering og at miljøvennlige løsninger velges bort fordi man undervurderer besparelsene de kan medføre.

Det overordnede målet med denne masteroppgaven er å forbedre dagens metode for beregning av effektbehov til oppvarming. Dette gjøres ved å gjennomgå relevant litteratur om emnet og utprøve nye metoder for beregning på fire eksempel-bygninger. Målt effekt til oppvarming er hentet fra bygningenes SD-anlegg og er sammenlignet med installert varmekapasitet. Dette er vurdert opp mot simuleringer i IDA ICE, hvor forskjellige metoder er testet ut.

De fire eksempel-bygningene som er med i oppgaven er Baard Iversens veg 7 (GKBT), Otto Nielsens veg 12E (ONV12E), Sluppenvegen 17B (STG) og Vestre Rosten 69 (HENT). Alle disse er nyere høyisolerte kontorbygg i Trondheim. Varmepumpe og fjernvarme er brukt som grunnlast og topplast i samtlige bygg.

For GKBT blir tilstedeværelse i cellekontor, møterom og total tilstedeværelse undersøkt. For HENT blir kun total tilstedeværelse undersøkt. Total tilstedeværelse i GKBT blir sammenlignet med flere relevante standarder, samt en relevant studie. Resultatene viste at tilstedeværelse fra NS 3031 og TS 3031 er innenfor det målte standardavviket for tilstedeværelse. Elektrisitet til belysning blir målt i GKBT og ONV12E, og deretter sammenlignet med relevante standarder. Sammenligning mellom GKBT og ONV12E viste at GKBT har litt høyere intensitet og tidligere oppstart enn ONV12E. Sammenligningen mellom GKBT og standarder viste at samtlige standarder overdriver intensiteten. Intensiteten fra NS 3701 passer best, mens varigheten ligger en plass mellom TS 3031 og NS 3701. Strøm til teknisk utstyr blir også målt på GKBT og ONV12E. Som for belysning er oppstarten for GKBT litt tidligere enn for ONV12E. Begge bygningene måler forbruk utenfor driftstiden. Sammenligningen mellom GKBT og standarder viste at alle standarder overdriver intensiteten, samt at alle antar at det ikke er noe forbruk utenfor driftstiden. Resultatene viste også at intensiteten til NS 3701 treffer best, mens TS 3031 treffer best på driftsperiode.

Det konkluderes med at målt tilstedeværelse ikke gir ny innsikt, men støtter opp om funnene i litteraturstudiet. For lys kan det tyde på at intensiteten er overdrevet i standardene. Det samme gjelder for teknisk utstyr, men målingene tyder på at det er forbruk utenfor driftstiden. Internlaster anbefales å brukes i beregninger for dimensjonering av varmepumper, men det trengs mer forskning på internlaster

da dette kan variere kraftig avhengig av type bygg og brukermønster.

Sammenligning mellom målt og installert effekt til oppvarming antyder at tre av fire bygg har overdimensjonert topplast-system, mens to av fire bygg har overdimensjonert varmepumpe. Dette kan føre til dårligere regulering, høyere investeringskostnad, høyere driftskostnader og kortere levetid.

Det blir i denne oppgaven foreslått å bruke bygningers tidskonstant for å ta hensyn til termisk masse når dimensjonerende utetemperatur bestemmes. Dette testes ved å simulere en sprangrespons for å finne tidskonstanten for hvert bygg. Varmesystemet blir deretter dimensjonert etter den resulterende dimensjonerende utetemperaturen basert på tidskonstanten ved en statisk simulering. Til slutt utføres det dynamiske simuleringer med faktiske værdata fra 2005-2018 for å se hvordan varmesystemene fungerer ved denne metoden. Antall timer hvor systemene ikke klarer å opprettholde settpunkt-temperatur blir logget. Resultatene viser at det vil oppstå noen timer med for lav innetemperatur i 2010. Dette er ikke uventet, da 2010 var det kaldeste året i Trondheim på 50 år. Med denne metoden ble beregnet topplast redusert med 11,9 % i forhold til statisk dimensjonering med dimensjonerende utetemperatur på -19 °C. Det konkluderes med at overdimensjonering av oppvarmingssystemer kan reduseres ved bruk av denne metoden.

Dynamisk simulering er utført med målte værdata fra 2010 for å studere det resulterende romoppvarmingsbehovet. Internlaster er også inkludert for å se hvordan romoppvarmingsbehovet påvirkes. Det er simulert med og uten solstråling. For tilstedeværelse er verdier fra TS 3031 brukt, mens lys og teknisk utstyr er hentet fra NS 3701. Ved å inkludere 100 % internlaster ble beregnet topplast til romoppvarming redusert med 23,5 % uten solstråling og 24,1 % med solstråling, sammenliknet med beregninger uten internlaster.

Det er også gjennomført en validering av modellen for GKBT, der målt effekt til oppvarming er sammenlignet med simulert effekt. Målte internlaster og værdata fra 2018 er brukt i simuleringen for å få så likt sammenligningsgrunnlag som mulig. Resultatene viste at simulert romoppvarmingsbehov var 10,9 % større enn det som ble målt, noe som tyder på at man kan oppnå relativt representative resultater med en enkel modell dersom innverdiene er korrekte.

Table of Contents

List of Tables

List of Figures

Abbreviations

AHU	=	Air Handling Unit
AMS	=	Advanced Measuring and control system
AMY	=	Actual Meteorological Year
BEM	=	Building Energy Model
BMS	=	Building Management System
BPG	=	Building Performance Gap
CAV	=	Constant Air Volume
COP	=	Coefficient Of Performance
DCV	=	Demand Controlled Ventilation
DH	=	District Heating
DHW	=	Domestic Hot Water
DOT	=	Design Outdoor Temperature
GKBT	=	Baard Iversens veg 7
HENT	=	Vestre Rosten 69
HP	=	Heat Pump
HVAC	=	Heating, Ventilation, and Air Conditioning
IWEC2	=	International Weather for Energy Calculations v 2.0
ONV12E	=	Otto Nielsens vei 12E
PCM	=	Phase Changing Material
PLF	=	Part-Load Factor
PLR	=	Part-Load Ratio
PMV	=	Predicted Mean Vote
PPD	=	Predicted Percentage of Dissatisfied
SCOP	=	Seasonal Coefficient Of Performance
SD	=	Standard Deviation
STG	=	Sluppenvegen 17B
TMY	=	Typical Meteorological Year
VAV	=	Variable Air Volume
ZEN	=	Zero Emission Neighborhood
τ	=	Building Time Constant [h]
$\sim$	=	Approximately

Chapter 1

Introduction

The main vision of this project is to develop a new method for heat load calculations to ensure accurate boundary conditions for an optimal HVAC system design.

1.1 Motivation

Regulations and requirements regarding building performance are constantly getting stricter, caused by different political and socioeconomic drivers. For example, UN's Sustainability Goals, a worldwide strategy to eradicate poverty and diversity, and stop climate change, includes *7: Clean energy for all* and *11: Sustainable cities and societies*.[1] Another example, the Paris Agreement, is an international agreement that requires every country to adapt to climate change.[2] With a total of 4.2 million buildings in Norway (as of 2018-01-01)[3], the Norwegian building stock stands for approximately 36 %[4] of Norway's total energy use. It is therefore clear that the performance of buildings are important to ensure minimal energy use in order to reach the Sustainability Goals.

To improve building performance, it is crucial to have good understanding of the power and energy consumption of buildings in order to design social, economical and environmentally sustainable buildings. However, experience have shown that the understanding is not that good: peak loads tend to be overestimated and energy use tends to be underestimated. This can cause heating and cooling systems to be optimized for conditions that do not represent the real case. As a result, HVAC systems are known to be oversized, reducing both energy and economical savings and using more materials than needed. In addition, contractors can decide to use less environmentally friendly systems as they underestimates the savings they can achieve.[5] For example, heat pumps are known to be extra sensitive to misleading power and energy calculations, as the life cycle cost analysis is dependent on investment costs, NOK/kW, and operational costs, NOK/kWh.

1.2 Problem description

Oversized components in HVAC systems results in reduced system performance, increased operating costs, mechanical wear, and unnecessary high investment costs. With increasing requirements regarding energy efficiency in buildings, the heating demand is decreasing significantly. This calls for more cost-effective solutions in the future than what is common practice today.

In this project, different causes for oversizing shall be studied. Thermal dynamic (and static) simulations using IDA ICE will be performed and compared to measurements for a number of highly-insulated office buildings. Based on these simulations, improvements to guidelines and standard power sizing procedures shall be proposed for office buildings. Finally, technical and economic consequences of chosen input parameters for sizing of the HVAC system shall be evaluated and discussed.

The report should contain a detailed literature review of of standards and existing procedures to evaluate the nominal space heating of buildings. The literature should also report about standard sizing procedures of heat pump systems. Potential sources of oversizing should be recognized from the literature review. Further, building energy models (BEM) should be developed for existing buildings in order to compare simulated heating power and needs of the buildings to measured and installed power. Improvements to current design methods should be proposed and discussed.

This Master's thesis is a continuation of the Specialization Project completed December 2018.

1.2.1 Scope

Based on the findings in the literature review, and the findings in the previous Specialization Project, the scope of this theses is to focus on the following topics:

- Measure internal gains in office buildings and compare to standards
- Validate how IDA ICE considers periodic penetration depth in thermal mass
- Finding the building time constant and perform static heat load simulations with a new-found design outdoor temperature based on the building time constant
- Perform dynamic heat load simulations with different amounts of internal gains
- Compare results from simulations to installed and measured heat capacities using four test buildings

This thesis focuses on methods and procedures for heat load calculations, thus cooling energy/power and heating energy is excluded.

Re-use of the Specialization Project (Dec. 2018)

As preparatory work for this Master's thesis, the Authors have together completed a Specialization Project with a similar topic, entitled *Power sizing procedures for heat pump systems in highly-insulated office buildings*. As this is the Authors own work, parts of the project work has been re-used. This includes the first paragraph in the summary and large parts of the literature review: chapter 2.1-2.3.7, 2.4.1, 2.4.3-2.4.4, 2.4.6, and 2.5. IDA ICE is used as tool in both projects, thus chapter 3.1 is re-used. As the building energy model of GKBT is the same as in the Specialization Project, parts of chapter 3.2.1 and 5.4.1 is re-used as well. Additionally, parts of the problem motivation and description in 1.1 and 1.2 is similar to that of the Specialization Project, as this thesis is a continuation of the same issue. Finally, appendix A.1 is re-used. The material has been reviewed, edited, extended and improved, but the reader should be aware that similarities can be found if the mentioned parts are compared to the previous work.

Chapter 2

Theory

In this chapter, theory regarding building performance, standards, thermal mass, heat pumps, and other factors that influence power and energy in buildings will be presented, focusing on power consumption.

2.1 Building energy and power profiles

2.1.1 Building performance gap

Calculating and predicting the performance of a building is an extensive process, with many factors that need to be addressed. To ease the calculations, it is common practice to use a simulation tool. However, the complexity and dynamics of a building can make the computations time consuming.[6] The building complexity and the uncertainties in predictions of the future, normally results in deviation between calculated energy performance and actual energy performance. This deviation is commonly referred to as the *building performance gap* (BPG).[7]

Menezes, Cripps, Bouchlaghem, and Buswell (2012) lists several causes for why a BPG takes place, split into causal factors regarding *predicted performance* and *actual performance*.[7]

For the predicted performance, there are causal factors connected to *design assumptions* and *modelling tools*. Design assumptions are assumptions that are made in the design stage of a project, regarding input values for performance calculations. In the early stages of a project, there are different aspects that are not known, which gives *epistemic uncertainties* in the results [8]. Regarding modelling tools, a causal factor can be fundamental errors in the software's code, which can lead to inapplicable results. Additionally, it is important to use a simulation software that fits the addressed problem, with the right balance of simplifications and accuracy for that specific problem.[7]

Regarding building performance, Menezes et al. (2012) describes *management and control*, *occupancy behaviour*, and *build quality* as causal factors for BPG. These causal factors will be elaborated in Chapter 2.4.

In the same way that it is known to appear discrepancies between calculated and measured energy, an equivalent discrepancy appears for power calculations. There are lots of articles describing accuracy in energy calculation, but it appears to be a lack of literature that deals with peak loads. However, there is a common experience in the HVAC (Heating, Ventilation, and Air Conditioning) industry that calculated peak loads for buildings are overestimated [9]. The reason why energy is more extensively studied, may be that energy use has a direct impact on the operating costs. Estimated power on the other hand, is more relevant in the design phase, especially when deciding heating and cooling strategies. Calculated power may impact the energy use indirectly, for example it can be a determining factor when deciding if a heat pump should be installed and how big this heat pump should be. With new smart electricity meters (AMS) installed, it will also be more common to pay for the peak load, which means that the building user will pay for used power in a more direct manner.[10]

2.1.2 Power duration diagrams

A duration diagram is a graphical presentation of the relationship between power and duration hours. The power needed, for example for heating at each hour of a year, is sorted into decreasing or increasing power. Duration diagrams often present net heating demand and gross heat load at design outdoor temperature (DOT). Net heating demand is presented as this shows the amount of heating energy that the heating system should deliver when all gains, such as solar radiation, occupants, lighting, and technical equipment, are accounted for. Gross heat load is heat load without gains, and is sometimes used because the norm is to size the the heating system after this. In reality, the gross heat load will never occur as the building will always have some heat gains, which can result in oversized HVAC systems.[5]

When sizing a base-load heating system the net heat load becomes important. For example, heat pumps are often sized for 40-70 %[5] of net heat load. The difference between gross and net heat load vary based on the building type. Residential buildings often have a lower deviation between gross and net heat load, regardless of the build quality and the climate zone, the deviation is often less than 10 %. This is not the case for non-residential buildings, as the gap between gross and net heat load varies between 10-40 %; based on build quality, climate zone and building type.[5]

The build quality, location, and type of building affects the amount of energy used and power needed in order to function properly. The amount of insulation used in high quality buildings like low-energy and passive houses reduces the heating demand and heat load significantly. This is shown in figure 2.1 where the specific heat load and specific heating demand is presented for different build qualities.[5]

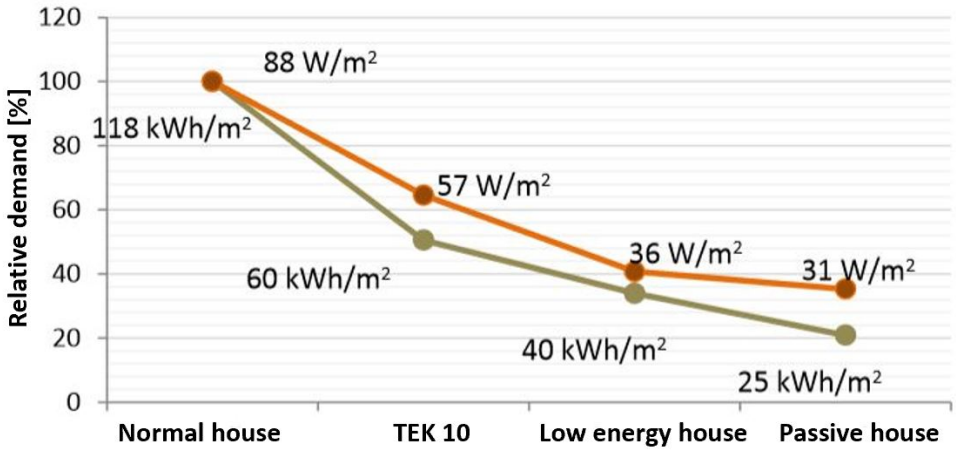

Figure 2.1: Specific heat load at DOT (W/m^2) and annual specific heat demand (kWh/m^2) in an office building with varying build quality in Oslo climate.[5]

On average, the heat load and annual heating demand will decrease by roughly 60 % and 80 % respectively when the build quality changes from *Normal house* to *Passive house*. Another result of high build quality is that the operating hours for the heating system decreases.[5]

The effect of increased build quality on the heating season is shown in figure 2.2. It is shown that the heating season decreases from 5900 hours (Normal house) to 4200 hours (Passive house). Decreased heating season will give lower operating time for the heating system, which can increase the life time of some heating system like heat pumps [5]. However, as shorter heating season is a result of, among other things, decreased envelope U-value, it can often mean longer cooling season.

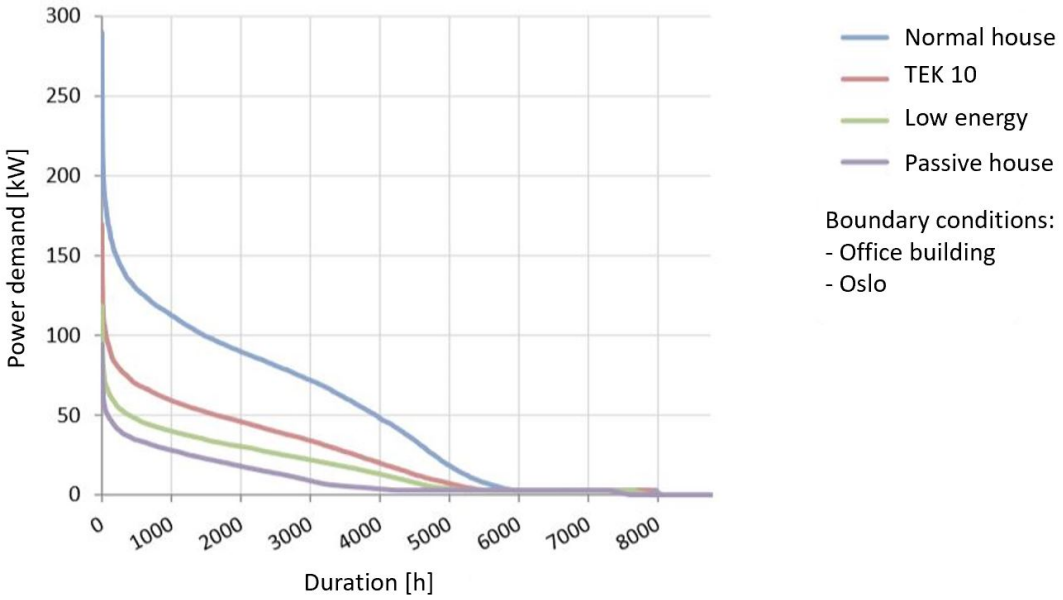

Figure 2.2: Duration diagram for an office building with varying build quality, Oslo climate.[5]

Figure 2.3 shows that the distribution of heat changes with the build quality. As the build quality increases, the share of DHW (Domestic Hot Water) increases from 16 to 58 % of the total heating demand. This means that temperature-independent heating, such as DHW, becomes more important than before.[5]

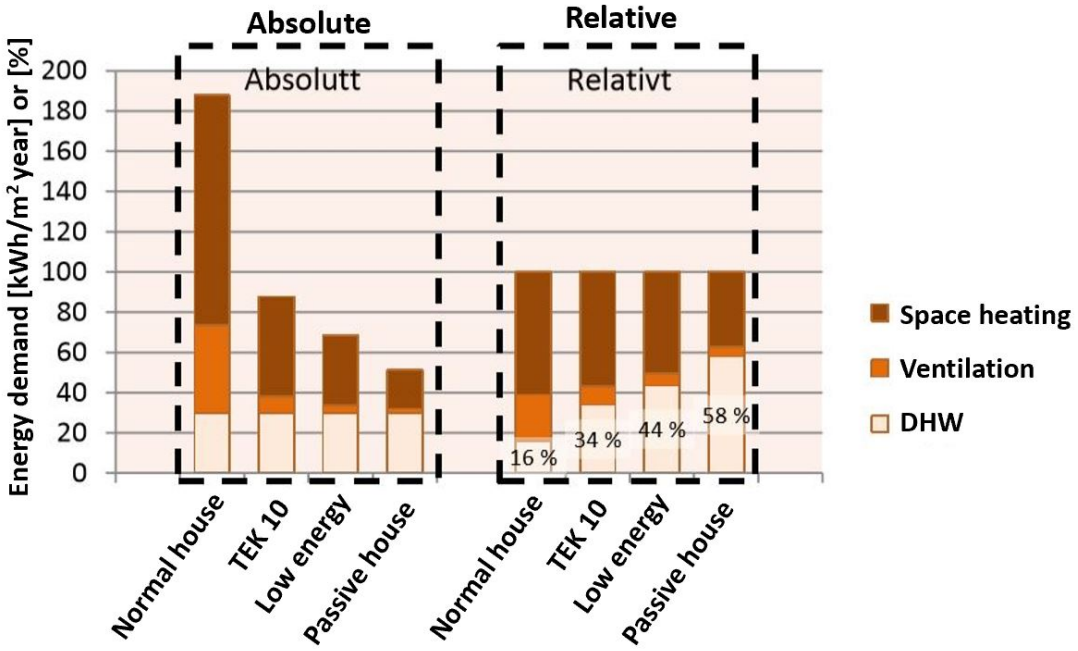

Figure 2.3: Heat distribution for a residential building in Oslo for varying build quality.[5]

2.2 Regulations in Scandinavia

Technical Regulations (TEK) in Norway gives two methods to satisfy legal energy requirements: the *Energy Budget Method* and the *Energy-saving Measures Method*. If the Energy Budget Method is used, authorities demand that energy simulations are preformed. The energy simulations should be based on NS 3031, using nominal climate for Oslo, in order to find net energy demand and compare it to the demands for the corresponding building category. Results from the energy simulations are not mandatory to deliver to the authorities, but must be available.[11]

When designing an HVAC system, the method and system design have to meet the laws and regulations that are given by the government in the country of operation. To ensure that the design is within legal requirements in Norway, the requirements from TEK 10:17 (referred to as TEK17) is used. When studying requirements regarding thermal environment in TEK17, it is referred to NS-EN 15251:2007+NA:2014 *Indoor environmental input parameters for design and assessment of energy performance of buildings addressing indoor air quality, thermal environment,lighting and acoustics*. This standard refers to another standard; the standard NS-EN 12831 *Energy performance of buildings - Method for calculation of the design heat load*. This means that for the building to be within legal

requirements, the design heat load should be designed according to NS-EN 12831. The method given in the standard is elaborated in chapter 2.3.4

Sweden requires that total measured energy use is reported after 24 months of operation, and that the reported measurements should be logged over a period of 12 months. This requirement was introduced in 2009 to verify calculations against measurement, and to follow-up on the energy use. To improve the quality of the energy simulations done in Sweden, a set of standardized input values that can be used in the energy calculations (*Standardize and verify energy performance in buildings - SVEBY*) was created by the building- and property industry. These input values should preferably be as close as possible to real values. Guidelines for follow-up on the energy demands during the construction process have also been developed. These guidelines recommend that energy calculations should be done in early- and detailing phase of the project, in addition to when the building is raised. This is to ensure that the calculated energy use is the same as what is measured.[11]

Denmark uses delivered energy distributed by gross heated area for evaluations. It is divided into space heating, ventilation, cooling, DHW, and lighting. An energy labelling system was introduced in 2006 and is used for energy certificates and building permits. As Denmark is trying to reduce the use of electricity for heating, a penalty factor of 2.5 for electrical heating is included in the energy labelling system.[12]

2.3 Standards

Some of the most common standards in Norwegian design and calculation procedures are presented, in addition to other standards that are relevant for this Master's thesis.

2.3.1 NS 3031

NS 3031:2014 *Calculation of energy performance of buildings - Method and data* is used for energy calculations for comparison to Norwegian building regulations. The standard provides input values and guidelines regarding boundary conditions, regardless of the calculation method. It also elaborates different methods for calculating energy performance, but only monthly calculations are explained in detail. Based on building type, different calculation procedures can be used and the standard gives directives about which procedure should be used. Note that NS 3031:2014 is currently withdrawn, and there is per 2019-05-09 no new version to replace it.[13]

2.3.2 SN/TS 3031

SN/TS 3031:2016 *Energy performance of buildings - Calculation of energy needs and energy supply* is an addition to NS 3031:2014. TS 3031 was produced based on experiences using NS 3031. In TS 3031, monthly calculations are removed, leaving only dynamic calculation with a time step of one hour or shorter. New schedules for occupancy, technical equipment, lighting, and DHW are given. The new schedules presented in TS 3031 give the same energy use over 24 hours as in NS 3031, but the distribution of power vary by the hour rather than being evenly distributed solely based on occupied and unoccupied hours. Note that the schedules and input values in the standard is only supposed to be used for nominal calculations, and for verifying against regulations. For actual power and energy demand, actual values and schedules are required, as the standard values does not necessarily represent the reality.[14]

2.3.3 NS 3701

NS 3701:2012 *Criteria for passive houses and low energy buildings, Non-residential buildings* is the Norwegian answer to the German concept *Passivhaus* [15]. The need for a Norwegian passive house standard occurred as the words *passive house* and *low energy building* more frequently appeared in applications for public funding, while the German definitions was not well suited for Norwegian conditions. In addition, as stated in the standard's preface, the Norwegian government wanted to influence the demand for low energy buildings and needed clear definitions in their communication.

The standard gives definitions for two levels of energy efficient buildings: low energy buildings and passive houses. Overall requirements regarding heat loss factors, heating and cooling need, energy for lighting and energy supply are presented. In addition, minimum requirements regarding building parts, components, systems and leakage number are given. Finally, normative input values for energy calculations are listed.[15]

2.3.4 NS-EN 12831-1

NS-EN 12831-1:2017 *Energy performance of buildings - Method for calculation of the design heat load - Part 1: Space heating load* can be used for heat load calculations for new buildings or extensive reconstruction measures. The method in the standard can be divided into calculation of heat loads in rooms, building entities, or buildings.[16]

The simplified method for calculation of the building design heat load is as shown in equation 2.1-2.3. Note that this method is meant for determination of building heat load prior to real measurements. The simplified method is limited to buildings with natural ventilation, residential buildings or buildings of

similar use and existing buildings.[16]

$$\Phi_{HL,build} = \Phi_{T,build} + \Phi_{V,build} \tag{2.1}$$

$$\Phi_{T,build} = \sum_k (\Phi_{T,k}) = \sum_k \langle A_k \cdot (U_k + \Delta U_{TB}) f_{x,k} \rangle \cdot (\theta_{int,build} - \theta_e) \tag{2.2}$$

$$\Phi_{V,build} = V_{build} \cdot n_{build} \cdot \rho_L \cdot C_{p,L} \cdot (\theta_{int,build} - \theta_e) \tag{2.3}$$

Where

$\Phi_{HL,build}$	=	Design heat load [W],
$\theta_{T,build}$	=	Transmission losses [W],
$\Phi_{V,build}$	=	Ventilation heat loss [W],
A_k	=	Area of the building element k [m^2],
U_k	=	U-value for the building element k [W/m^2K],
ΔU_{TB}	=	Normalized thermal bridge value [W/m^2K],
$f_{x,k}$	=	Temperature adjustment factor [-],
$\theta_{int,build}$	=	Internal room temperature [°C],
θ_e	=	Design outdoor temperature [°C],
V_{build}	=	Air volume of the building [m^3],
n_{build}	=	Air exchange rate [h^{-1}],
ρ_L	=	Air density [kg/m^3],
$C_{p,L}$	=	Specific heat capacity of air [J/kgK].

The standard method for calculating design heat load is presented in equation 2.4. This method does not have any restrictions and is typically meant for sizing of components in heating systems in new buildings or extensive reconstructive measures.[16]

$$\Phi_{HL,build} = \sum_i \langle \Phi_{T,ie} + \Phi_{T,iae} + \Phi_{T,ig} \rangle + \Phi_{V,build} + \sum_i \langle \Phi_{hu,i} \rangle - \sum_i \langle \Phi_{gain,i} \rangle \tag{2.4}$$

The design heat load for a building, $\Phi_{HL,build}$, is based on both indirect and direct transmission losses to the exterior, $\sum_i (\Phi_{T,ie} + \Phi_{T,iae} + \Phi_{T,ig})$, losses related to ventilation, $\Phi_{V,build}$, and any additional heating power, $\sum_i (\Phi_{hu,i})$. Heat gains, $\sum_i (\Phi_{gain,i})$, can also be included if national regulations allows it. During the literature review, there are not found any statements that this apply for Norway. Therefore, it must be assumed that this does not apply, as it is not specified in TEK. To avoid oversized heating system, only the heating powers that occur simultaneous should be included.[16]

The standard also gives a method for adjusting DOT by taking variances in climatic conditions, height differences, and the building's time constant into consideration. The ordinary DOT is often adequate, but for high-rise buildings, and buildings with large variations in thermal capacity per floor, adjustment may be needed in order to get satisfactory results. The method is presented in appendix A.1.

2.3.5 ISO 17772-1

ISO 17772-1:2017 *Energy performance of buildings - Indoor environmental quality - Part 1: Indoor environmental input parameters for design and assessment of energy performance of buildings* specify criteria for the cooling and heating season, and other factors that may significantly impact the energy and power demand of buildings. The criteria listed in this standard are not meant directly for energy calculations, but rather for sizing the HVAC systems. Different schedules and values regarding internal gains are also presented in this standard. These can be used for different types of occupancy patterns, buildings, climate and national differences. These input values and schedules are *"... examples that can be used as input to calculations of energy use in a building..."*. However, real values and schedules for internal gains should be used for calculation regarding building performance if they are known.[17]

2.3.6 ISO 7730

ISO 7730:2005 *Ergonomics of the thermal environment, Analytical determination and interpretation of thermal comfort using calculation of the PMV and PPD indices and local thermal comfort criteria* is a standard that defines relevant parameters to evaluate thermal comfort on the basis of the *Predicted Mean Vote* (PMV) and *Predicted Percentage of Dissatisfied* (PPD).[18]

2.3.7 NS-EN 15251

NS-EN 15251:2007 *Indoor environmental input parameters for design and assessment of energy performance of buildings addressing indoor air quality, thermal environment, lighting and acoustics* is an European standard concerning how different indoor climatic conditions influences the energy use. It gives methods for long term evaluation of the indoor climate, and defines how different categories for the indoor environment can be used. Parameters for sizing of HVAC systems are given, while the methods themselves are excluded.[19]

2.3.8 NS-EN 15193-1

NS-EN 15193-1:2017 *Energy performance of buildings - Energy requirements for lighting* is a standard dedicated to evaluate the energy performance of lighting systems. Methods for calculating and measure energy required or used for lighting are given. It is stated that this standard assumes that *"...the buildings can have access to daylight to provide all or some illumination required...in addition there will be an adequate amount of electric lighting installed..."*.[20]

2.3.9 ISO 13612-1

ISO 13612-1:2014 *Heating and cooling systems in buildings - Method for calculation of the system performance and system design for heat pump system - Part 1: Design and dimensioning* is an international standard that deals with heat pumps for space heating and space cooling, heat pumps with combined space heating/cooling and DHW, and heat pumps for hot water production. This part of the standard gives calculation methods, required inputs and outputs for space heating and DHW, and control of the heat pump system. Sizing the boundary conditions for the heat pump design (such as space heating and DHW load) are not in focus, as the main objectives are the heat pump itself, as well as it's distribution system, the emission system, and the control system.[21]

2.4 Factors that influence building performance

2.4.1 Internal gains

Occupancy

Duarte, Wymelenberg, and Reiger (2013) has in their study *Revealing occupancy patterns in an office building through the use of occupancy sensor data* [22] looked at a large, multi tenant, commercial office building in order to remove some uncertainties about occupancy for energy modellers. The case building was comprised of several different room types, such as private (single/cell) offices, open (landscape) offices, conference/meeting rooms, break rooms, hallways, and rest rooms. In the study it was found a discrepancy between the diversity factor in ASHRAE 90.1 2004 and measured occupancy of 46 % [22]. In the study, the diversity factor is defined as actual occupancy level divided by total possible occupancy.[22] Further, Duarte et al. (2013) states:

"...ASHRAE 90.1-2007 provide guidance for the minimal requirements of energy-efficient new building design. This standard leaves the determination of occupancy schedules up to the modeler and approval up to the rating authority. ...Modelers often refer back to ASHRAE 90.1-2004 which includes standardized occupancy diversity factors...".

This suggests that standards that are not meant for system design is used in an unintended way [22]. Duarte et al. (2013) also found that different days and months had an effect on the occupancy in the building. Both days and months could be separated into three different groups: high, medium, and low level of occupancy. The months included in the group with high occupancy are January, March, April, May, June, September, and October. The other groups and their respective months can be seen in figure 2.4.

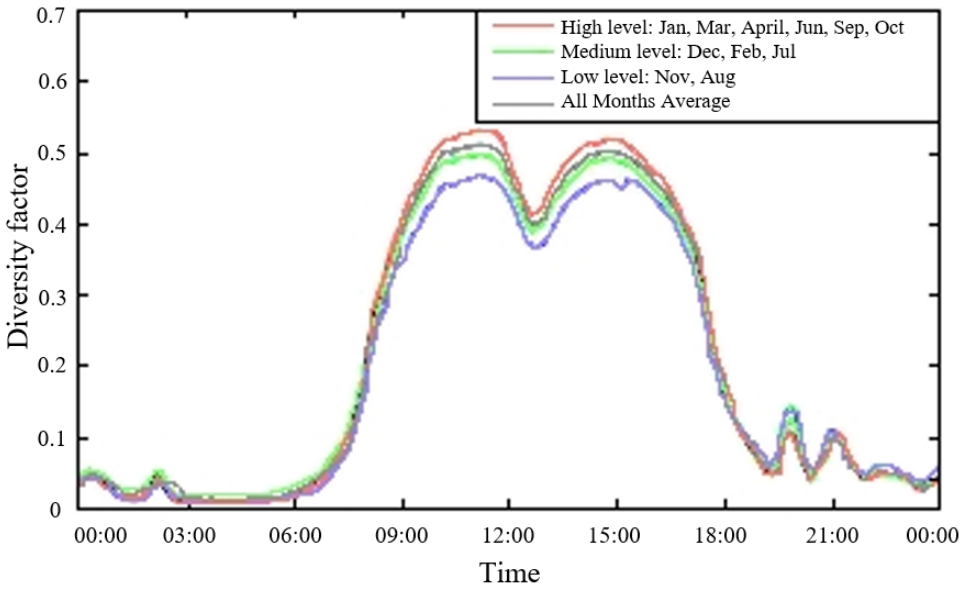

Figure 2.4: Level of occupancy on monthly basis in the different groups, showing high, medium, and low level of occupancy.[22]

Regarding the different weekdays, Monday is in the group with high occupancy, Tuesday-Thursday is in the medium level group, and the lowest level of occupancy is found on Friday. This is shown in figure 2.5.

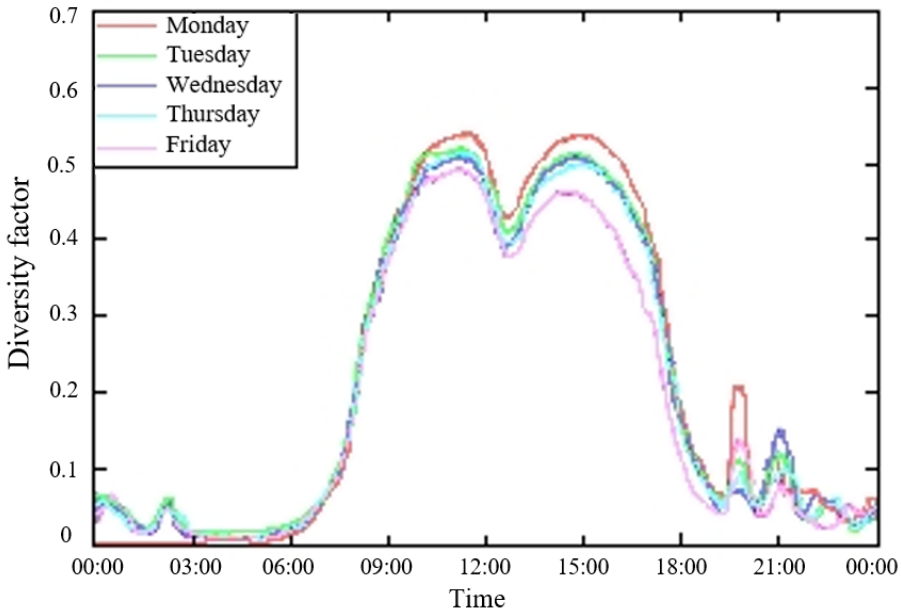

Figure 2.5: Level of occupancy on a daily basis in the different groups, showing high, medium, and low level of occupancy.[22]

The diversity factor found in Duarte et al. (2013) matches with the results Halvarsson (2012) found in his study, *Occupancy patterns in office buildings*[23] as shown in figure 2.5. Halvarsson (2012) stated

that the measured occupancy in a single office have a average diversity factor of 0.4, varying between 0.2 to 0.6 in Norwegian offices on workdays between 08:00 and 17:00.

According to Duarte et al. (2013), there is there a significant difference in the occupancy before and after a holiday. Both before and after the holiday, lower occupancy can be expected.[22]

Table 2.1: Values regarding occupancy from ISO 17772-1.[17]

Room type	**Total heat [W/m^2]**	**Dry heat [W/m^2]**	**Moisture production [g/(m^{2}h)]**	**CO_2 production [l/(m^{2}h)]**	**Occupant density [m^2/pers]**
Landscape office	7.0	4.7	3.53	1.10	17
Meeting room	59.2	40.1	30.0	9.35	2
Single office	11.8	8.0	6.0	1.87	10

Input values and schedules for occupancy in single offices, landscape offices and meeting rooms from ISO 17772-1:2017 are presented in table 2.1 and figures A.1-A.3. During weekends, the diversity factor is set to zero for all the presented room types.[17]

Table 2.2: Relevant occupant behavior from ISO 17772-1:2017.

Room type	**Office landscape**	**Meeting room**	**Single office**
Base diversity factor (unoccupied) [%]	0	0	0
Peak diversity factor (occupied) [%]	70	90	100
Occupied start time	08:00	09:00	10:00
Occupied stop time	19:00	18:00	17:00
Peak diversity factor duration [h]	4	1	6
Occupied duration [h]	11	9	7

Table 2.2 presents relevant parameters from ISO 17772-1 for single offices, meeting rooms, and open landscapes. The schedules from the standard is presented in the appendix, see figures A.1 - A.3. These schedules are not only for occupancy, but for electricity to lighting and technical equipment as well.

Measurements of occupancy in office buildings are often based on measurements in offices, either cell or landscape. However, these measurements only describes occupancy in the primary areas and not secondary areas. According to NS 3701, primary areas in office buildings are defined as offices and meeting rooms, while secondary areas are defined as corridors, toilets, stairwells, wardrobes, and other rooms where occupants are not intended to stay over longer time spans.[15]

Both NS 3701 and NS 3031 use that 65 % and 35 % of the building are primary and secondary areas respectively, when calculating energy demand for demand controlled ventilation (DCV). Occupancy density in primary areas is assumed to be 5 m^2/person, while the lowest occupancy level is assumed to be 60 %.[13, 15]

When studying occupancy, Halvarson (2012) defines an occupancy factor, OF_p. This is calculated as shown in equation 2.5.

$$OF_p = \frac{\sum_{x=1}^{n} p_x}{\sum_{x=1}^{n} p_x^d} \tag{2.5}$$

Where

OF_p = Occupancy factor for design occupancy load [-],
p_x = Number of occupants in sub-zone *ix* [-] ,
p_x^d = Number of occupants the sub-zone *ix* is designed for [-].

The following assumptions are made in the study by Halvarsson (2012): each person emits 80 W of sensible heat, there is 15 m^2 per person, and a single cell office is on average 10 m^2 [23]. By using these assumptions, Halvarsson (2012) states that the occupancy factor used in NS 3031 is 0.75 for the entire building as one and 0.5 for cell offices. This means that 75 % of the design occupancy load is present during the operating hours on average when studying primary and secondary areas as one, and 50 % when only addressing cell offices. However, Halvarsson stresses that the values stated in NS 3031 are for control calculations against building code requirements, and not design values for HVAC systems. Furthermore, Halvarsson (2012) concludes that it would be more accurate to *"... specify diversity factor for different types of office space, for example, differentiate between space for individual work, meeting/conference rooms, and other types of space."*.[23]

Lighting

NS-EN 15193-1:2017 *Energy performance of buildings - Energy requirements for lighting* gives values for the *Absence factor*, F_A, used for lighting calculations. Absence factors are listed for several building types, table 2.3 showing the absence factor for office buildings.[20]

Table 2.3: Absence factor for office building from table B.6 in NS-EN 15193-1.[20]

Overall building calculation	F_A	Room by room calculation		F_A
Offices	0.20	Offices	Cellular office 1 person	0.40
			Cellular office 2-6 persons	0.30
			Open plan office >6 persons (sensing/30m)	0.00
			Open plan office >6 persons (sensing/10m)	0.20
			Corridor (dimmed)	0.40
			Entrance hall	0.00
			Showroom/Expo	0.60
			Bathroom	0.90
			Rest room	0.50
			Storage room/Cloakroom	0.90
			Technical plant room	0.98
			Copying/Server room	0.50
			Conference room	0.50
			Archives	0.98

Absence factor is the fraction of time when a zone or a room is unoccupied during the reference operating time (2500 hours for offices). This factor, as wells as the *Control function factor* F_{OC} is used to calculate the *Occupancy dependency factor* F_O, by the use of equation 2.6.[20]

$$F_O = min\{1 - [(1 - F_{OC}) \cdot F_A/0.2]; (F_{OC} + 0.2 - F_A); [7 - (10 \cdot F_{OC})] \cdot (F_A - 1)\} \tag{2.6}$$

Occupancy dependence factor is, according to Halvarsson (2012), multiplied with the total installed lighting power in the zone or room to consider the impact of occupancy and control system has on lighting. Halvarsson also states that the *utilization rate* (the average occupancy factor for a zone over specified time period) is equal to (1-F_A).[23]

As for technical equipment, ISO 17772-1 gives schedules for lighting, presented in the appendix (figure A.1-A.3). The diversity factor in weekends is set to zero. No specific values for heat gain is presented in the standard, but an illuminance of 500 lux is recommended for office workplaces [24]. *Brukarindata* (Eng.: User input values) from SVEBY states that in an normal office the lighting has an heat gain of 7.6 W/m^2[25]. NS 3031 states a nominal value of 8 W/m^2[13] for control calculations against regulations, which can be reduced by 20 % if a daylight control system is used. TS 3031 states 9.62 W/m^2[14] during occupied hours. Emergency lighting can also be considered; Martirano (2011) [26] states that emergency lighting can be estimated by adding 1 kWh/m^2/year to the energy consumption for lighting. Assuming

that the emergency lighting is constant throughout the year, this yields an average of 0.11 W/m^2.

Technical equipment

Acker, Duarte, and Wymelenberg (2012) study measurements of technical equipment in six different offices in their study *Office space plug load profiles and energy saving interventions* [27]. Measurements from the offices were collected over a year to exclude any seasonal variations. The offices included in this study range from private to public, and different business types as land records (1), world wide logistics (2), architects (3), elections office (4), regulatory agency (5) and investment analytics (6). Note that the numbers refer to the columns in table 2.4. The offices differ in size and employees (from seven to a hundred). Technical equipment were logged every 15 minutes, while other load circuits, like HVAC or lighting were excluded in order to isolate technical equipment like computers, monitors, and copying machines.[27]

Table 2.4: Measured electricity to technical equipment from Acker et al. (2012).[27]

Site	**1**	**2**	**3**	**4**	**5**	**6**
Peak hours	06-18	07-18	08-17	07-17	08-17	07-18
Area [m^2]	422	1272	120	144	1214	1272
Weekday peak [kW]	6.25	10.5	1.5	1.25	9.5	28
Weekday peak [W/m^2]	14.8	8.3	12.5	8.7	7.8	22
Weekday unoccupied peak [kW]	2.75	2	0.75	0.25	4.75	22
Weekday unoccupied peak [W/m^2]	6.5	1.6	6.3	1.7	3.9	17.3
Weekend peak [kW]	2	1.75	0.6	0.35	2.5	21
Weekend peak [W/m^2]	4.7	1.4	5	2.4	2.1	16.5
Holiday peak [kW]	3	5	0.5	0.35	3.5	23
Holiday peak [W/m^2]	7.1	3.9	4.2	2.4	2.9	18.1

Results from Acker et al. (2012) shows that site 2 and 4 have the lowest energy use in average, cf. table 2.4. The study states that *"...this value agrees with some of the previous research that report 2.19 kWh/(ft^2 year)..."*. It is also noted that site 1 and 3 measures about twice as much. Site 6 is even higher, with almost 5 times as much as the reported value. Because of the different business types, the offices have different amounts of technical equipment. Site 1-4 is considered to have an average amount. Site 5 and 6 use above average; these offices are in industries that require large amount of computer power and is therefore considered as computer intensive.[27]

The technical equipment profiles found in Acker et al. (2012) is presented in figure 2.6. The figure shows the measured load for site 2, but the profiles for all the other sites have near the same shape with different magnitude. The profile for site 5 differs to some degree from the other sites, as the power in unoccupied

hours were higher than the rest. The reason was thought to be *"...an IT policy prohibiting employees from turning computers off in weekday evenings to allow network maintenance."*.[27]

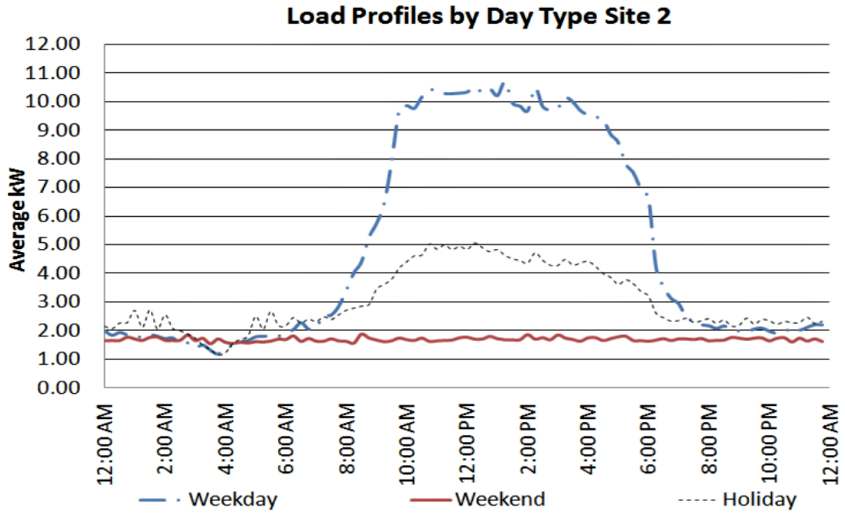

Figure 2.6: Technical equipment profile for site 2.[27]

The profiles for technical equipment from ISO 17772-1 are the same as for occupancy and lighting. The input value for technical equipment is 12 W/m^2 for all room types, while the diversity factor in the weekends is set to zero.[17]

2.4.2 Electrical consumption and occupancy

Menezes et al. (2012) [7] has in their study *Predicted vs. actual energy performance of non-domestic buildings: Using post-occupancy evaluation data to reduce the performance gap* investigated reasons for the performance gap. They studied an office building with four different tenants distributed over seven floors and a basement. The study showed that the electricity consumption differed between the tenants, due to different routines; some of the tenants had a policy to always keep technical equipment turned on. This emphasize the fact that different tenants have different user behaviour, which will yield different heat gains.[7]

In addition, Menezes et al. (2012) performed detailed analysis of the electrical consumption; measured electricity consumption for one of the office spaces is shown in figure 2.7. The peak that occurs during weekdays between 20:00 and 21:00 is the cleaning personnel triggering the light sensors and using vacuum cleaners. Some relevant values from figure 2.7 are presented in table 2.5.[7]

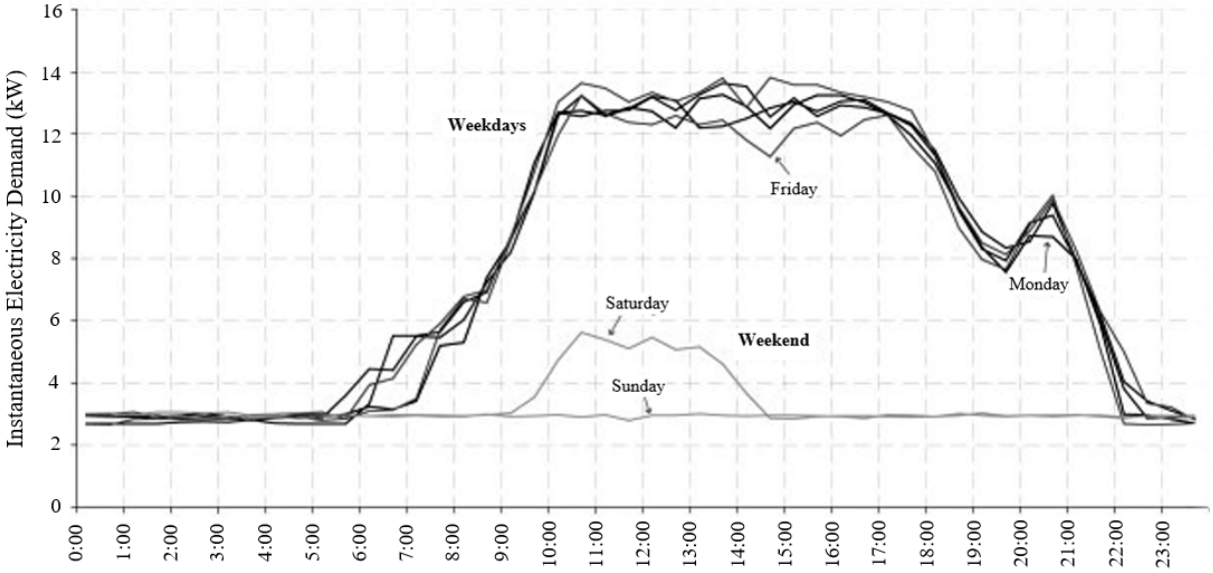

Figure 2.7: Measured electrical consumption for one part of the case building.[7]

Table 2.5: Results of measured electrical consumption for the case building.[7]

Day	Weekdays	Weekend
Base load (unoccupied) [kW]	3	3
Peak load (occupied) [kW]	13	5.5
Occupied start time	06:00	09:00
Occupied stop time	19:30	15:00
Occupied duration [h]	13.5	6
Rise time unoccupied to occupied [h]	4	1.5
Descend time occupied to unoccupied [h]	2	2.5

In order to investigate the correlation between occupancy and electrical consumption, Menezes et al. (2012) measured occupancy for each tenant. The results for one of the tenants are shown in figure 2.8, where it can be seen that the measured electrical consumption coincided quite well with the measured occupancy with the excepted valley around 13:00. This valley in measured occupancy, occurs since the occupants were leaving for lunch. However, their office equipment were not shut off, causing the same electricity consumption without any occupants present. The figure also include the occupancy profile from *SBEM Standard* for comparison. SBEM (Simplified Building Energy Model) is a software used to analyze a building's energy consumption where several CEN standards are available.[28]

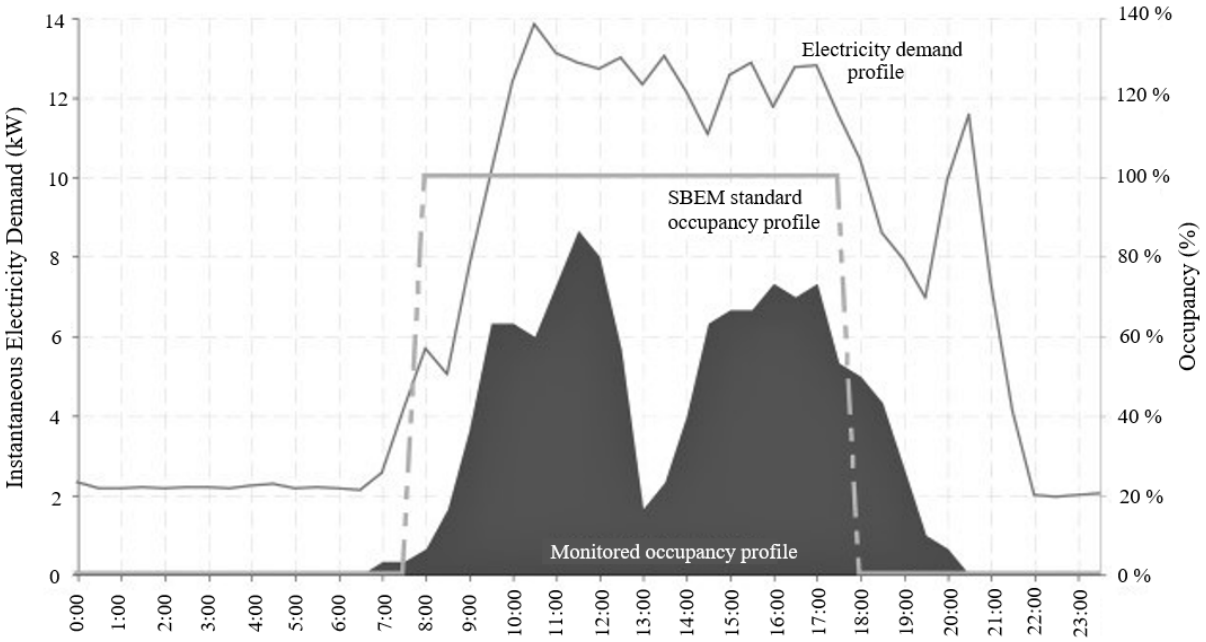

Figure 2.8: Comparison between measured electrical consumption and occupancy.[7]

2.4.3 Domestic hot water

Domestic hot water consumption can be a large part of the annual energy consumption for a low-energy building. The total use of DHW is assumed to be more or less constant, and it is said that it has not changed much since the buildings built according to TEK49 and older [9]. As the energy use for space heating has decreased over the years, DHW takes a bigger share of the energy use, as shown in figure 2.9.

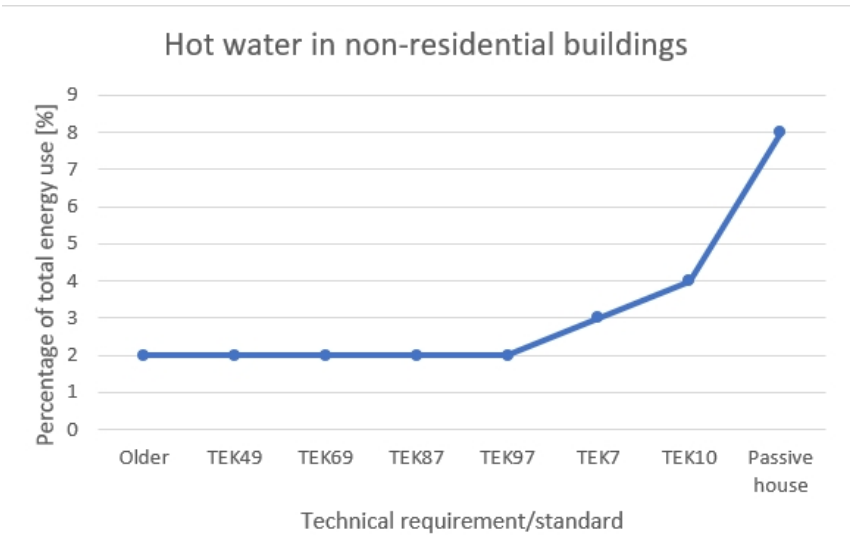

Figure 2.9: Energy consumption for DHW in non-residential buildings presented as percentage of total energy consumption.2.9

Power used for DHW is mainly dependent on the heating strategy. The most common method is using accumulator/storage tanks to store hot water for whenever it is needed. This way, the water can be heated when heat is available, using low power, and stored in well-insulated tanks. The other solution is direct heating, where the hot water is heated continuously when it is needed. If the DHW use is small, this can be a more energy efficient solution, as a tank can introduce heat losses. However, this calls for high power installations.[29]

Sintef states that knowledge about actual hot water use is limited. Therefore, there is an ongoing research project, lasting from 2017 to 2021, named *VarmtVann2030* (Eng.: HotWater2030). The aim of this project is to increase knowledge about usage and system solutions to develop new technical solutions, and smart control systems.[30]

2.4.4 Indoor thermal environment

One of the most important aims of an HVAC system is to achieve acceptable indoor environment. Therefore, there can be no doubt that the desired indoor environment affects the power and energy consumption in a building.

Studies have shown that the performance of an office worker are connected to thermal comfort. As can be seen in figure 2.10, the relative performance decreases when the temperature deviates from the optimal operative temperature [31]. Salaries to office workers is a large share of the total operating costs of an office building. The cost of reduced relative performance caused by thermal discomfort can easily outrun the extra investment cost needed for an HVAC system to maintain optimal operative temperature [32]. Figure 2.10 also shows that the optimal temperature is different from summer to winter, as the level of clothing (clo) is different for the two.

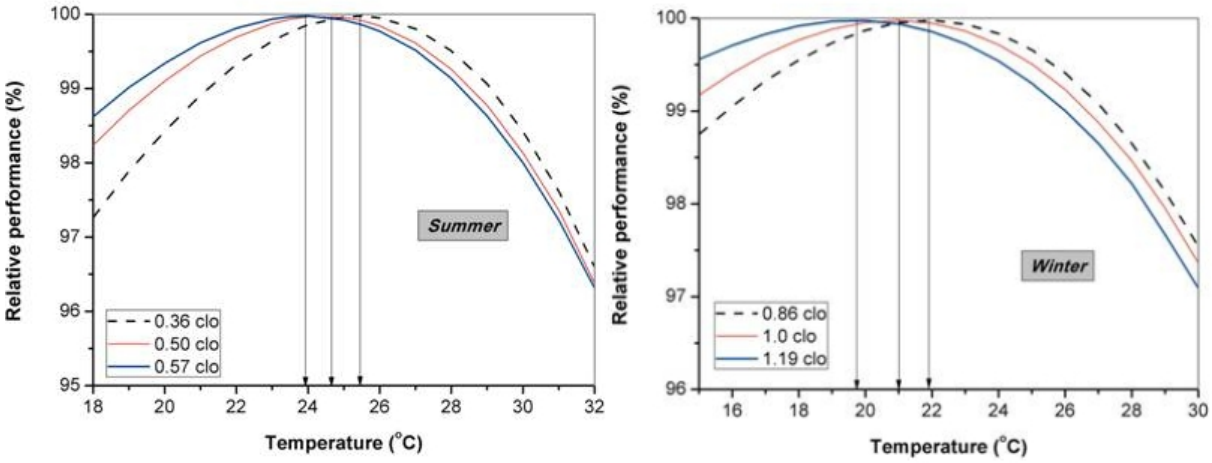

Figure 2.10: Relative performance of an office worker as a function of temperature during summer and winter conditions.[31]

There are two main models for thermal comfort: *Heat balance model* (Fanger's Comfort Model) and the *Adaptive Thermal Comfort Model*. What comfort model is used during building performance calculations can affect the estimated energy and power use.

Table 2.6: Design criteria for an office during summer (RH=60%, 0.5clo) and winter (RH=40%, 1.0clo) with a metabolic rate of 1.2 met as listed in ISO 7730 and NS-EN 15251 depending on the thermal comfort model.[18, 19]

Thermal comfort model	Category	Operative temperature [°C]	
		Summer	Winter
Heat balance model	A	24.5 ± 1.0	22.0 ± 1.0
	B	24.5 ± 1.5	22.0 ± 2.0
	C	24.5 ± 2.5	22.0 ± 3.0
Adaptive comfort model	I	< 25.5	> 21.0
	II	< 26.0	> 20.0
	III	< 27.0	> 19.0

Fanger's Comfort Model is a heat balance model that estimates thermal comfort based on heat exchange between the human body and the surroundings. This model is the basis for calculation of PMV and PPD, and has lead to the commonly used standard ISO 7730 [33]. This standard sets temperature limits to achieve thermal comfort for three different building performance categories, see table 2.6. It is also differentiated between winter and summer.

Adaptive comfort models allow a larger temperature range, as it is assumed that occupants have the ability to take measures to achieve thermal comfort. Such models are not based on a heat balance, but on empirical studies of comfort temperatures as a function of outdoor temperature [33]. This means that the level of thermal comfort can depend on several factors such as gender, age, nationality, and health. Therefore, adaptive models are not as strict as the heat balance models. However, it is stated that a persons adaptive abilities does not in fact change the comfort temperature, only the ability to withstand uncomfortable thermal conditions [33]. NS-EN 15251[19] sets maximum temperature for the cooling season and minimum temperature for the heating season.

According to NS-EN 15251, PMV/PPD should be used when sizing HVAC systems in buildings with mechanical heating/cooling. On the other hand, if the building do not have mechanical cooling, it is also possible to use adaptive models, due to *"...the different expectations of the building occupants and their adaptation to warmer conditions."* [19]. As the adaptive comfort model is not as strict as Fanger's comfort model and allows for a wider range of temperatures, it is clear that the chosen thermal comfort model will affect the building performance. The heating and cooling set point will affect the energy consumption and the peak power substantially.[34]

2.4.5 Thermal mass

Building materials and components have the ability to absorb and emit heat, and store heat over time. During summer, building components can absorb heat during the day, and then flush during nighttime in order to avoid over heating and reduce the cooling needs, see figure 2.11.[35]

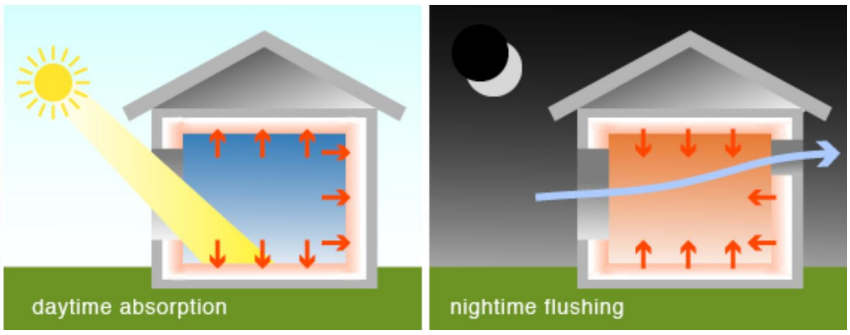

Figure 2.11: Cooling effect of thermal mass during summer.[35]

During winter, thermal mass can be used to reduce heating needs, by absorbing heat when excess heat is available and release it when it is needed. This is shown in figure 2.12.[35]

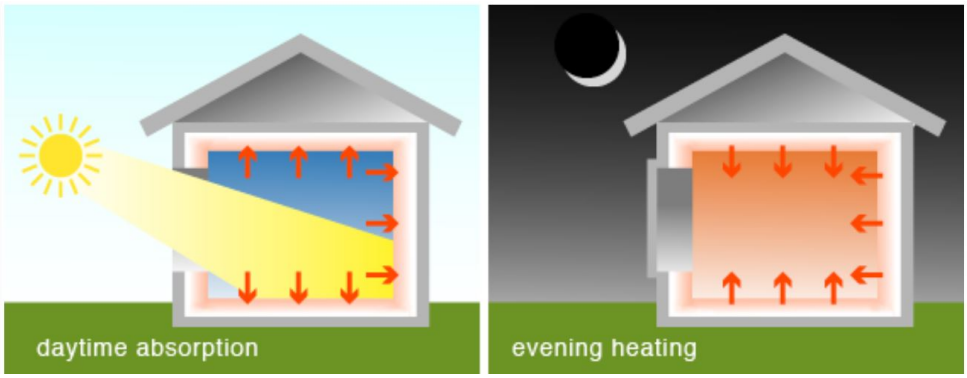

Figure 2.12: Heating effect of thermal mass during winter.[35]

Temperature fluctuations in outdoor and indoor air, and their correlation is greatly affected by thermal mass. This is shown in figure 2.13, where the internal temperature fluctuations are dampened by thermal mass, resulting in lower amplitude for the temperature fluctuations. Higher thermal mass will increase the dampening effect. The temperature fluctuations will also have a phase shift, *phase lag* ϕ. The phase lag appears when the temperature development happens through different materials, e.g.from air to concrete and from concrete to air.[36]

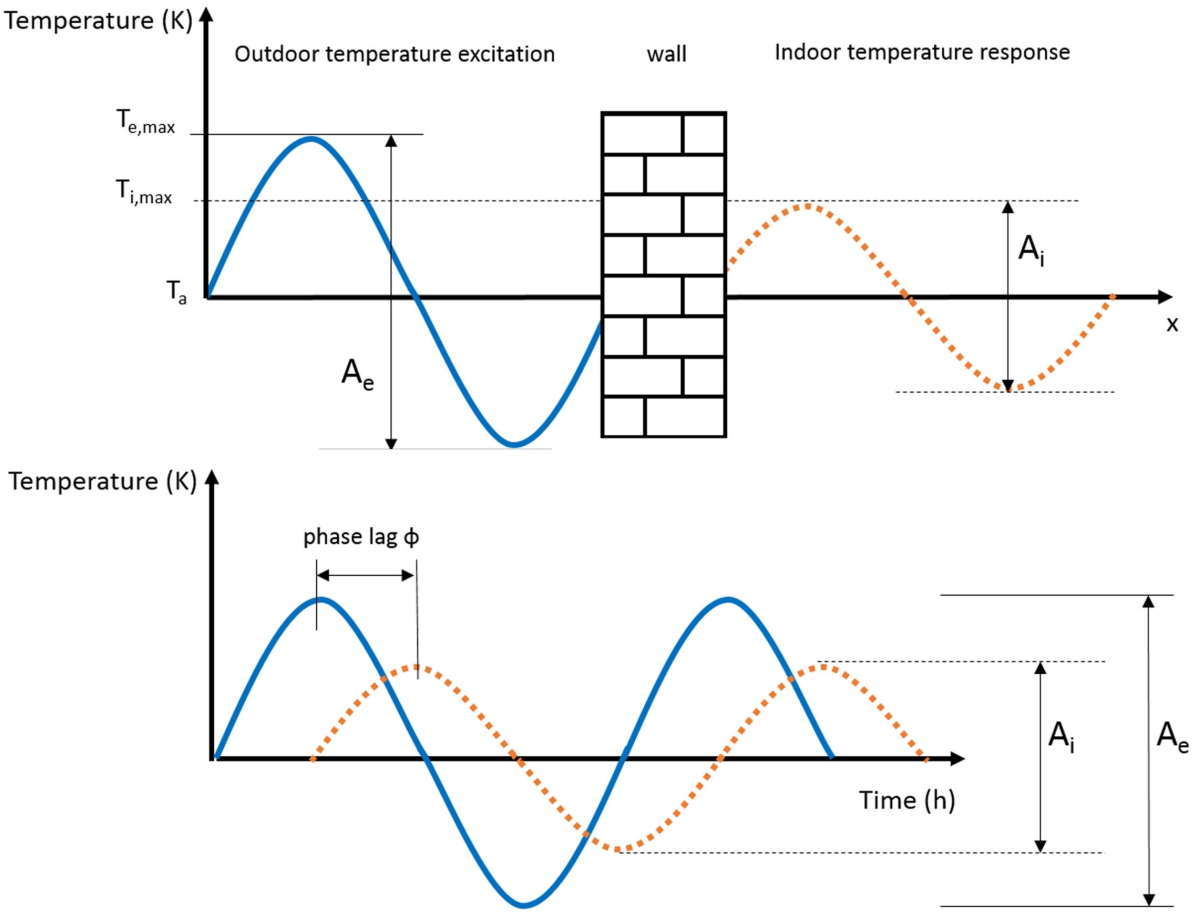

Figure 2.13: Thermal mass affecting internal temperature.[36]

As shown in figure 2.14, a building with high thermal mass has slower reactions to variations than a building with low thermal mass. In the figure, the building is in steady state when the heating system is shut off, thereby starting a cooling process as the indoor air temperature is reduced towards the outdoor temperature T_0. The building with high thermal mass (A) reacts slower than the building with low thermal mass (B). Thus, this can affect the thermal environment in the building, as buildings with high thermal mass can achieve a better thermal environment with less temperature fluctuations [37]. On the other hand, it can be a reason for thermal discomfort as the preheating and pre-cooling periods are increased.[38]

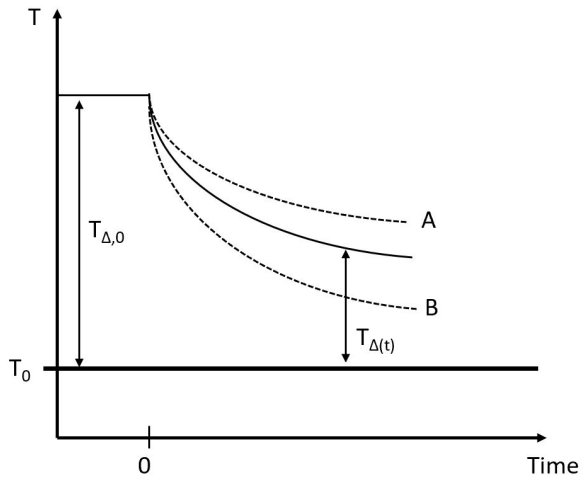

Figure 2.14: Cooling curve for an idealized building with high (A) and low (B) thermal mass.[37]

It is clear that thermal mass can affect building performance. In their study *The impact of thermal mass on building energy consumption*, Reilly and Kinnane (2017) [39] investigated the effect of thermal mass of buildings in cold climates and the importance of including it in calculations regarding both energy and power. A case study revealed that steady state and dynamic models could differ with more than twice the amount of required energy for a typical office.[39]

Situations where thermal mass was found to lower energy consumption and power requirements, were in warm climates, especially if the location had large variations in temperature and the building had intermittent occupancy patterns [39]. Slee, Parkinson, and Hyde (2013) [40] states that increased thermal mass is not unconditionally equivalent to higher building performance. Studies have shown that the energy saving potential is low in Nordic countries, as the heat gain during daytime is limited. On the contrary, it can cause increased energy need as the heating system needs to keep the large mass heated. For example, Reilly and Kinnane (2017) states:

"In this case of a wall with thermal mass, extra heat is needed to heat up the wall at the start of each day. Although this reduces the amount of heating needed the next day, the net effect is that more heat is lost overall - and this effect will always dominate."[39]

However, by utilizing thermal mass as a buffer to reduce fluctuations, it can be a useful tool to reduce peak loads for heating and cooling, as the coldest and warmest extremes are evened out.[39]

Thermal mass is a function of three main parameters: specific heat capacity (C_p), thermal conductivity (k), and density (ρ). Together, these factors decides the thermal storage effectiveness. For example, brick (C_p=800 J/kgK, k=0.73 W/mK, ρ=1700 kg/m^3) have high effectiveness, while mineral fibre insulation (C_p=1000 J/kgK, k=0.035 W/mK, have low effectiveness [35]. Different materials do not only have different energy storage capacities, but also different optimal thicknesses, as can be seen in figure 2.15. After a certain wall thickness, heat fluxes from heat stored from previous days will disrupt the heat fluxes

from absorbed heat from the surroundings, thus reducing the total energy stored.[41]

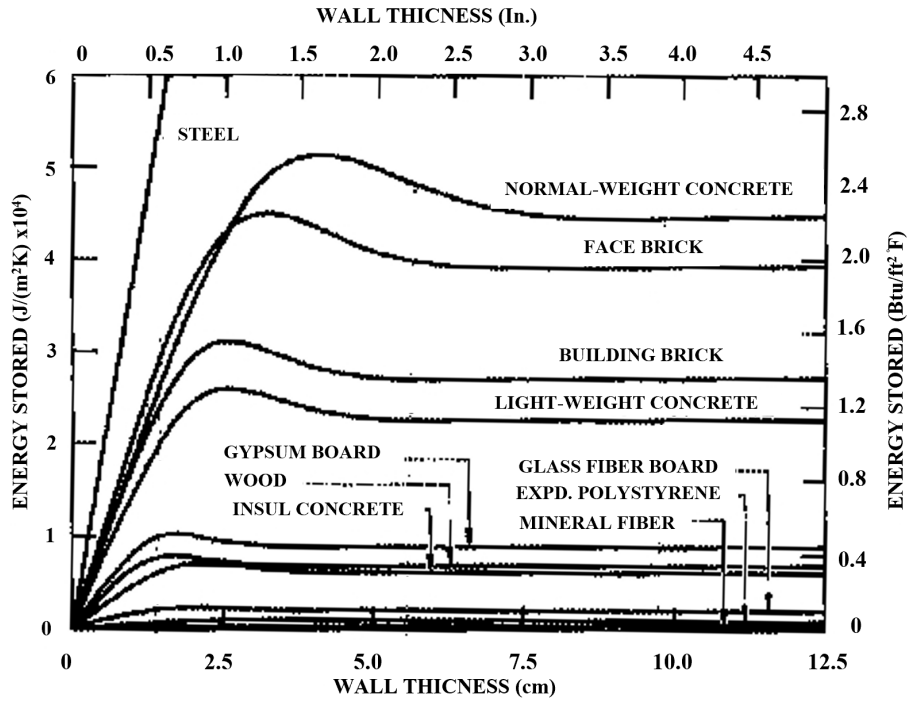

Figure 2.15: Optimal wall thickness to maximize stored energy for different materials.[41]

When assessing energy storage in thermal mass, it is differentiated between sensible and latent heat storage. Sensible heat is stored by increasing the temperature of the building component, while latent heat is stored by changing the phase of a phase changing material (PCM). The equations for stored sensible heat is shown in equation 2.7, while the equation 2.8 and 2.9 show stored latent heat.[42]

$$Q_S = \int_{T_1}^{T_2} m \cdot C_p \cdot dT = m\overline{C}_p \cdot (T_2 - T_1) \tag{2.7}$$

$$Q_L = m \cdot a_m \cdot \Delta H_m + \int_{T_1}^{T_m} m \cdot C_p \cdot dT + \int_{T_m}^{T_2} m \cdot C_p \cdot dT \tag{2.8}$$

$$Q_L = m[\cdot a_m \cdot \Delta H_m + m \cdot \overline{C}_{p,S} \cdot (T_m - T_1) + \overline{C}_{p,L} \cdot (T_2 - T_m)] \tag{2.9}$$

Where

Q_S	=	Stored sensible heat [kJ],
Q_L	=	Stored latent heat [kJ],
T_1	=	Start temperature [K],
T_2	=	End temperature [K],
C_p	=	Specific heat capacity [kJ/kgK],
m	=	Mass [kg],
H_m	=	Latent heat of melting [kJ/kg],
a_m	=	Melting coefficient [-].

During the natural fluctuation in outdoor temperature and solar radiation, the energy storage capacity are not the only thing that need to be considered: the thermal admittance (Y-value), also referred to as the heat transfer coefficient, is important for the energy storage to be utilized. The thermal admittance describes the rate at which materials absorb and emit heat (W/m^{2}K), see equation 2.10.[35]

$$Y = \frac{\Delta Q}{A \cdot \Delta T} \tag{2.10}$$

Where

ΔQ = Absorbed or emitted heat [W],
A = Area of the thermal mass [m^2],
ΔT = Difference between surface temperature and adjacent air temperature [K].

In a building performance perspective, total amount of stored heat will affect the energy need, while the thermal admittance is important regarding power and power-shifting. More detailed dynamic calculations of building components' thermal properties are elaborated in the standard ISO 13786:2017.[43]

Periodic penetration depth in thermal mass

Babiak, Minárová and Olesen (2007) have in their study *What is the effective thickness of thermally activated concrete slab?* [44] looked at how much of the concrete slab contributes to storing energy. Several different floor coverings are analyzed, such as raised floor, acoustic insulation, tiles, wood, and no covering. To test the active depth, the room temperature drifts between 20 and 26 °C, and the depth is analyzed by using a two-dimensional thermal conductance equation. The study shows that the differences between daily maximum and minimum temperature decreases as the depth increases, see figure 2.16.[44]

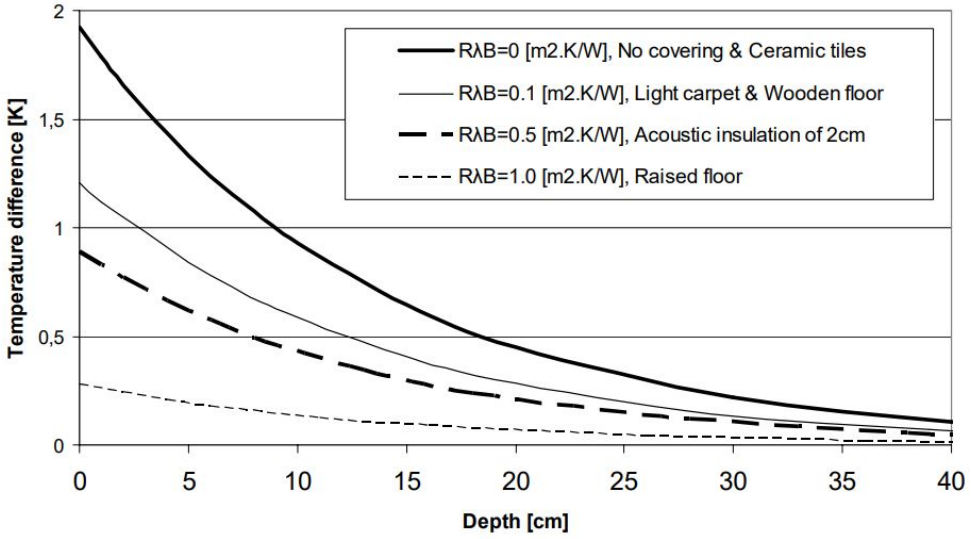

Figure 2.16: Temperature difference between daily maximum and minimum in concrete floor with different coverings.[44]

When assessing stored thermal energy, Babiak et al. (2007) concludes that ceiling slabs should not be thicker than 100-150 mm. Thicker slabs will have higher thermal mass capacity, but will not contribute on a daily or weekly basis as the additional part of the slab will be more or less thermally passive. It is also stated that the temperature fluctuations depend mostly on depth, not covering.[44]

Table 2.7: Periodic penetration depth [m] for different materials.[37]

Material	1 hour	24 hours	1 week
Concrete	0.029	0.143	0.377
Aerated concrete	0.019	0.091	0.240
Wood	0.014	0.067	0.177

Table 2.7 shows different penetration depth for different materials over different time spans.[37]

Operation strategies utilizing thermal mass

Night-time setback is a way to operate the heating or cooling system in order to save energy. It works by letting the building glide outside its temperature limits when the building is not occupied. In a heating perspective, this means letting the building cool down and reduce the heating need.[36]

Using intermittent heating means that when the building should heat up, the heating system will have to heat up the indoor air as well as the thermal mass. Depending on the amount of thermal mass this could require larger capacity in the heating system. Buildings with low thermal mass require less capacity to heat up the thermal mass, and thereby the energy saving potential is bigger without affecting the capacity of the heating system [36]. When utilizing nighttime set-back, it is important to find the optimal time to start the reheating. Starting the reheating to early reduces the amount of energy saved, while starting the reheating to late will call for high power usage.

Verbeke and Audenaert (2018) [36] states that with proper use of the buildings thermal mass, operational cost for heating and cooling can be reduced. Furthermore, capacities in HVAC system can be lower with peak load shifting, making it possible to ”undersize” HVAC systems. Installing lower capacities in HVAC systems reduces the investments cost of the building. One example of such a strategy is using night ventilation to cool down the thermal mass in the building during summer. This reduces the cooling load when the building is occupied, and can in some cases remove the total cooling demand. The study concludes that with the correct control strategy, thermal mass can be used to reduce both heating and cooling loads.[36]

Karlsson, Wadsö and Öberg (2013) does in their article *A conceptual model that simulates the influence of thermal inertia in building structures* [45] discuss if peak heat load reduces during cold-spells in buildings with high interior thermal inertia. The authors state that this depends on how the heating is

controlled. In buildings where the temperature is allowed to decrease significantly during cold-spells the heating power can be reduced as heat is allowed to transfer from the building structure and into the room. However, if the building does not allow the indoor temperature to drop, there will be little to no temperature changes in the building structure thus little to no heat transfer into the room, meaning that the heating power will not be affected. This is regardless of the amount of thermal mass in the building.[45]

The building time constant

The time constant of a building is calculated by the formula:

$$\tau_b = \sum(m_i \cdot c_i)/H_T \tag{2.11}$$

Where $\sum(m_i \cdot c_i)$ is the heat capacity [J/K] of all material layers within the insulated layer, including joists and internal walls up to 10 cm, and H_T is the heat loss coefficient [W/K] [46]. Another method to find the time constant to a building or a room is shown in equation 2.12.

$$\Delta\Theta_t = \Delta\Theta_0 \cdot e^{\frac{-t}{\tau}} \tag{2.12}$$

Where $\Delta\Theta_t$ is the temperature difference between indoor and outdoor with respect to time, $\Delta\Theta_0$ is the temperature difference between indoor and outdoor when the cooling starts, t is time, and τ is the time constant. Note that the time constant is defined as the time it takes for 63.2 % of the temperature reduction to take place. However, it is important to keep in mind that a building will consists of several different time constant, for different cases and conditions. One example is the room time constant, which can vary from room to room based on location in the building and building materials inside the room.[37]

2.4.6 Climatic conditions

Design outdoor temperature

Design outdoor temperature is used in heat load calculations as the lowest outdoor temperature that the heating system should be able to provide thermal comfort. Usually the lowest three day average temperature over a thirty year period is used.[47]

Another way of adjusting DOT is by using equation 2.13 which gives the change in indoor temperature ($\Delta\Theta_i$) based on change in outdoor temperature ($\Delta\Theta_e$), time (t), and building time constant (τ). By the use of this method, the DOT is adjusted based on accepted reduction in indoor temperature and the thermal inertia of the building.[37]

$$\Delta\Theta_i = \Delta\Theta_e \cdot (1 - e^{\frac{-t}{\tau}}) \tag{2.13}$$

Swedish Forum for energy efficient buildings (FEBY) gives recommendations for choosing DOT when calculating heat load for highly insulated buildings. FEBY12 recommends to relate the building's thermal mass to the amount of days that should be considered in the selection of DOT. Higher thermal mass means that a longer time period should be considered as it delays the changes in indoor air temperature due to thermal inertia. The number of days that is included in the calculation of the lowest average temperature is usually referred to as *n* in *n-day average temperature*.[46]

Table 2.8: DOT for variable n-day average temperature for some locations in Sweden, based on the time period from 1978 to 2008.[46]

Location	1-day	2-days	3-days	4-days	5-days	6-days	7-days	8-days	9-days	10-days	11-days	12-days
Kiruna airport	-30.3	-29.4	-28.6	-28.0	-26.8	-26.1	-25.7	-25.3	-25.0	-24.8	-24.7	-24.3
Jokkmokk	-34.8	-34.0	-33.2	-32.0	-31.2	-30.9	-29.9	-29.5	-29.1	-29.0	-28.5	-28.1
Luleå	-27.7	-26.9	-26.1	-25.6	-25.0	-24.4	-24.4	-23.7	-23.2	-22.9	-22.7	-22.4

In table 2.8, the n-day average temperature is presented for one to twelve days. The average temperature difference between 3-day average temperature, which is common practice to use in Norway, and 12-day average temperature, which can be used for semi heavy and heavy buildings in Sweden, for these three locations is 4.4 K.

In the updated version of FEBY, FEBY18, it is possible to choose the lowest 3-day average temperature for heat load calculations independent on the building's thermal mass. Another change is that DOT can be calculated with a more recent time period, which in some cases can give increased DOT [48]. For comparison, the Swedish DOT is based on temperatures from 1981 to 2010[46], whereas the Norwegian DOT is often based on the period from 1971 to 2000 [47]. According to NS-EN ISO 15927-5:2004, source weather data must be based on *"...measurement recorded over a continuous period of at least 20 years..."*.[49]

Other climatic factors

Of the environmental factors, solar radiation and outdoor temperature are the most important in terms of energy performance. In the latitudes of Norway, the radiation will affect south faced facades most during spring and fall, when it is useful as heat gain. During summer the radiation will affect east and west faced facades most, creating a cooling demand. There are three main ways to receive radiation during daytime: direct radiation from the sun, diffuse radiation from the sky, and reflected radiation from the ground and other elements. The intensity of the solar radiation depends on several factors, as position of the sun, altitude above sea level, cloudiness number, cleanliness of the atmosphere, shading and reflectance.[37]

Wind is one of the main contributors to natural ventilation, but it may also cause heat loss (through infiltration) and draught. For old buildings with higher leakage number, wind may contribute to a large part of the heat loss and could require special considerations when sizing the heating system [37]. Mean annual values for wind can be used to asses if there is a lot of wind on the building location. However, average values do not represent wind conditions for one specific place. For example, buildings in cities with lots of surrounding obstacles can experience lower local wind velocity than the surrounding terrain.[37]

If there are no requirements to indoor relative humidity (RH), humidity in outdoor air will only have a marginal influence on the power consumption of the building. The amount of moisture in porous materials are determined by the amount of humidity in the air. This moisture affects the heat conductivity of the material. Normal humidity variations will have very little influence on the heat transmission. However, if the building has requirements to relative humidity, the vapour content in outdoor air has an impact on the amount of heat needed in the processing of ventilation air.[37]

Weather data from meteorological stations gives information about the characteristic weather in the region. One aspect to consider is that the local weather at the building site can vary quite a lot from where the weather data is collected. Most of the time, it is impossible to get local climate data and one must use macro-climate data as a starting point for the building. Special climate factors can be based on own observation of the topography, snow, and vegetation. Another possibility is to use statements from locals.[37]

Weather files for BPS

International Weather for Energy Calculations v 2.0 (IWEC2) is a weather file for one year that consists of weather observations with an average time step for measurements of at least four times per day. The weather parameters that are observed are sky cover, wind speed and direction, visibility, dry-bulb temperature, dew-point temperature, atmospheric pressure, and liquid precipitation. The data is collected over a time period of 12 to 25 years depending on the location [50]. There are also other file-formats depending on the use. Some examples are *Design Day Year* (DDY), *Design Summer Year* (DSY) and *Typical Meteorological Year* (TMY).[51]

2.5 Heat pump as energy supply

Estimated power and energy demand is important when sizing HVAC systems. Discrepancies between actual and calculated power can have a big influence on the performance of the system. One installation that is especially sensitive to discrepancies between calculated and actual energy and power demand are heat pumps, due to life cycle cost analysis. NVE estimates that heat pumps delivered 15 TWh heat to Norwegian buildings, using 6.5 TWh electricity, in 2015. Extrapolating the current incline in number of heat pumps, it will be delivered 18-20 TWh of heat in 2030 [52]. It is clear that reduced performance of the heat pumps can give large socioeconomic costs.

2.5.1 COP and energy savings

When performing load calculations to size the heat pump, both the available heat to the evaporator and needed heat on the condenser side will affect the performance and power to the heat pump. This is shown in equation 2.14 and 2.15.[53]

$$Q_c = Q_e + W \tag{2.14}$$

$$COP = \frac{Q_c}{W} = \frac{Q_e + W}{W} \tag{2.15}$$

$$\Delta E = (\frac{1}{\eta_{alt}} - \frac{1}{COP}) \cdot 100\% \tag{2.16}$$

Where

Q_c	=	Condenser power [kW],
Q_e	=	Evaporator power [kW],
W	=	Compressor power [kW],
COP	=	Coefficient of performance,
ΔE	=	Relative energy savings [%],
η_{alt}	=	Efficiency of the alternative heat source [-].

Equation 2.16 shows the relative energy savings of a heat pump in comparison to an alternative heat source with the efficiency η_{alt}. In the case of an electric boiler with the ideal efficiency of $\eta_{alt} = 1$, the energy savings will follow the function $(1 - 1/COP)$, as shown in figure 2.17. For heat pumps with relatively low COP, a small change in the COP (Coefficient Of Performance) will have a large effect on the relative energy saving. On the other hand, changes in COP when the COP is high will give small changes in the relative energy saving. This means that heat pumps with higher COP will, in an energy saving perspective, be more robust regarding changes in the heat load and the heat source.[53]

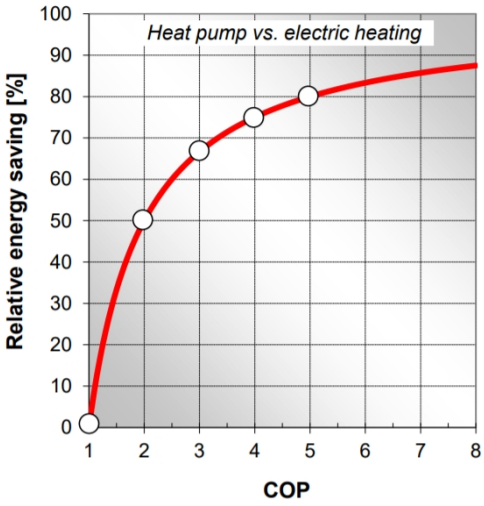

Figure 2.17: Relative energy savings as a function of COP.[54]

2.5.2 Controlling the output power

Heat pumps are usually used as base load, which means that the heat pump preferably covers most of the energy use, not the highest peak loads. As the heat demand varies from hour to hour, delivered energy from the heat pump must be controlled. This is mainly done by controlling the compressor. The main compressor types for an office building are scroll, piston, and screw compressor, while there are, depending on the compressor type, different types of capacity control strategies, see figure 2.18 [55]. When sizing, it is important to keep in mind that the heat pump should operate within the capacity control range. If not, the heat pump will start cycling (intermittent start/stop), which reduce the efficiency and life time of the heat pump.

Properties	Scroll	Piston	Screw	Turbo
Compressor volume – capacity	Low	Low → medium	Medium → high	Very high
Result when pressure ratio deviates from nominal conditions	Under or over compression	Suction / discharge valves	Under or over compression	By-pass at "surging"
Methods for capacity control	1. Intermittent 2. Inverter/VSD	1. Intermittent 2. Cylinder unloading 3. Inverter/VSD	1. Slide valve 2. Inverter/VSD	1. Guide vanes 2. By-pass 3. Intermittent
Efficiency at part load conditions	1. Good **2. Superior**	1. Good 2. Very good **3. Superior**	**1. Bad** **2. Superior** incl. v_i-control	**1. Superior** **2. Bad** 3. Good
Max. number of start/stops per hour at intermittent operation	Approx. 4	Approx. 4	Approx. 2	Approx. 2
Lowest heating/cooling capacity for the compressor type at part load operation	1. 100 % 2. 15-20 %	1. 100 % 2. 20-25 % 3. 20-50 %	1. 10 % 2. 50 %	1. 40-50 % 2. 30 % 3. 100 %

Figure 2.18: Different compressor types compared regarding capacity control strategies.[55]

When operating at part load with reduced heat delivery, it is desirable that the input power to the compressor is reduced linearly in order to reduce losses. However, figure 2.19 shows that this is not always the case for all compressor types.

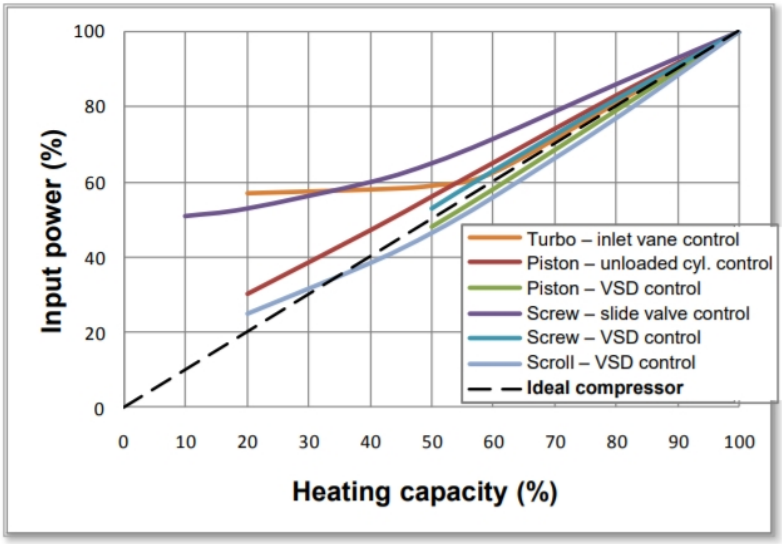

Figure 2.19: Real input power to the compressor at part loads compared to the ideal compressor.[55]

2.5.3 Sizing the heat pump

Using a heat pump should be a sustainable solution, both environmentally and economically. Unfortunately, sizing the heat pump is not straight forward, and a bad design can have a large effect on the costs. If the heat pump is designed to cover the entire heat load, the investment costs will be very high and the Seasonal Coefficient Of Performance (SCOP) reduced, as the heat pump will run at part load most of the year [56]. At the same time, if the heat pump is undersized, the energy coverage will be low and the annual costs for heating will be high. Finding the right balance between power and energy coverage is therefore the key to an optimal heat pump design.

To understand and analyze the relationship between power and energy consumption in a building, it is common practice to use a net heat load duration diagram, as presented in chapter 2.1.2. In this diagram the power coverage factor and the energy coverage factor are studied to find the factors that lead to the lowest annual costs. The power coverage typically varies from 40-70 %, while the energy coverage varies from 70-95 %. For air source heat pumps, it is natural to expect lower energy coverage, typically 60-80 %, because the air temperature, thus the evaporator temperature, drops during winter.[57]

ISO 13612-1:2014 *Heating and cooling systems in buildings - Method for calculation of the system performance and system design for heat pump system - Design and dimensioning* [21] can be used for sizing heat pump systems. The standard states that the heat pump system must be designed in such a way that the system will achieve the highest possible SCOP based on the chosen heat source. Equation

2.17 gives the formula for sizing of heat supply systems where heat pumps are used. Note that if the heat supply system consists of a heat pump and a peak load system, it should be designed in such way that the energy supplied by the peak load system is reduced to a minimum, especially if the peak load system is not renewable.[21]

$$\Phi_{SU} = f_{HL} \cdot \Phi_{HL} + f_{DHW} \cdot \Phi_{DHW} + f_{AS} \cdot \Phi_{AS} \tag{2.17}$$

Where

Φ_{SU} = Heat supply system capacity [kW],
f_{HL} = Design factor heat load [-],
Φ_{HL} = Heat load capacity [kW],
f_{DHW} = Design factor domestic hot water [-],
Φ_{DHW} = Domestiv hot water capacity [kW],
f_{AS} = Design factor attached systems [-],
Φ_{AS} = Attached systems capacity [kW].

Table 2.9: Design factors for heat pump systems.[21]

Load	**Heat pump design factor**	**Design criteria**	**Default value for the design factor**
Heat load	f_{HL}	Low mass building (raised floor and suspended ceiling, light walls)	1.00
		Medium mass buidling (Concrete floors and ceiling, light walls)	0.95
		Heavy building (Concrete floors and ceiling, concrete walls or brick)	0.90
Domestic hot water	f_{DHW}	Standard class of sanitary system	1
Attached systems	f_{AS}		1

Table 2.9 gives default values for design factors for heat pump systems based on building construction. These are used as input in equation 2.17.[21]

Cost efficiency

Expressing the costs (including investment, operation and energy savings) as a function of power, the criteria for optimum heat pump capacity is shown in equation 2.18. Further evaluating the capital costs

and operating costs of installing 1 watt more or less for both the base load and peak load system, as in equation 2.19-2.20, the optimal duration time is found (equation 2.21). The optimum heat pump capacity is read from the duration diagram at the found duration time T.[57]

$$\frac{dC}{dP} = 0 \tag{2.18}$$

$$dP \cdot [I_{BL} \cdot a + (\frac{e_{BL}}{\eta_{BL}}) \cdot T] = dP \cdot [I_{PL} \cdot a + (\frac{e_{PL}}{\eta_{PL}}) \cdot T] \tag{2.19}$$

$$\Leftrightarrow$$

$$(I_{BL} - I_{PL}) \cdot a = (\frac{e_{PL}}{\eta_{PL}} - \frac{e_{BL}}{\eta_{BL}}) \cdot T \tag{2.20}$$

$$\Leftrightarrow$$

$$T = \frac{(I_{BL} - I_{PL}) \cdot a}{(\frac{e_{PL}}{\eta_{PL}} - \frac{e_{BL}}{\eta_{BL}})} \tag{2.21}$$

Where

dC	=	Cost change [€],
dP	=	Power change [kW],
T	=	Duration [h],
C	=	Total costs [€],
I	=	Investment costs [€/kW],
e	=	Energy prices [€/kWh],
a	=	Annuity factor [-],
η	=	Efficiency [-],
BL	=	Base load [kW],
PL	=	Peak load [kW].

To solve this optimization problem, it is needed high-quality input variables, which depend on the design phase. As it can be both difficult and time consuming to collect accurate data, it is not unusual that the designer choose a power coverage factor based on experience. However, Stene (2018) stresses that an energy-economical analysis should be performed. It is further mentioned that it should be performed a sensitivity analysis to evaluate maximum investment costs and minimum earnings. Furthermore, Stene (2018) list the following factors which can contribute to determine the power coverage factor[57]:

- Power duration diagram
- Heat source - type and temperature level
- Heat distribution system - temperature level
- Heat pump unit - COP at different operating conditions
- Specific investment costs for heat pump and peak load
- Energy prices

Stene (2019) [58] suggests, for the early design phase calculation, that investment cost for heat pumps range from 4500-6500 NOK/kW based on quality, in addition to another 30 % for installation. In a real-life example, the investment costs for district heating were 450 000 NOK for the capacity and an additional 80 000 NOK for the heat exchanger. However, Stene (2019) stresses that investment cost for district heating vary a lot based on the supply company and distance between the building and the district heating grid [58]. According to *Statkraft varme*'s energy calculator [59], the investment cost for district heating in an office building in Trondheim with energy label B is 250 000 NOK if the building only uses district heating. This price is a deal between the customer and Statkraft, where Statkraft reduces the investment costs since the building only uses district heating. However, if the building has another heat source in combination with district heating, the investment cost increases to 750 000 NOK. Each of these prices includes 80 m of tubing for connecting the building to the district heating grid. If the building is located more than 80 m from the grid, the costumer has to pay for the extra tubing. These prices are based on experiences from both Statkraft and consultants.[59]

Cycling and duration hours

Heat pump cycling can be used to size the capacity of the heat pump. This design method requires a buffer tank in order to limit the times the heat pump cycles on/off. According to Stene (2019) [60], the rule-of-thumb is that the heat pump should not cycle on/off more than four times per hour to reduce wear and tear on the compressor. The buffer tank can be sized by assuming 20 liters/kW.[60]

Djunaedy, Wymelenberg, Acker and Thimmana (2011) have in their study *Oversizing of HVAC system: Signatures and penalties* [61] looked at oversized Roof-Top Units and what characterizes them based on cycling rate [cycle/h] (equation 2.22), and run-time fraction (RTF) (equation 2.23). They concluded that a combination of high cycling rate and low run-time fraction on a design, or "near" design, day is a sure sign of an oversized unit.[61]

$$N = \frac{1}{t_{Cycle}} \tag{2.22}$$

$$RTF = \frac{t_{ON}}{t_{Cycle}} \tag{2.23}$$

2.6 Oversized HVAC systems

Thomas and Moller (2006) has in their case study *HVAC system size - Getting it right* [62] looked at oversized HVAC systems and their effects on regulation and system efficiency. They found that oversized HVAC systems have effects on the whole project. For example, a bigger system would need larger pipes, pumps, valves, and cooling towers. Often will HVAC system be provided with a certain capacity.

Even tough a large system often have a smaller cost per kW, the total cost for the project will increase considerably because of the bigger parts needed. An oversized AHU (Air Handling Unit) has the risk of not being able to sustain thermal comfort, as too large systems might not be able to run well on low capacity, causing either too much conditioning or not being able to provide stable operation, i.e poor part load operation. Oversized motors or other electrical equipment can also create penalty tariffs for large current loads on the electrical distribution grid. Larger current loads also require higher capacity electrical boards and cables, which also increase costs.[62]

Thomas and Moller (2006) lists several factors for oversizing, such as occupancy loads, internal loads, temperature set-points, discrete design process, and conservative design approach. Especially the last factor is discussed in detail. For example, not considering the surroundings yield a higher calculated cooling load, as shading from surrounding buildings is neglected. A reason why designers might do this is that they assume that nearby buildings might be demolished at a later date creating a higher cooling demand. Also, if the tenants in the building are unknown, it may force the designer to size a cooling system for a worst case scenario. To avoid oversizing, these recommendations are given: [62]

- Avoid the use of safety factors
- Do not use rule-of-thumb methods
- Use load estimation programs that can account for thermal storage in the building
- Specify equipment with good part load efficiency to ensure good part load operation
- Use data specific to the location
- Design for flexibility with respect to different occupants

Gorter (2011) has in her article *HVAC Equipment Right-sizing: Occupant Comfort and Energy Saving Potential* [63] looked at how HVAC equipment size affect buildings. Often, engineers and designers have to go through a tender process to get a project. To reduce costs of the building, the lowest priced offer wins. The price is often lowered by reducing the project's working hours, resulting in systems that work, but not necessarily with the most optimized design. Another reason for oversizing is that neither designers nor contractors want to be responsible for an HVAC system that is not able to satisfy the demand in the building. Therefore, the systems are design to handle a worst case criteria, and sometimes multiplying by a safety factor. Thus, the system is design for a scenario that will never occur.[63]

Due to oversizing, HVAC systems achieve higher investments costs, higher energy consumption, shorter equipment lifetime, and also higher equipment replacement rate than necessary. Right-sized equipment reduces both investment and operation costs, extends lifetime of the equipment, and improves occupant comfort. Owners and contractors should consider increasing the amount of time used in the design phase as right-sized equipment will pay off.[63]

Chapter 3

Methodology

3.1 IDA ICE

First released in 1998, IDA ICE is a building simulation tool to simulate energy consumption, indoor air quality and thermal comfort. It is written in *Neutral Model Format* (NMF), allowing acausal algebraic equations and two-ways flow of information, the opposite of the causal form traditionally used in computer programming.[64]

A great advantage of IDA ICE is the user friendly interface and a 3D-view that make it simple for the user to get an overview of the input data and physical properties of the model. Some of the most relevant outputs of IDA ICE are[64]:

- Power for system components
- Energy for system components
- Energy balance for every zone
- Air temperature, operating temperature, PMV and PPD
- Airflow through openings and between zones

Further, IDA ICE is a well tested international software, thoroughly validated by for example *ASHRAE 140*, *EN 15255*, *EN 15265*, and *International Energy Agency SHC Task 34*. This means that if IDA ICE is used correctly, it can be a powerful tool to evaluate a buildings performance.[65]

IDA ICE provides detailed IWEC2 weather files, in order to run dynamic simulations for different locations throughout the world. It is also possible to use self-made weather files. Furthermore, it can be implemented detailed schedules for occupancy, lighting, technical equipment, fan operation etc.

This gives detailed results for indoor climate and energy. However, this also makes the computations heavy and time-demanding. Additionally, the licence is relatively expensive. Therefore, some consultant companies use simpler tools for energy calculations and IDA ICE if there is need for detailed indoor environment analysis.

3.2 Case buildings

To realize the aims of this Master's thesis, four different office buildings are used to test different methods and weather data: Baard Iversens veg 7 (the *GK Building Trondheim*, GKBT), Otto Nielsens vei 12E (ONV12E), Sluppenvegen 17B (*Stålgården*, STG), and Vestre Rosten 69 (HENT). Firstly, the buildings are briefly compared in table 3.1. Further, GKBT, ONV12E, STG, and HENT are presented in details in chapter 3.2.1, 3.2.2, 3.2.3, and 3.2.4 respectively. Here, relevant information and input values used in the construction of the building energy models (BEM) are given.

The abbreviations for the different buildings are used strictly for simplification, and should not under any circumstances be connected to the existing companies that bear names similar to the abbreviations used in this Master's thesis.

Table 3.1: Overview of the case buildings.

Site	**GKBT**	**ONV12E**	**STG**	**HENT**
Size [m^2]	5000	8940	13150	10000
Heating strategy	Air heated. Air-source HP+DH.	Hydronic radiators and floor heating. Ground-source HP.	Active thermal slabs (hydronic heating). Air-source HP+DH.	Air heated. Air-source HP+DH.
Cooling strategy	Air-cooling. Air-source HP.	Air-cooling. Ground-source HP.	Air-cooling. Air-source HP.	Air-cooling. Air-source HP.
DHW heating strategy	Storage tank (600 L)	Unknown	Storage tank (unknown size)	Direct heating

Air supply control strategy	Cell offices: VAV Temp. control. Meeting rooms: DCV CO_2 + Temp. control. Open landscape: VAV Temp. control.	Cell offices: VAV Temp. control. Meeting rooms: DCV CO_2 + Temp. control. Open landscape: VAV Temp. control.	Unknown.	Cell offices: VAV Temp. control. Meeting rooms: DCV CO_2 + Temp. control. Open landscape: VAV Temp. control.
Occupancy	Logged every ten minutes.	Started logging 2019-02, logging changes.	Not logged.	Logged every fifteen minutes.
Lighting	1 el. meter per floor, 3 floors. Logged hourly.	2 el. meters per floor, 4 floors. Logged hourly.	Not logged.	Not logged.
Technical equipment	1 el.meter per floor, 3 floors. Logged hourly.	2 el. meters per floor, 3 floors. Logged hourly.	Not logged.	Not logged.
Total electricity (light+tech)	Lighting + technical equipment.	Lighting + technical equipment.	Measured per tenant, 12 tenants in total. Logged hourly.	3 el. meters per floor, 3 floors. Logged hourly.

Table 3.2: Different heating capacities installed in each of the case buildings

	Heating capacity [kW]			
	GKBT	**ONV12E**	**STG**	**HENT**
Heat pump	80	230	275	281
District heating	350	Unknown	670	975
Domestic hot water	10.5	Unknown	300	250
Technical room(s)	2.5	Unknown	Unknown	5.7
Aerotemper parking garage	30	Unknown	40	150
Snow melting system	45	Unknown	30	0
Estimated space heating	262	Unknown	300	569.3

Table 3.2 presents the different heating capacities for each site. Information for every site except ONV12E is gathered from the respective HVAC system scheme. The HVAC systems will be further explained in chapters 3.2.1 - 3.2.4.

3.2.1 Baard Iversens veg 7 - GKBT

GKBT was raised 2017 in Trondheim, and is a four storey office building with a three level underground parking. The underground parking should keep the temperature above 5°C, but is not a part of the BEM. Instead, the external floor is simulated with a constant temperature of 5°C on the outside. The ground floor, meant for industry and cafeteria/bar, is projected to meet the requirements in TEK10. First to fourth floor consist of offices, and shall meet the requirements for a low energy building according to NS 3701. Today, GK occupies first to third floor, while Erichsen & Horgen and Karl Knudsen share the fourth floor. The technical room is placed on the roof. Input data for the BEM is given in table 3.3.

Table 3.3: Input parameters used to construct a base case building energy model of GKBT.

Element	Value	Unit	Note
Wall towards free area, U-value	0.21	$W/(m^2 \cdot K)$	From energy concept. Light wooden walls.
Wall towards ground, U-value	0.55	$W/(m^2 \cdot K)$	From energy concept. Double gypsym, insulated wall.
Internal walls, U-value	1.7	$W/(m^2 \cdot K)$	Internal wall without insulation, only between zones with same set point temperatures.
External floor, U-value	0.18	$W/(m^2 \cdot K)$	From energy concept.
Internal floor, U-value	1.64	$W/(m^2 \cdot K)$	From energy concept. Hollow core concrete slabs.
Roof, U-value	0.16	$W/(m^2 \cdot K)$	From energy concept. Light insulated wooden roof.
Glazing/windows, U-value	0.7	$W/(m^2 \cdot K)$	From energy concept. Using simple 3-pane glazing with integrated internal blinds.
Orientation	12.28	$degrees$	Measured from IFC-file.
Normalized thermal bridge value	0.05	$W/(m^2 \cdot K)$	From energy concept. Note that this value is per floor area, while the standard unit in IDA ICE is per envelope.

Infiltration	0.3	$ACH(h^{-1})$	From energy concept. Wind driven flow, at pressure difference 50 Pa, semi-exposed building.
DHW	5	$kWh/m^2/year$	From NS 3031.
Set point temperature heating	21.5	$°C$	Set point found from the building management system.
Set point temperature cooling	-	$°C$	Not relevant.
Ventilation, offices	10	$m^3/(h \cdot m^2)$	Balanced constant air volume. Recommended flow rate from NS 3031 Appendix B. Reduced to 20% outside operation time.
Heat exchanger efficiency	85	$\%$	From energy concept. Rotary heat exchanger, minimum allowed leaving temperature -30 °C.
Door construction, U-value	0.21	$W/(m^2 \cdot K)$	Same as wall constructions, with leakage area of 0.01 m^2, except for glass doors, which are configured as windows with the standard glazing.

In GKBT, an 80 kW air-to-water heat pump is used as base load, and 350 kW district heating for peak load. The heat pump also works as a liquid chiller when cooling is needed. The heat supply system delivers heat to the different AHUs, DHW, and snow melting system by a hydronic heating system. Originally, electrical heaters were planned in each corner of the building, but these are not in use. Assuming that district heating is sized to cover the total heat load at DOT, in case of heat pump maintenance, would mean that the design heat load for GKBT is 350 kW. However, the space heating demand is assumed to be 262 kW, if removing heating of DHW, technical room, parking garage, and snow melting system from the design heat load (see table 3.2). GKBT is heated by ventilation air, which calls for complex regulation. It uses advanced Lindinvent diffusers that measures room temperature, occupancy (on/off), air temperature in ventilation ducts, and supply air flow rate in order to control the indoor environment in the building.

In this project, the object of evaluation is power *need*. Detailed evaluations of the existing heating systems is less relevant, justifying ideal heaters and coolers with no system losses and ideal efficiencies (COP of 1). Other input data that may not be specified above, is left as default values provided by the software.

In figure 3.1, the 3D-view of the building energy model of GKBT is presented. As shown in the figure, shading from nearby buildings are included.

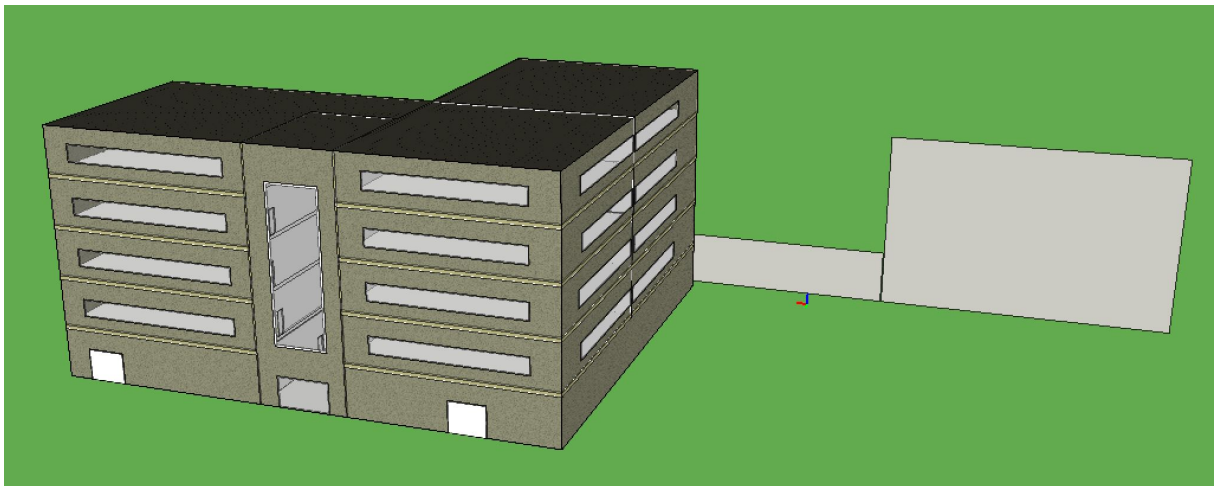

Figure 3.1: 3D-view of the BEM of GKBT.

Figure 3.2 shows the thermal zoning of GKBT. The zoning is based on the layout of the AHUs, however the entrance area (small rectangular zone) is simulated as one zone due to it's height and difference in internal gains.

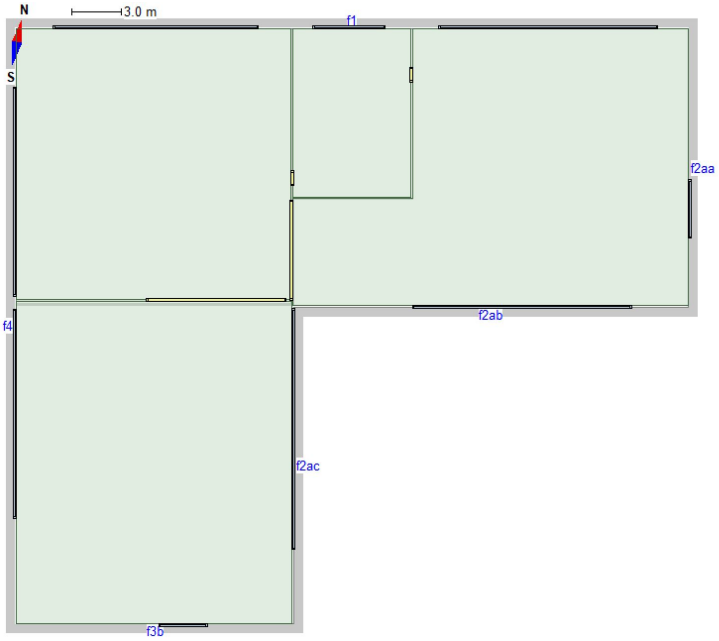

Figure 3.2: Thermal zoning in the BEM of GKBT.

3.2.2 Otto Nielsens vei 12E - ONV12E

ONV12E, raised in January 2016, is a near passive house office building with a BREEAM Excellent rating. The building has a total heated area of 8940 m^2 distributed over 4 floors and a parking garage. The heating and cooling system consists of a heat pump/liquid chiller which covers the total space heating and cooling (space- and process cooling) demand, and almost all of the DHW heating. The heat pump/liquid chiller system is developed based on the tenants in the building which require a large cooling capacity for process cooling. Due to the more or less constant process cooling demand, the excess heat produced from the system is transferred to Otto Nielsens Vei 12 A-D. Because of this connection to the other buildings, ONV12E is a part of the Zero Emission Neighbourhood (ZEN) research program.[66]

In total, the heat pump/liquid chiller system should have an energy coverage of 100 %, but due to maintenance, is it roughly 95 %. During maintenance and peak load, district heating is used as back up, through the connection with ONV12 A-D. The heat pump has a heating capacity of 230 kW in heating mode, and 290 kW heating capacity in cooling mode, while the hydronic system in ONV12E is sized for 395 kW.[66]

The BEM has an area of 5461.2 m^2, since the parking garage is excluded from the model. This model is based on the model created by Florent Dulac in his Master's thesis *Investigation of the detailed design of a multifunctional heat pump system* [67]. However, as the original model had over 200 zones, it had to be simplified to be used in this Master's thesis. The simplifications were mainly performed on the geometry, windows, and the thermal zones. Note that the values for the building construction in table 3.4 are based on Dulac's model, due to lack of access to the project folder of ONV12E.

Table 3.4: Input parameters used to construct a building energy model of Otto Nielsens vei 12E.

Element	Value	Unit	Note
External wall, U-value	0.16	$W/(m^2 \cdot K)$	Light timber construction.
Internal walls, U-value	0.25	$W/(m^2 \cdot K)$	Internal wall with insulation.
External floor, U-value	0.24	$W/(m^2 \cdot K)$	Heavy concrete construction.
Internal floor, U-value	1.64	$W/(m^2 \cdot K)$	Assumed hollow core concrete slabs.
Roof, U-value	0.10	$W/(m^2 \cdot K)$	Light insulated concrete roof.
Glazing/windows, U-value	0.81	$W/(m^2 \cdot K)$	Using simple 3-pane glazing with integrated external blinds and a heat gain coefficient of 0.31.
Orientation	28.08	$degrees$	Measured from Dulac's model.

Normalized thermal bridge value	0.03	$W/(m^2 \cdot K)$	Note that this value is per floor area. Assumption based on thermal bridge value from NS 3701.
Infiltration	0.3	$ACH(h^{-1})$	Wind-driven flow, at pressure difference 50 Pa. Configured as ”semi-exposed building”.
DHW	5	$kWh/m^2/year$	From NS 3031.
Set point temperature heating	21.5	$°C$	From building management system.
Set point temperature cooling	-	$°C$	Not relevant.
Ventilation, offices	10	$m^3/(h \cdot m^2)$	Balanced constant air volume. Recommended flow-rate from NS 3031 Appendix B. Reduced to 20% outside operation hours.
Door construction, U-value	0.16	$W/(m^2 \cdot K)$	Same as wall constructions, with leakage area of 0.01 m^2, except for glass doors, which are configured as windows with the standard glazing.

Figure 3.3 show the 3D-view of the BEM of ONV12E created in IDA ICE. As shown in the figure, shading from nearby buildings and structural elements on the building are included.

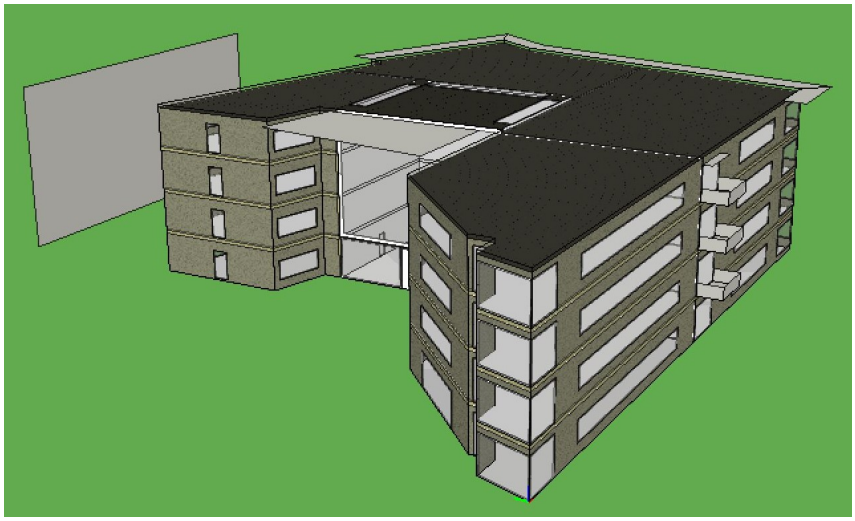

Figure 3.3: 3D-view of the BEM of ONV12E.

In figure 3.4, the thermal zoning in the BEM is presented. The zones are developed similar to the distribution of the AHUs. Also, the entrance area (square zone in the middle) is chosen to be simulated as one separate zone due to its difference in heat gains and height.

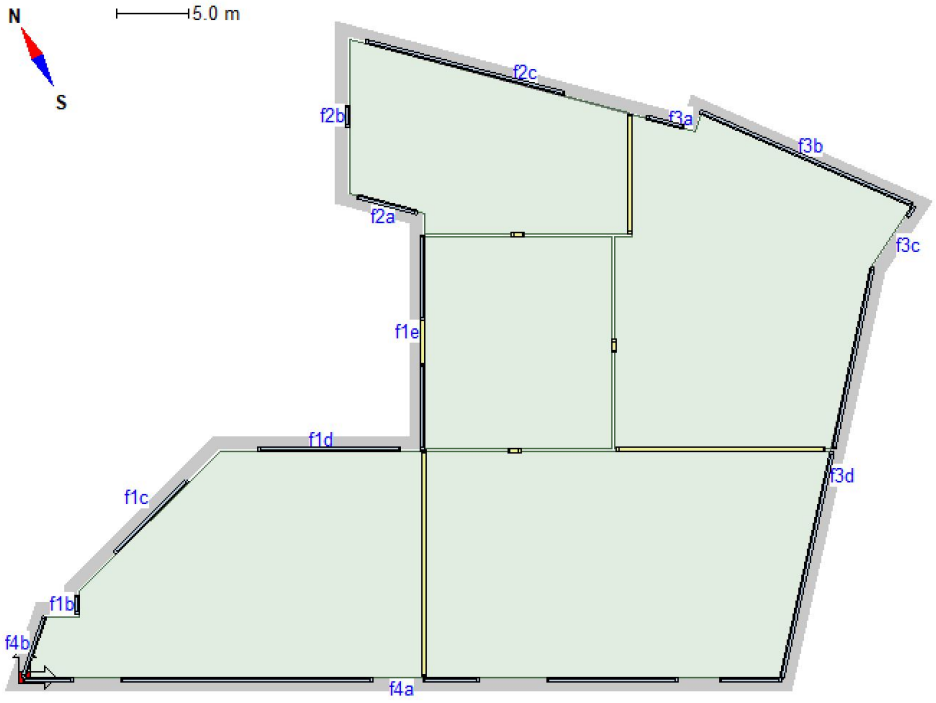

Figure 3.4: Thermal zoning in the BEM of ONV12E.

3.2.3 Sluppenvegen 17B - STG

STG was built in 2015 and satisfy the requirements for a passive house office building. The building received funding from Enova due to the use of active thermal slabs. The ground floor contains a restaurant, a gym, locker rooms, and meeting rooms. A parking garage is located underneath the building. The rest of the 8 story building contains offices, both cell and landscape. In total, the building has an area of 13 150 m^2 including the parking garage.[68]

The heating supply system in the building consists of a heat pump of 275 kW for base load, and district heating as peak load with a capacity of 670 kW. The heating demand in the building consists of space heating, DHW, heating of ventilation air, and a snow melting system. Since the heat pump uses R410a as working fluid, it stops working when the outside temperature drops below -10 °C, meaning that the district heating is sized to cover the total heating demand of 670 kW [69]. As shown in table 3.2, the DHW is sized for 300 kW, the aerotempers in the parking garage are sized for 40 kW, while the snow melting system is sized for 30 kW. Based on these heating capacities, the space heating demand for the building, excluding the parking garage and snow melting system, is assumed to be 300 kW. The HVAC system scheme does not give enough information to evaluate the size of the DHW sizing, however, by

assuming a temperature difference of 60 °C in the district heating DHW-exchanger, 300 kW is estimated.

Table 3.5: Input parameters used to construct a building energy model of STG.

Element	Value	Unit	Note
External wall, U-value	0.14	$W/(m^2 \cdot K)$	From energy concept. Light timber construction. Clad with steel plates.
Outer surface shortwave reflectance	0.726	-	IDA ICE default for brushed aluminum to simulate the steel cladding.
Internal walls, U-value	0.62	$W/(m^2 \cdot K)$	Internal wall with insulation.
External floor, U-value	0.18	$W/(m^2 \cdot K)$	From energy concept. Concrete floor with light insulation, topped with chip board.
Internal floor, U-value	2.71	$W/(m^2 \cdot K)$	From energy concept. Heavy concrete slab (0.304 m thick).
Roof, U-value	0.13	$W/(m^2 \cdot K)$	From energy concept. Light insulated wooden construction.
Glazing/windows, U-value	0.8	$W/(m^2 \cdot K)$	From energy concept. Using simple 3-pane glazing with integrated external blinds on the east, south and west facade. Heat gain coefficient of 0.35.
Orientation	285	$degrees$	Measured from IFC-file.
Normalized thermal bridge value	0.09	$W/(m^2 \cdot K)$	From energy concept. Note that this value is per floor area, while the standard unit in IDA ICE is per envelope.
Infiltration	0.24	$ACH(h^{-1})$	From energy concept. Wind-driven flow, at pressure difference 50 Pa. Configured as ”semi-exposed building”.
DHW	5	$kWh/m^2/year$	From NS 3031.
Set point temperature heating	21.5	$°C$	Assumption based on set point temperature in GKBT, ONV12E, and HENT.
Set point temperature cooling	-	$°C$	Not relevant.

Ventilation, offices	10	$m^3/(h \cdot m^2)$	Balanced constant air volume. Recommended flow-rate from NS 3031 Appendix B. Reduced to 20% outside operation hours.
Heat exchanger efficiency (AHU)	85	%	From energy concept. Rotary heat exchanger, minimum allowed leaving temperature -30 °C.
Door construction, U-value	0.14	$W/(m^2 \cdot K)$	Same as wall constructions, with leakage area of 0.01 m^2, except for glass doors, which are configured as windows with the standard glazing.

In figure 3.5, the 3D-view of STG's BEM is presented. As shown in the figure, shading from nearby buildings is considered.

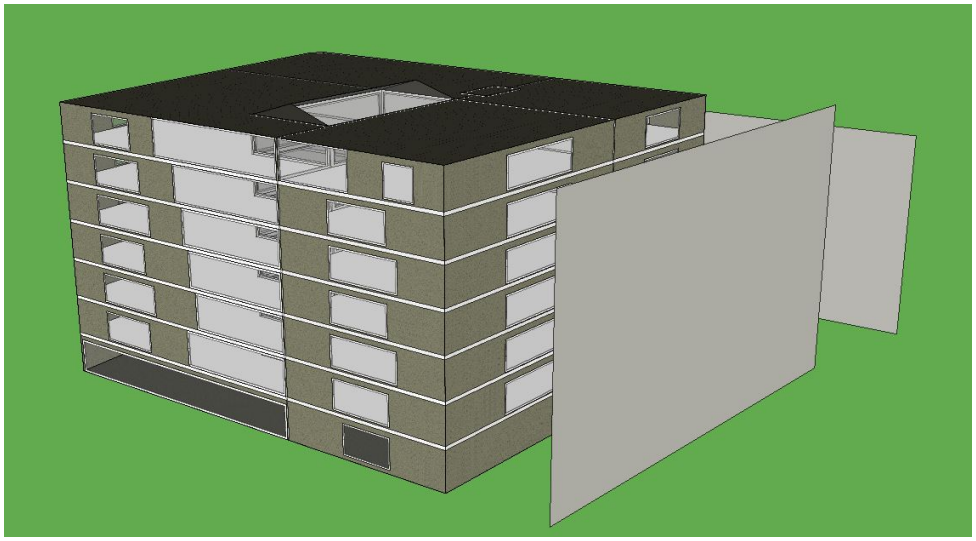

Figure 3.5: 3D-view of the BEM of STG.

Figure 3.6 shows the thermal zones in STG. These are based on orientation, but the aula and the stairwell are created as separate zones because of their different heights and internal gains.

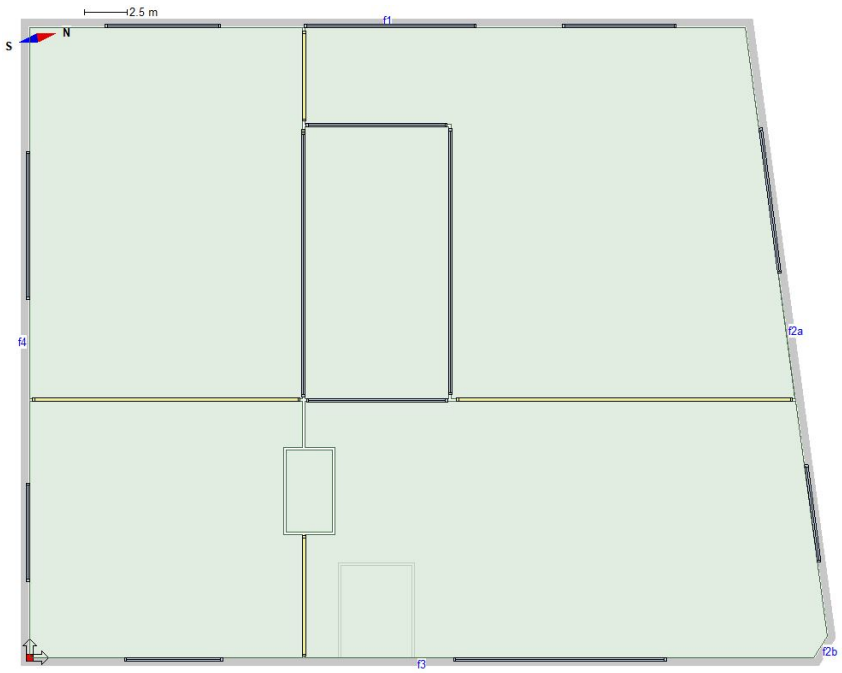

Figure 3.6: Thermal zoning in the BEM of STG.

3.2.4 Vestre Rosten 69 - HENT

HENT is located at Vestre Rosten 69 in Trondheim and is an 10000 m^2 (gross area) office building, raised 2014/15, with an energy label B. The building consists of 4 floors with offices and a ground floor with cafeteria, locker rooms, and other technical rooms, and a parking garage.[70] The building is heated by ventilation air, and utilizes the same Lindinvent system as in GKBT.[71]

The HVAC system in the building consists of a heat pump with a heating capacity of 281 kW, 725 kW district heating for space heating, and 250 kW district heating for DHW. The heating system includes aerotempers in the parking garage with a total capacity of 150 kW and two aerotempers with a combined capacity of 5.7 kW for heating the technical rooms on the roof. Based on these heating capacities, the space heating demand is assumed to be 569.3 kW, excluding parking garage and technical room (see table 3.2).

Table 3.6: Input parameters used to construct the BEM of HENT.

Element	Value	Unit	Note
Wall towards free area, U-value	0.21	$W/(m^2 \cdot K)$	From energy concept. Light wooden walls.
Wall towards ground, U-value	0.2	$W/(m^2 \cdot K)$	From energy concept. Double gypsym, insulated wall.

Internal walls, U-value	0.62	$W/(m^2 \cdot K)$	Internal wall with insulation, only between zones with same set point temperatures.
External floor, U-value	0.15	$W/(m^2 \cdot K)$	From energy concept.
Internal floor, U-value	1.64	$W/(m^2 \cdot K)$	From civil engineer's IFC-model, hollow core concrete slabs.
Roof, U-value	0.13	$W/(m^2 \cdot K)$	From energy concept. Light insulated wooden roof.
Glazing/windows, U-value	0.79	$W/(m^2 \cdot K)$	From energy concept. Using simple 3-pane glazing with integrated internal blinds.
Orientation	11.35	$degrees$	Measured from IFC-file.
Normalized thermal bridge value	0.09	$W/(m^2 \cdot K)$	From energy concept. Note that this value is per floor area, while the standard unit in IDA ICE is per envelope.
Infiltration	0.6	$ACH(h^{-1})$	From energy concept. Wind driven flow, at pressure difference 50 Pa, semi-exposed building.
DHW	5	$kWh/m^2/year$	From NS 3031.
Set point temperature heating	21.5	$°C$	From building management system.
Set point temperature cooling	-	$°C$	Not relevant.
Ventilation	9.2	$m^3/(h \cdot m^2)$	Balanced constant air volume. Reduced to 35 % outside operation time. From energy concept.
Heat exchanger	84	%	From energy concept. Rotary heat exchanger, minimum allowed leaving temperature -30 °C.
Door construction, U-value	0.21	$W/(m^2 \cdot K)$	Same as wall constructions, with leakage area of 0.01 m^2, except for glass doors, which are configured as windows with the standard glazing.

In figure 3.7, the 3D-view of the BEM for HENT is presented. As shown in the figure, the parking garage is excluded from the model, but is considered by connecting the walls that would in reality be connected to the parking garage to a fixed temperature of 5 °C.

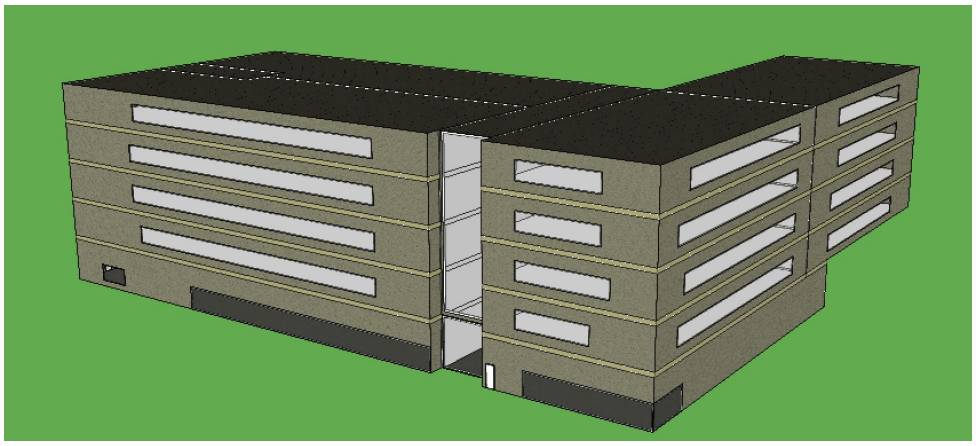

Figure 3.7: 3D-view of the BEM of HENT.

Figure 3.8 shows the thermal zoning of HENT. This is based on the layout of the AHUs, as for the other buildings. The open glass area North in the building, and the entrance area, are simulated as separated zones due to their height and difference in internal gains.

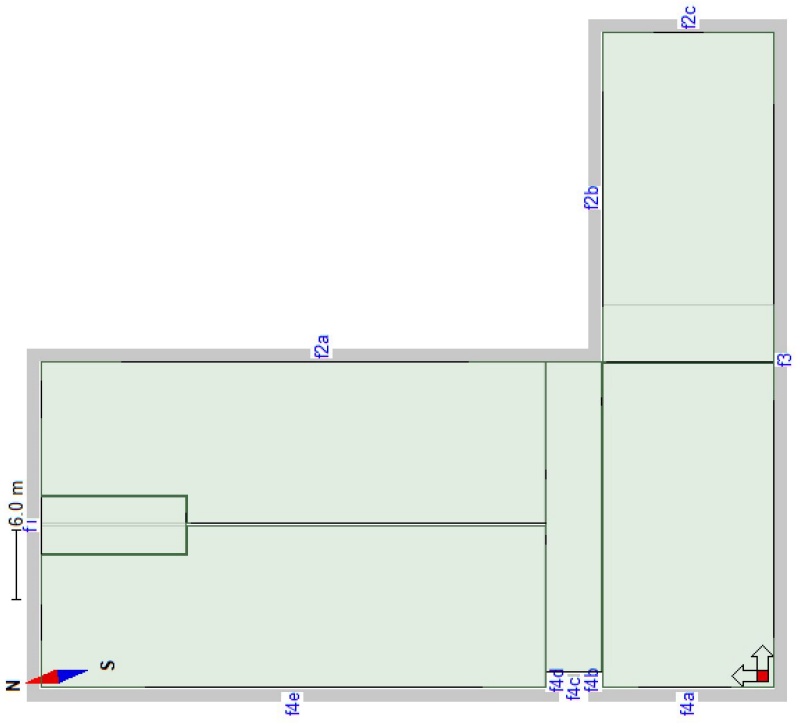

Figure 3.8: Thermal zoning in the BEM of HENT.

3.3 Measuring internal gains

In this thesis, different standards and studies of internal gains are studied to evaluate their feasibility. To get a better understanding of the accuracy of these studies/standards, they are compared to measurements mainly based on GKBT. This building is chosen as the main basis for comparison due to the measuring equipment available in the building, and the quality of the measurements. For most of the internal gains evaluations, the entire year of 2018 is studied. When studying internal gains as averages, arithmetic averages are used.

3.3.1 Occupancy

Both GKBT and HENT are equipped with active *Lindinvent* air diffusers. For each diffuser, a motion sensor recognizes occupants and digitally logs the occupancy every tenth minute (every fifteenth minute for HENT). The installed motion sensors are of the type *Lindinvent XPIR*, which *"...detects changes in infrared radiation resulting from the movement of a person (or object) with a temperature different from its surroundings."*, and registers movements with the magnitude of 20 cm with an observation angle of 51.3.°[72] The occupancy is logged as On (1) or Off (0) and is available at Lindab's building management system (BMS) *Lindinspect*. It is assumed that 1 or 0 means that the room is occupied/not occupied the next ten (fifteen) minutes.

The simplest way to evaluate occupancy is to read the total diversity factor directly from the BMS. This diversity factor tells how many of all the diffusers that are triggered (On), divided by the total number of diffusers. However, the accuracy of this method is limited. Therefore, it is interesting to study cell offices and meeting rooms in detail. In the landscape areas, the ventilation is temperature controlled. Even though the diffusers are equipped with motion sensors, they will only tell if anyone is present- not the actual number of occupants. Therefore, occupancy in the open landscape is not studied in detail. In the meeting rooms, there are demand controlled ventilation, thus CO_2 concentration is measured. This can be used to estimate the total number of occupants in the meeting rooms.

It is important to be aware that there are some issues with the logging. Firstly, the data set naturally have some holes, i.e. time steps where the occupancy is not logged. The main problem is that these time steps are entirely removed from the data set instead of logged as "not available" or an empty value. The second issue is that the time step is not constantly ten minutes, but for some reason is shifted by a couple of seconds for every other time step. As a result, evaluating the data becomes very time consuming to ensure that the data are interpreted correctly.

In ONV12E, logging of occupancy was started in February 2019, meaning that supplementing measurements were available in the late phase of this Master's thesis. However, the occupancy is only logged whenever a change appears. This irregular logging makes processing the data even more time

consuming. Thus, the results are excluded from this thesis, but are available for further work.

Cell offices

As GKBT comprises of 104 one-man cell offices, the diffusers will give a detailed and accurate presentation of the occupancy in these cell offices even though it is only logged as On/Off. For the cell offices, the occupancy-values are exported from Lindinspect as digital values. Lindinspect gives the data as a continuous series of zeros and ones. Therefore, MatLab is used as a tool to separate this data set into the different weekdays and months of 2018. A quantitative inspection of the data from GKBT showed that there were small to none differences between the different weekdays (Monday-Friday). Therefore, data is analyzed as weekday and weekend averages.

At each time step, the diversity factor is found by adding the occupancy (0 or 1) for each cell office, and dividing on the total number of cell offices. This means that a diversity factor of 1 means that all the 104 cell offices are occupied at the same time, while a diversity factor of 0 means that no one are present.

It is desirable to compare the measured occupancy to findings from the literature review. To realize this, the occupancy has to be converted to W/m^2 which is the standard unit for heat from occupants found in the literature. The average one-man cell office in GKBT is found to be 10.9 m^2. This gives an average of 0.0917 persons/m^2. Assuming light office work (1.2 met$\approx$126 W/person [73]), gives 0.0917 persons/m$^2\cdot$126 W/person=11.56 W/m^2, thus a diversity factor of 1 is defined as 11.56 W/m^2 for occupancy in the cell offices.

Meeting rooms

The case buildings consists of several meeting rooms. Some meeting rooms are excluded because of inconsistencies in the measured data. To make occupancy schedules for the meeting rooms, 12 rooms from GKBT with a total area of 233.9 m^2, ranging from 13.3 m^2 to 41.8 m^2, are studied. Active Lindinvent diffusers are also placed in the meeting rooms, giving an accurate presentation of presence in the rooms. However, as the sensors only logs digital values, they do not give any information about the number of persons present in the rooms. As mentioned, CO_2 concentration, as well as air flow rates, are measured and logged by the Lindinvent diffusers. This means that the number of persons present can be estimated by performing a mass balance calculation on each room. The method of estimating occupancy by the CO_2 mass balance is studied in detail by Ansanay-Alex (2013)[74]. The mass balance for a pollutant in a ventilated room is presented in equation 3.1 [75]. It is assumed that the the air is fully mixed, so that the pollution concentration in the room is uniform and equal to the concentration in the return air.

$$V\frac{dC_r}{dt} = C_s \cdot \dot{V}_s + \dot{M} - C_r \cdot \dot{V}_r \tag{3.1}$$

Where

V	=	Room volume [m^3],
$\frac{dC_r}{dt}$	=	Accumulation of pollutants in the room [µg/h],
C_s	=	Pollutant concentration in supply air [µg/m^3],
$\dot{V}_s$	=	Supply air flow [m^3/h],
$\dot{M}$	=	Pollutant strength [m^3/h],
C_r	=	Pollutant concentration in return air [µg/m^3],
$\dot{V}_r$	=	Return air flow [m^3/h].

$$\dot{M} = n \cdot \dot{V}_{occu} \tag{3.2}$$

The pollution strength, $\dot{M}$, is estimated as a function of number of persons, n, and CO_2 generation rate per person, $\dot{V}_{occu}$. A study by Persily and deJonge (2017) estimates $\dot{V}_{occu}$=4.8 mL/s.[76]

$$\frac{dC_r}{dt} \approx \frac{[C_r]^{n+1} - [C_r]^n}{\Delta t} \tag{3.3}$$

By discretizing the continuous equation, the accumulation of pollutants can be expressed as in equation 3.3, where $[C_r]^{n+1}$ is the concentration in the next time step, $[C_r]^n$ is the concentration in the current time step, and Δt is the length of each time step in seconds. For this case, the time step is 10 min., i.e. 600 s. Further, it is assumed balanced ventilation, so that $\dot{V}_r = \dot{V}_s$. Rearranging equation 3.1, converting the units to better fit the measurements (assuming ideal gas at 1 atm and 25°C), and combining 3.2 with 3.3 results in equation 3.4.

$$n = \frac{1}{\dot{V}_{occu}}(V \cdot \frac{[C_r]^{n+1} - [C_r]^n}{\Delta t} - 0.001 \cdot \dot{V}_s(C_s - C_r)) \tag{3.4}$$

Where

n	=	Number of occupants,
$\dot{V}_{occu}$	=	CO_2 generation rate per person [mL/s],
V	=	Room volume [m^3],
$[C_r]^{n+1}$	=	CO_2 concentration in next time step [ppm],
$[C_r]^n$	=	CO_2 concentration in current time step [ppm]
dt	=	Time step [s],
$\dot{V}_s$	=	Supply air flow [L/s],
C_s	=	CO_2 Concentration in supply air [ppm],
C_r	=	CO_2 Concentration in return air [ppm].

A challenge of using this method is that the CO_2-concentration in the supply air is not measured. Another challenge is that quantitative studies of the measured data suggests that the diffuser's CO_2 meter is not

properly calibrated. To deal with these challenges, the lowest measured concentration outside occupied hours is studied. It is assumed that the lowest measured concentration of CO_2 in each room is the same concentration as in the supply air at all times. This assumption involves the assumption that the CO_2-concentration outside the building is constant. Even though these assumptions will not give the real CO_2-concentration, they can be used to describe the changes due to occupancy.

After implementing these calculations in Excel, the data is exported to MatLab for processing. When studying the resulting diversity factors for meeting rooms, a diversity factor of 1 is the highest occupancy that occurred simultaneously in the measured time period (2018-01-01 to 2018-12-31), not to be confused with fully occupied for the cell offices.

3.3.2 Lighting and technical equipment

In both GKBT and ONV12E, electricity to lighting and technical equipment is logged separately every hour. In GKBT, each floor has a number of energy meters that each hour logs the energy consumption (kWh) in the previous hour. This is the equivalent to the average power consumption (kW) in the previous hour. In ONV12E the current meter reading is logged hourly, giving accumulated values for kWh used. Here, the slope of the accumulation is used to describe the average power consumption (kW) for each hour.

Each electricity meter logs the consumption for a specific part of the building, so that the power consumption given by each meter can be presented as power per floor area (W/m^2). A diversity factor of 1 is here defined as the highest power intensity per floor area measured by a single electricity meter. Further, the area weighted average of all electricity meters is divided by the highest intensity found for a single electricity meter, giving the diversity factor. Thus, the buildings are evaluated separately, split into diversity factors for lighting and for technical equipment.

In HENT, the total electricity for both lighting and technical equipment are logged as one. The total electricity is logged in the same manner as in GKBT, i.e. the average power consumption in the previous hour. Even though HENT will not give details about lighting and technical equipment separately, it can be useful to see if the same trends can be found in this building. For GKBT and ONV12E, the total electricity is therefore found by adding the electricity used by lighting and technical equipment. The energy meters for technical equipment and lighting in each specific part of the buildings are added and divided by the floor area. Again, the highest intensity defines the diversity factor of 1. HENT can be said to be more of a multipurpose building than GKBT and ONV12E. To ensure a good basis for comparison, only electricity consumption to the office part in HENT is included.

STG logs the total electricity use in the same manner as in HENT, with one electricity meter per tenant. However, the tenants have been switched out and moved around, as the building is rather new. In addition,

the electricity meters have been faulty a couple of times over longer time periods, giving hiccups and overshoots in the measurements. STG is therefore excluded completely when studying internal loads, as the quality of the data is considered too low.

3.4 Measurements from the building management systems

Power measurements from each building's BMS is used to find the actual heat load required by the buildings, and to compare this to the installed heating capacities. Note that the power measurements are consumption per hour (kWh/h), giving average power consumption for each hour.

The measurement equipment in STG were faulty a period during the summer of 2018, resulting in little to no measurements during the cooling season. However, as cooling is not of interest in this thesis, it is not considered to be a problem. Since the heating demand is quite small in this period, the missing measurements are filled by linear interpolation. This is to consider temperature independent heating such as DHW. Note that the interpolated values are used only when actual measurements are missing.

Scatter plots

To further investigate the installed power compared to measured data, scatter plots for each of the buildings are created. Firstly, the hour in which the peak heat load occurs are found from the measured data for each buildings. Then, the measured power for each day in this hour is plotted in relation to the average outdoor dry bulb temperature in the previous twenty-four hours. It is shown that there should be a good correlation between power consumption and outdoor temperature for the previous day. In this way, the relation between temperature and power can be estimated by a linearization of the measured data.[77]

The aim of this method is to estimate what the peak power would be at the design outdoor temperature for the actual building, based on measurements. This estimation should provide insight in the net power consumption for space heating at design conditions. Further, this can be used to suggest how large the heat pumps should be if only power coverage is considered, in hindsight. Installed heat pump capacity (heating mode) and total installed space heating capacity is also included in the figures for comparison.

As four different buildings are evaluated, the available data is different for each building. Therefore, the plotted data is taken from different time periods. For GKBT, ONV12E, and STG, the measurements are from 2018-01-01 to 2018-12-31, while for HENT the measured time period 2018-03-26 to 2019-03-25. Temperatures are given by Eklima[78] for Voll Weather station.

3.5 Weather data

In order to perform tests on the case buildings, actual weather data is needed. This weather data can be used to study how the heating system would have worked in the past, and how much of the time an hypothetical undersized heating system would not be able to achieve thermal comfort. A large range of weather data will also give a better picture of how the system works, as TMY and IWEC2 files often represent trends considered as typical, without extremes, the opposite of measured weather data used to create AMY (Actual Meteorological Year) weather files.

In order to have AMYs for several years, the creator of Shiny Weather Data, Ph.D. Lukas Lundström, was contacted. Lundström provided solar radiation data for Trondheim from February 2004 to December 2018 based on data from Copernicus. Hourly values for air temperature, relative humidity, wind speed and direction were extracted from Eklima. According to Lundström, all this data could be compiled into AMY weather files.[79] The missing values are filled by using the same values as the day before. This will affect the quality of the weather files, and will be discussed in chapter 5.4.2. Since the data from 2004 does not include a full year worth of measurements, this year is excluded.

To be able to create *.prn* weather files, the values were placed in an Excel-sheet in the following order: time, air temperature, relative humidity, wind in x-direction (East) , wind in y-direction (North), direct irridiance, and diffuse irridiance. It is important to have enough space between the columns in the Excel sheet, so that the headers does not overlap each other. The weather file is finalized by saving the sheet in the format *.prn*, which can directly be imported in IDA ICE. An example of such a weather file can be seen in figure 3.9.

# Time	Tair	RelHum	WindX	WindY	IDirNorm	IDiffHor
0	17.6	64	-0.88	-1.46	0	0
1	16.3	74	-1.11	-1.42	0	0
2	15.5	78	-0.71	-1.76	0	0
3	14.7	81	-0.78	-0.78	0	0.47
4	14.5	82	-0.46	-0.53	0	6.33
5	14.9	79	-1.11	-1	20.23	49.67
6	17	70	-0.7	-0.57	261.37	87.61
7	18.9	66	-0.43	0.42	481.99	103.83
8	18.3	77	0.47	1.63	374.2	149.72
9	19.8	71	0.51	1.2	362	239.16
10	20.3	70	0.49	1.84	380.76	285.6
11	21.8	58	0.61	1.37	492.47	272.22
12	23.6	51	0.46	1.43	652.25	200.04
13	23.9	53	1.08	1.8	655.07	202.83
14	24	48	-0.24	2.69	352.45	315.96
15	24.3	47	-0.9	2.33	340.09	297.51
16	24	50	-2.02	1.64	381.66	264.27
17	24.1	46	-0.6	2.22	301.44	223.15
18	22.9	51	-2.26	1.97	132.85	172.06
19	22.9	46	-1.94	1.57	126.97	124.5
20	21.9	47	-2.41	-1.23	173.6	83.64
21	20.1	59	-1.64	-1.76	8.16	42.25
22	18.2	65	-1.54	-1.71	0	5.61
23	16.9	68	-0.8	-1.5	0	0.3
24	16.1	73	-0.39	-2.47	0	0

Figure 3.9: Example of *.prn* weather file used in IDA ICE.

3.6 Periodic penetration depth in IDA ICE

To validate how IDA ICE treats periodic penetration depth (see chapter 2.4.5), a model similar to the model in the study *What is the effective thickness of thermally activated concrete slab?* [44] was created (figure 3.10), assisted by Mika Vuolle (EQUA). Object 1 is the source file, a weather file that represents air temperature based on a sine function that varies between 20 and 26 °C with 24 h periods. Object 2 is a mathematical model that splits temperature/power links into one-variable links. Object 3 is a mathematical model for an envelope surface that is not exposed to solar radiation. In the third object, the surface area is specified as 1 m^2, and the U-value is specified to 8 W/(m^2K) as in the aforementioned study. Object 4 is a mathematical model of a multi-layer component that represent the material in the wall. In this validation it chosen to only simulate one layer of concrete. In this layer, it is placed 100 cells to log the temperature at different depths in the concrete with a high resolution. Object 4 is connected to the source file on both sides, meaning that both sides will be subjected to the same temperature variations.

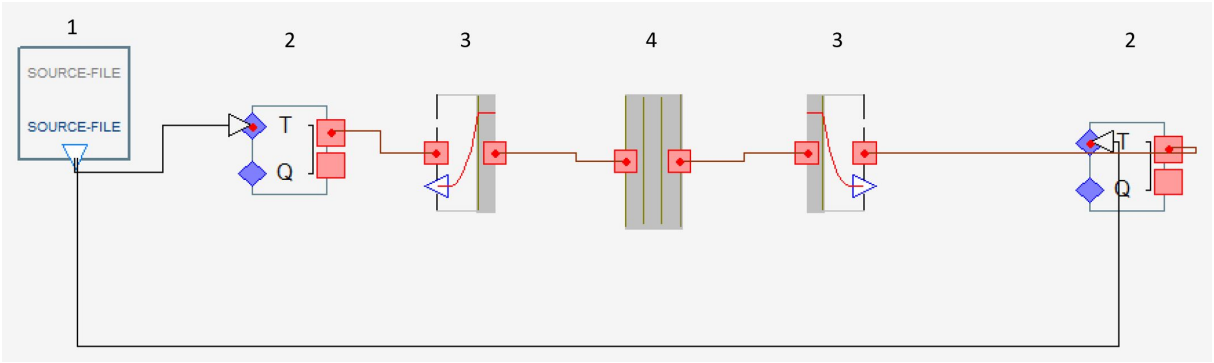

Figure 3.10: Mathematical model of a concrete wall subjected to fluctuating air temperature.

3.7 Peak heat load calculations based on the building time constant

When performing heat load calculations, one of the main parameters used is DOT, commonly the lowest 3-day average temperature. However, as elaborated in the literature review, a wrong DOT can be a cause for overestimating of the peak heat load. To reduce the gap between calculated and actual heat load, FEBY12 proposes to relate DOT to the building time constant (τ) (see chapter 2.4.6).

Based on this, it is of interest to calculate the resulting peak heat load if the DOT is based on τ in stead for the more commonly used lowest 3-day average temperature. It is also relevant to check whether or not this peak load will be sufficient to keep the thermal environment satisfactory. In order to evaluate the peak heat load and thermal performance of the test buildings, the following procedure is suggested and tested:

1. Conduct a step response
2. Find the building time constant (τ)
3. Find n-day average temperature based on τ
4. Perform heat load calculations with the found temperature
5. Limit the heating power in each zone
6. Checking unmet hours for the last fourteen years, regarding indoor temperature

Each step is further elaborated in the following chapters 3.7.1-3.7.6.

3.7.1 Conduct a step response

A weather file with fixed temperature of 0 °C, without solar radiation and average wind conditions is used to give constant outdoor boundary conditions. Solar radiation is excluded as this is often excluded in heat load calculations (see chapter 2.3.4). Internal gains are also excluded as there are large uncertainties about the duration and magnitude, and as these are often excluded from heat load calculations as well. Heat recovery in the AHU is included, as this will limit the ventilation losses and thereby affects the time constant. The supply air temperature is set to match the heating set-point temperature in order to use the full capacity of the heat recovery. The fan schedule is set to 80 % of max capacity to consider VAV, and the fans are set to "Always on" in order to make the losses in the step response more constant. All heating and cooling in the AHU is excluded, including the temperature increase in fans. All heating is provided by ideal heaters. The ideal heaters' controllers are used to conduct the step response by choosing the heating set-point temperature to be 21.5 °C until 1. April. Afterwards, all heaters are turned off (set to 0 °C) and the indoor temperature starts to decrease.

Note that the thickness of the internal slabs should be limited when performing a step response. This is due to the penetration depth (see chapter 2.4.5), since the period of the step response is long enough to utilize more thermal mass than what would be the case for day-to-day fluctuations. To limit the risk of too much thermal mass being considered when calculating the time constant, the thickness of solid concrete slabs are limited to 300 mm, as this gives 150 mm to each of the adjacent zones. 150 mm is the periodic penetration depth of concrete during a 24 hour time span [37, 44]. However, for GKBT, ONV12E, and HENT, hollow core concrete slabs are used. Since most of the concrete in hollow core slabs is close to the surface, the core containing large air gaps, the thickness will not be limited for these buildings.

3.7.2 Find the building time constant

After conducting a step response, the zone with the fastest decreasing temperature is chosen, so that the time constant is based on the temperature development in the worst performing zone, ensuring enough power for the other zones. Only zones that corresponds to primary areas are considered. The air temperature in this zone is extracted to find at what time 63.2 % of the temperature drop (from 21.5 °C to 0 °C) has occurred (see chapter 2.4.5). Thus, in this step response, the time constant is equal to the time it takes for the indoor temperature to drop to 7.9 °C.

The zone with the lowest time constant is used for defining the building time constant. This reduces the risk of choosing a too high design outdoor temperature, resulting in to small heating system. The worst zone would normally be the zone with largest external surface area compared to volume, as this gives the largest transmission losses and faster decreasing temperatures.

3.7.3 Find n-day average temperature based on the time constant

As explained in chapter 2.4.6 and FEBY12, the design outdoor temperature can be found based on the time constant. As an example, if τ is equal to 5 days, the lowest 5-day average temperature can be used as DOT.[46] It is used an accuracy of one decimal, and the n-day average temperature is interpolated. For example, if the time constant is 6.3 days, the temperature is interpolated between the 6- and 7-day average.

3.7.4 Perform heat load calculations with the found temperature

When the time constant is found and the new n-day temperature is chosen, a heating load simulation can be performed to size the heating system. The BEM input values are changed back to original, as stated in the tables 3.3 - 3.6. However, the ventilation schedule is set to constant 80 % to avoid peak loads at ventilation start up. Internal gains are excluded. The found temperature is set as a fixed temperature in IDA ICE's heating load simulation, which makes the software perform a steady-state simulation similar to the calculation method given in the standard NS 12831 (see chapter 2.3.4).

3.7.5 Limit the heating power in each zone

After conducting the heating load simulation, limitations are put in the ideal heaters for each zones. *Local heating units* are read from the heating load simulation results, and will be the limiting power in each zone. The value for local heating units are used since it expresses the heat that is supplied to each zone at the time of maximum total heat supply, thus simultaneity is considered.

3.7.6 Checking unmet hours

After limiting the heating power of the ideal heaters in every zone based on the heating load simulation, energy simulations are conducted with AMY weather files from 2005 to 2018. The ventilation schedules are changed back to the original stated in the tables 3.3 - 3.6, as the ventilation losses will decrease during unoccupied hours and the heating system will transfer potential excess heat into the thermal mass. Additionally, the temperature increase in the fans is changed back to 1 °C in order to get more realistic AHUs. The energy simulation is used, as it is a dynamic simulation where the building's thermal mass will be considered. Internal gains are still excluded from the simulations.

From the energy simulation results, number of unmet hours can be read. This expresses how many hours the indoor air temperature is lower than the heating set-point temperature with a certain number of degrees. As the temperature has to drop for the stored energy in the thermal mass to be utilized, it is decided to define unmet hours as the time the indoor air temperature is more than 1 °C lower than the heating set-point temperature. This is based on maximum recommended temperature fluctuations in a Category A indoor environment from ISO 7730, see table 2.6.

3.8 Dynamic heat load with internal gains from standards

3.8.1 Without solar radiation

Dynamic heat load calculations with different amounts of internal gains are conducted to study how user behaviour affect the calculated heat load. Including internal gains means that values and schedules for occupancy, lighting, and technical equipment has to be chosen. However, as there are many different standards and measurements that can be used as inputs, these should be chosen with caution as they can impact the resulting heat load.

Lighting and technical equipment from NS 3701 are used as these represents new and more energy efficient equipment that are often found in newer buildings like the case buildings. Occupancy from TS 3031 is used, as it has a more dynamic schedule than found in NS 3701. It should be mentioned that it is decided to use these input values after comparing the different standards to measured internal gains in chapter 4.1. The percentage of internal gains is gradually increased from 0 % to 100 %, increasing by 25 % for each step. The weekends are not separated, thus the simulation is run with seven working days a week. This is to ensure that the effect of internal gains is included even if the simulated peak load should occur during the weekend, even though this would not be the real case.

The weather file used for dynamic heating load simulations is based on actual weather data collected for the period from summer 2009 to summer 2010, as this includes the design period for Trondheim. Solar

radiation is excluded as this is not typically included in sizing procedures 2.3.4.

It was found that excluding heating of ventilation air in the AHU results in large peaks in the space heating system, as this will give rapid changes in the air temperature. As the simulations are run with unlimited ideal heaters, they will provide the required power instantly, giving unrealistically large peaks. To avoid this, the air is heated to 17 °C in the AHU. The heat is provided from a heating coil with efficiency of 100 %. Additionally, the heat exchanger in the AHU is assumed to be able to run regardless of the outdoor temperature, as all the buildings are equipped with rotary heat exchangers, in which frost formation is not considered to be a problem during normal conditions. The schedule used in the AHUs are the same as stated in the tables 3.3 - 3.6.

3.8.2 With solar radiation

Neither internal gains nor solar radiation are commonly included in standard design procedures in Norway. In the previous chapter, it is explained how the effects of internal gains are studied. In the same way, it is interesting to study the effect of solar radiation. Thus, the effect of including solar radiations in the dynamic heating load calculations is studied. The same method as described in the previous chapter is used- the main difference being that solar radiations based on measurements from Copernicus are included in the weather file.

3.9 Dynamic heat load calculations with measured internal gains

Finally, a dynamic heating load simulation is perform in order to validate the BEM of GKBT and the weather files created during this thesis. Calibrating models in IDA ICE is beyond the scope of this work, however it is interesting to briefly conduct a simulation to get an estimation of how valid the BEM is. All BEMs and all the weather files are constructed in similar ways, with the same logic and arguments. Thus, a simple validation can be used to roughly estimate the accuracy of this work.

By implementing the measured internal gains and using the weather file for 2018, a heating load calculation of GKBT is compared to measured data from the same year. Heating of the parking garage, snow melting system and the technical room are excluded from both the BEM and the measured heating load. The BEM is the same as stated in table 3.3. However, as stated above, measured internal gains are used. The measured internal gains used in this simulation is presented in the next chapter; in figure 4.1, 4.6, and 4.10 for occupancy, lighting, and technical equipment respectively.

Chapter 4

Results

In this chapter, the main results and findings will be presented.

4.1 Measured internal gains

4.1.1 Occupancy

Measured occupancy is plotted for each weekday day of 2018 and presented as thin black lines. Every time there is an overlap between days the area gets darker, representing the trends and expected occupancy. For the purpose of describing these results, occupied hours are defined as the period where the diversity factor exceeds 0.10.

The red line presents the annual average for each time step, while the red dashed lines presents the standard deviation (SD). As can be seen in figure 4.1, the red line is $\sim$0.05 below the darkest trend area. This is due to weekdays in holidays, which reduce the annual weekday average. These weekdays are shown as lighter gray lines between $\sim$0.10 and $\sim$0.30. Based on the results in figure 4.1, occupied hours are found to be between approximately 06:30 to 16:30. Between 08:00-11:00 and 12:00-14:30, the average diversity factor is relatively stable at $\sim$0.40, while the standard deviation ranges from $\sim$0.28 to $\sim$0.56. Between 11:00 and 12:00, there is a drop in the occupancy down to $\sim$0.17 most likely to be caused by lunch break. During weekends, the occupancy peaks at $\sim$0.05, which is the reason why it is not plotted in itself, as the occupancy is so low that it will give little to none heat gains.

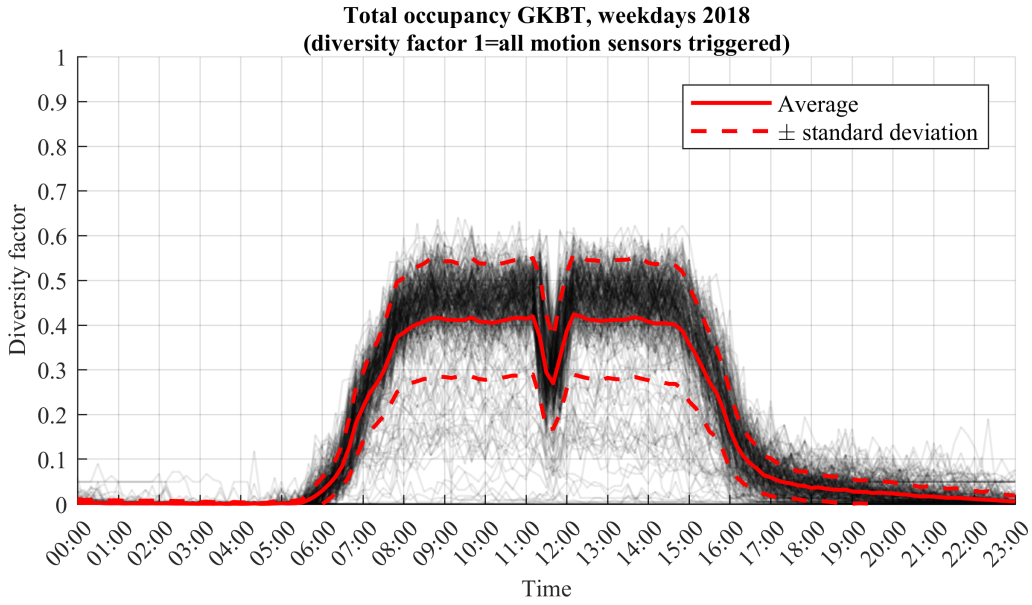

Figure 4.1: Measured total occupancy in GKBT during the weekdays of 2018, where a diversity factor of 1 means that all installed sensors are triggered.

When studying the total occupancy in HENT, see figure 4.2, it can be seen that the occupied hours start at 06:30, the same as in GKBT. However, the occupied hours end at 17:30, making the occupied period one hour longer than in GKBT. The average occupancy is more or less stable at ∼0.55. Compared to GKBT, the magnitude of the lunch break is smaller but the duration is approximately one hour longer. Additionally, it can be seen that between 16:00 and 21:00 there is an significant number of days that is outside the range of the standard deviation, suggesting that people are staying late a substantial number of days in the measured time period.

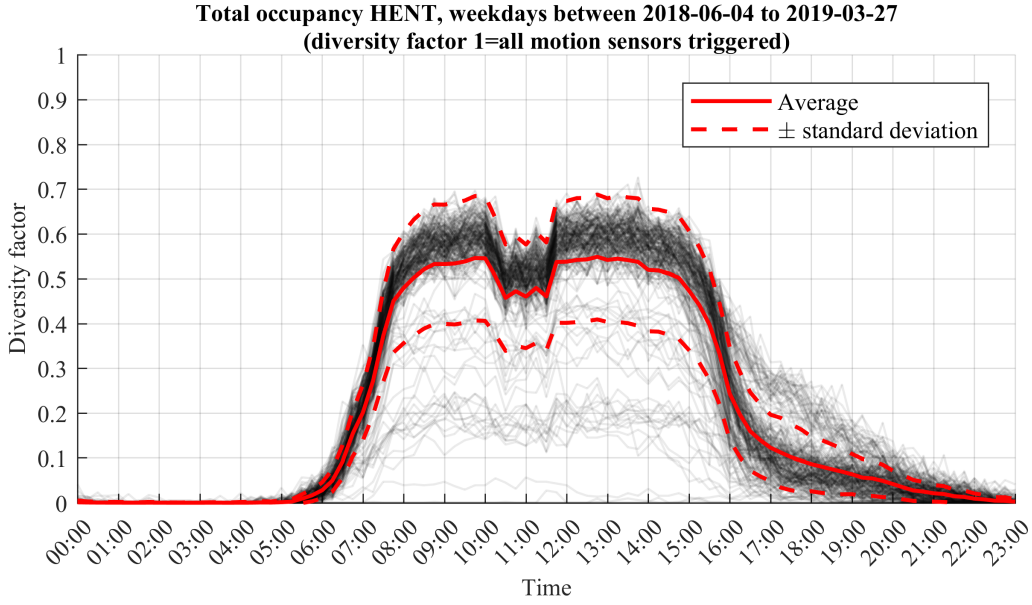

Figure 4.2: Measured total occupancy in HENT during the weekdays of 2018, where a diversity factor of 1 means that all installed sensors are triggered.

In figure 4.3, the diversity factor for occupancy in cell offices in GKBT is studied separately. Whereas the occupied hours are the same as in figure 4.1, the trend shows that the occupancy is marginally higher in the cell offices than for total occupancy.

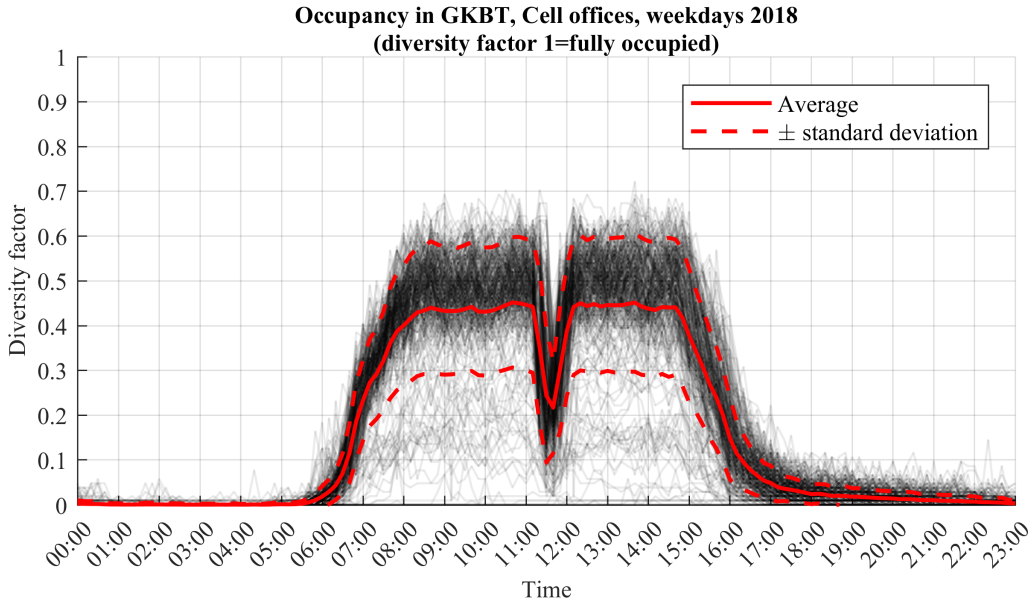

Figure 4.3: Measured occupancy for cell offices in GKBT during the weekdays of 2018, where a diversity factor of 1 means that all the offices are occupied.

By processing the measured data and performing mass balance calculations as described in chapter 3.3.1, the results for occupancy in meeting rooms are finally plotted in figure 4.4. Note that a diversity factor of 1 corresponds to the highest occupancy that occurred simultaneously during the measured time period, as described in chapter 3.3.1. The highest measured occupancy found was 27 persons, yielding 8.7 m^2 per person. The figure tells that the occupancy in meeting rooms are lower and much less predictable than in cell offices. The average occupancy is between $\sim$0.20 and $\sim$0.30, having the same decreasing trend during lunch time as for cell offices. At most, the standard deviation is $\sim$0.20, supporting that the occupancy appears to be more random than in cell offices. It is also shown a somewhat strange trend that there is a diversity factor of $\sim$0.05 during the night. With 12 meeting rooms in the study, this will mathematically mean $\sim$0.6 persons in one of the rooms, which has to be rounded to 1 because of the mass balance performed to achieve these results. This error will be further discussed in the next chapter.

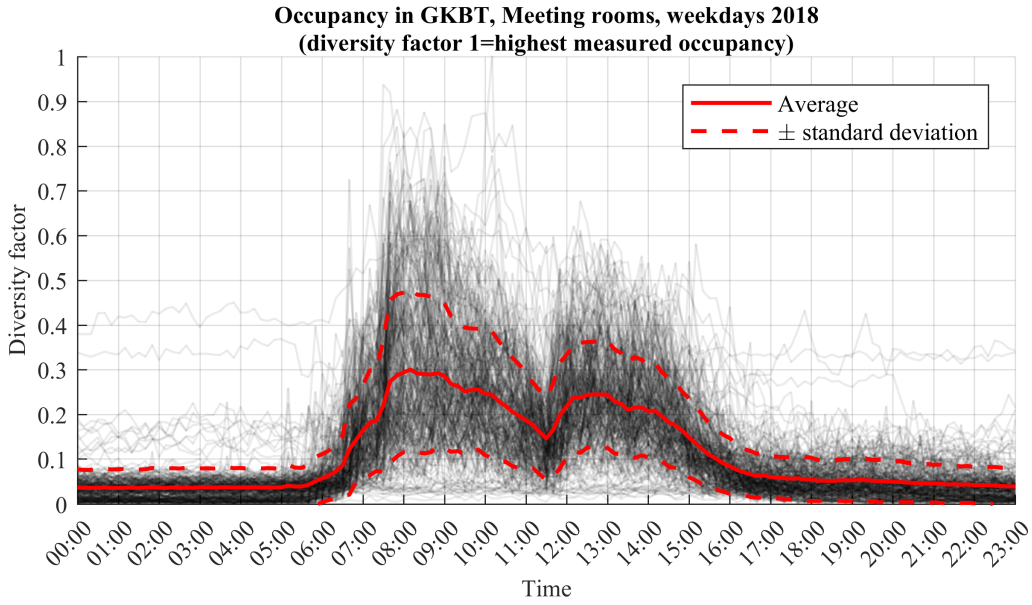

Figure 4.4: Measured occupancy for meeting rooms in GKBT during the weekdays of 2018, where a diversity factor of 1 is the highest measured occupancy (27 persons).

In figure 4.5, the measured total occupancy in GKBT is compared to the most common standards for calculations in Norway, TS 3031, in addition to ISO 17772-1 cell office, and the study of Duarte et al. (2013) which is presented in the literature review. It is noticed that the study of Duarte et al. (2013) is conforming with the measurements during the start-up period, while it exceeds the measured occupied hours in the evening by one hour, with a less prominent but longer lasting lunch break. Note that the lunch break and duration hours in Duarte et al. (2013) bear a resemblance to that of HENT as well, with somewhat longer duration hours and a similar (but shifted) lunch break.

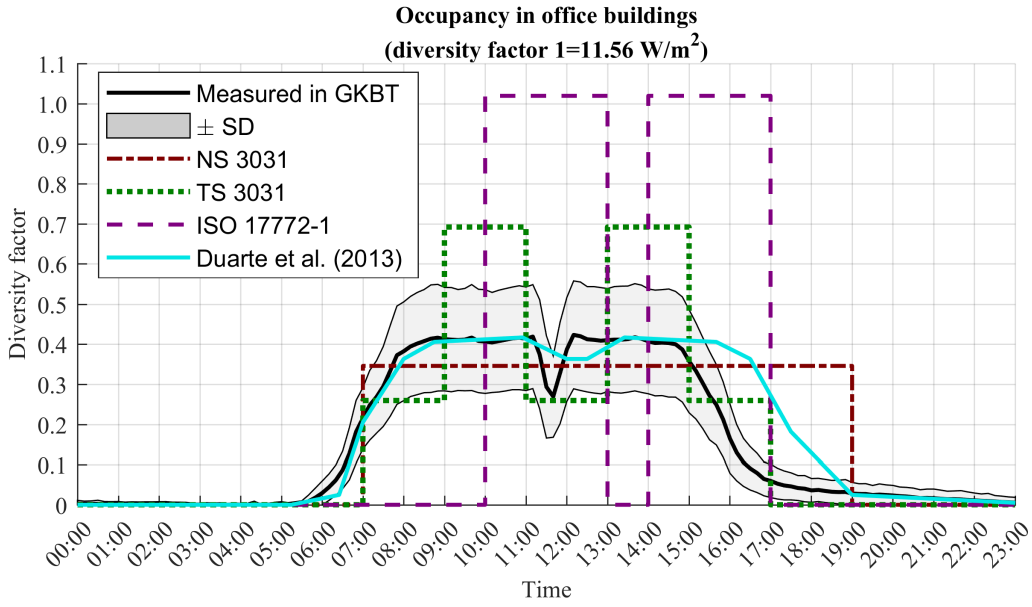

Figure 4.5: Measured total occupancy in GKBT compared to standards and studies, where a diversity factor of 1 corresponds to 11.56 W/m^2.

NS 3031 is the only compared standard with lower occupancy during up-time than what is measured, while this standard also exceeds the occupied hours. On the other hand, TS 3031 conforms better with the measurements, as it is a semi-dynamic step function taking the lunch break into consideration. With reduced peaks and a shortened lunch break, it will coincide quite good with the measurements. Measured occupancy for GKBT is chosen for comparison due to the quality of the measured data. However, when comparing figure 4.1 and 4.2, it is clear that the occupancy in HENT is higher. This would mean that if the occupancy in HENT were plotted in comparison to TS 3031, it would be a closer fit. Small resemblance can be found with ISO 17772-1 cell office, with high peaks, zero occupancy during the lunch break, and shifted by around 3 hours compared to the measurements. The diversity factor for cell offices from ISO 17772-1 is chosen for comparison as GKBT mostly comprises of cell offices. However, the measured total occupancy is found to be better presented by the diversity factor for landscape areas, see figure A.3.

Table 4.1: Summarized findings for occupancy.

	Measured total, GKBT			**NS 3031**	**TS 3031**	**ISO 17772-1**	**Duarte et al. (2013)**
	-SD	**Average**	**+SD**				
Min [W/m^2]	0	0	0	0	0	0	0
Mean [W/m^2]	1.11	1.80	2.49	2.00	2.08	4.00	2.72
Max [W/m^2]	3.34	4.90	6.46	4.00	8.00	11.80	4.82

In table 4.1, the main findings are summarized. Both NS 3031 and TS 3031 are within the range of standard deviation regarding average total occupancy in GKBT, while NS 3031 is the only standard that has its peak within the standard deviation. Duarte et al. (2013) is within the measured range of average and maximum values, while ISO 17772-1 is not within the measured range of average nor max values.

4.1.2 Lighting

For lighting, the highest measured electricity intensity is measured to be 4.24 W/m^2, in GKBT. Electricity to lighting per floor area in GKBT is shown in figure 4.6. Note that the up-time corresponds well to measured total occupancy in GKBT. It can be seen that the lighting is gradually turned on between 06:00 to 09:00, then remains relatively constant at $\sim$0.62 until it starts decreasing from 15:00 and more rapidly from 16:00. Only a slight decrease can be found between 11:00 and 12:00, suggesting that the lunch break has only a minor influence on the electricity consumption for lighting in GKBT. It should be noted that there is a diversity factor of $\sim$0.03 during the night, which can be ascribed to emergency lighting.

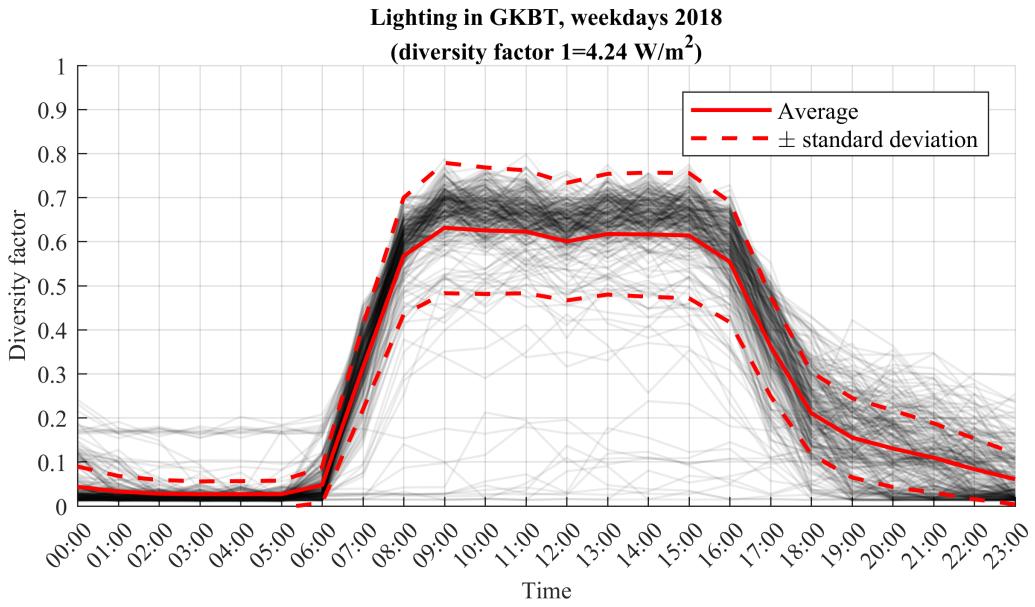

Figure 4.6: Measured electricity consumption for lighting in GKBT during the weekdays of 2018, where a diversity factor of 1 corresponds to 4.24 W/m^2.

For ONV12E, the results regarding measured electricity to lighting is presented in figure 4.7. The lighting increases from 06:00-07:00, and reaches its peak at 10:00 with a diversity factor of ∼0.50. A more prominent decrease down to ∼0.45 can be seen until 13:00 before the diversity factor stabilizes at ∼0.47 until 16:00-17:00.

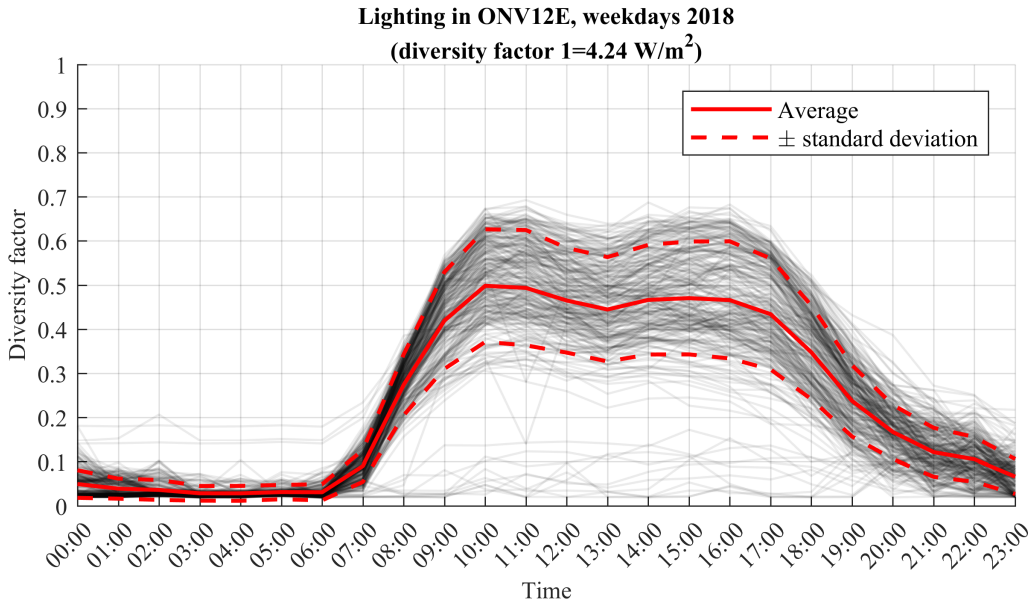

Figure 4.7: Measured electricity consumption for lighting in ONV12E during the weekdays of 2018, where a diversity factor of 1 corresponds to 4.24 W/m^2.

Figure 4.8 compares the measurements from GKBT and ONV12E. Compared to GKBT, the electricity to lighting turns on more gradually in ONV12E. It reaches its peak 10:00, one hour later than GKBT. The

figure gives the impression that the lighting in ONV12E is shifted one hour forward in relation to GKBT. Whereas GKBT peaks at ∼0.64, ONV12E peaks at ∼0.50. It should also be noted that a rather large standard deviation occurs during the occupied hours. When no one are present, electricity consumption to lighting overlaps almost perfectly, suggesting that the same consumption to emergency lighting finds place in both buildings.

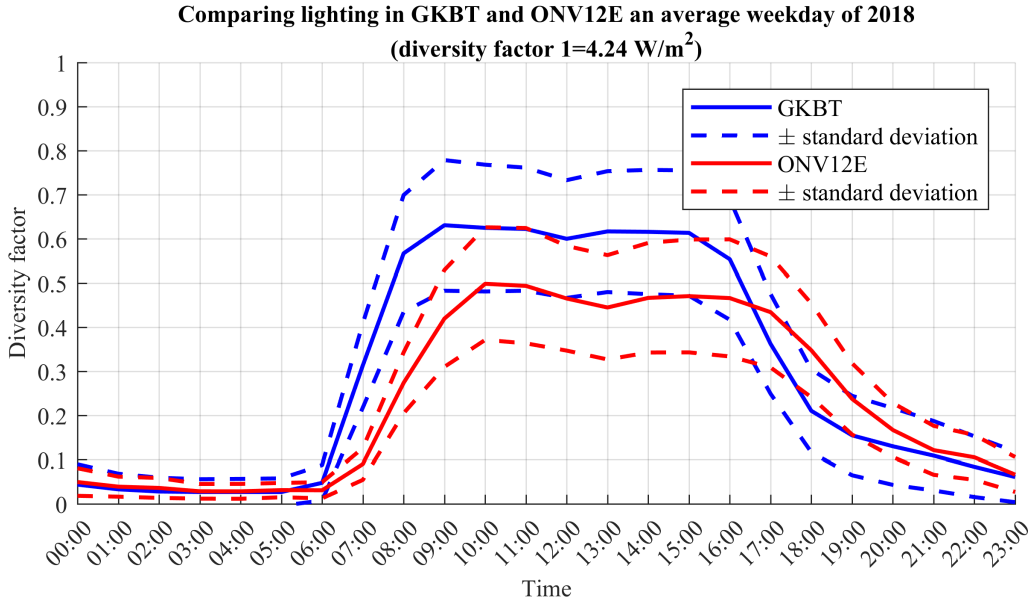

Figure 4.8: Comparison of electricity consumption for lighting in GKBT and ONV12E, where a diversity factor of 1 corresponds to 4.24 W/m^2.

In figure 4.9, measured electricity to lighting is compared to relevant standards. Data from GKBT is used due to the quality and reliability of the data. All evaluated cases have higher peaks than what is measured. NS 3031, TS 3031, and NS 3701 do all propose a realistic start-time for lighting, while the end-time seems to be somewhere between TS 3031 and NS 3031/NS 3701.

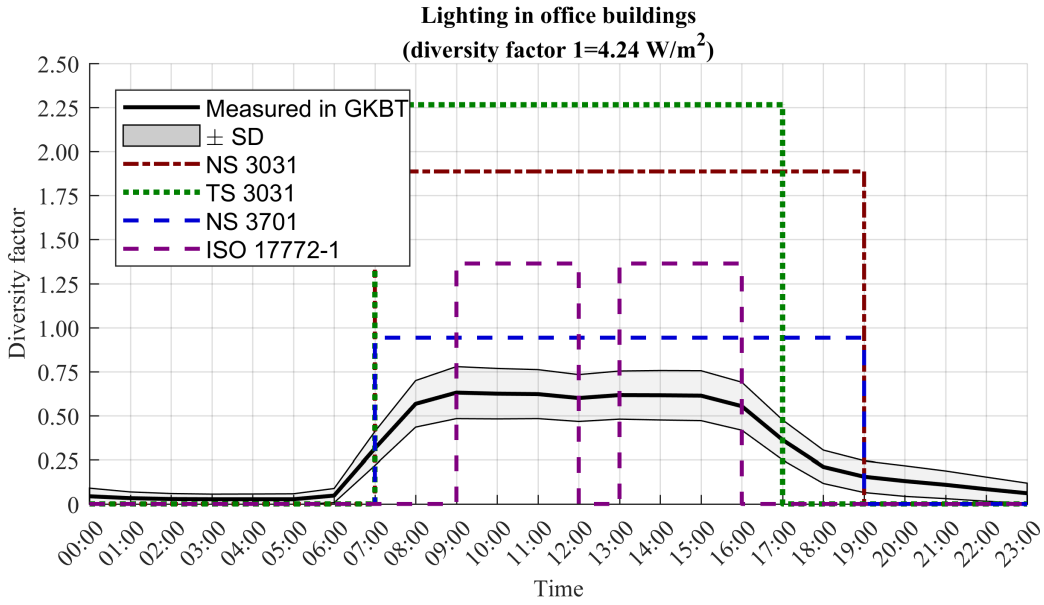

Figure 4.9: Measured electricity consumption for lighting in GKBT compared to standards, where a diversity factor of 1 corresponds to 4.24 W/m^2.

As for occupancy, the diversity factor for cell offices in ISO 17772-1 does not seem to fit the diversity factor for overall electricity consumption for lighting. It should also be noted that for all standards the diversity factors are step functions with either zero or max, which is not the case found from the measurements.

Table 4.2: Summarized findings for lighting.

	Measured, GKBT			NS 3031	TS 3031	NS 3701	ISO 17772-1
	-SD	Average	+SD				
Min [W/m^2]	0	0.13	0.25	0	0	0	0
Mean [W/m^2]	0.89	1.27	1.65	4.00	4.00	2.00	1.44
Max [W/m^2]	2.04	2.67	3.31	8.00	9.62	4.00	5.78

The main findings regarding electricity to lighting are summarized in table 4.8. It is shown that the minimum value should lie somewhere between 0 and 0.25 W/m^2. All standards have a minimum value of 0 W/m^2. Regarding mean values, ISO 17772-1 is the only standard that is within the range of the standard deviation. When assessing the maximum value, all the studied standards overshoot. NS 3701 is closest to the measured peak power, as the max standard deviation is 17.3 % lower than the peak in NS 3701.

4.1.3 Technical equipment

In the same way as for electricity to lighting, electricity to technical equipment is also studied. For GKBT, a brief field study showed that this involves electricity to computers, monitors, projectors, coffee makers, and refrigerators. The standard set-up for a work space in GKBT consists of one laptop, docked to two LED-monitors. For ONV12E and HENT, what kind of electrical equipment that are in use is unknown.

The highest intensity of electricity to technical equipment is higher than for lighting, with a peak intensity of 6.92 W/m^2. In figure 4.10, the diversity factor for technical equipment in GKBT is shown. The diversity factor peaks at ∼0.45, with a standard deviation of ∼0.10. A slight decrease can be seen during the middle of the day, supporting previous findings regarding the lunch break in GKBT. A strong trend shows that the diversity factor is ∼0.25±0.05 outside occupied hours. This suggests that computers and other technical equipment still are supplying a substantial amount of heat outside occupied hours, as it is decreased by only 44 % compared to the average's peak. A light grey area can be seen outside the range of the standard deviation during occupied hours, suggesting that there also is electricity consumption for technical equipment during holidays.

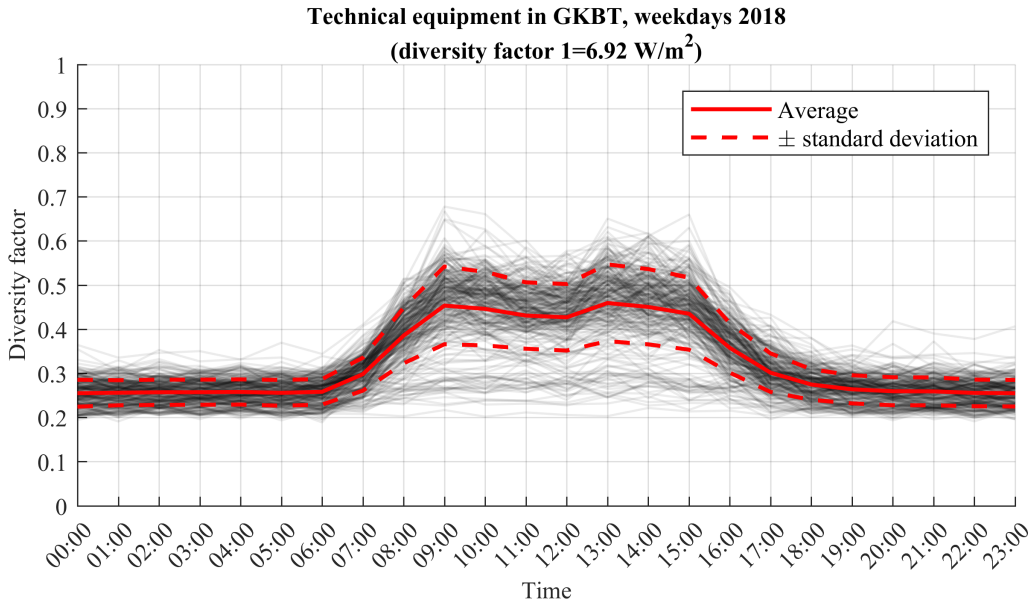

Figure 4.10: Measured electricity consumption for technical equipment in GKBT during the weekdays of 2018, where a diversity factor of 1 corresponds to 6.92 W/m^2.

The diversity factor for technical equipment in ONV12E is shown in figure 4.11. The diversity factor peaks at ∼0.40, with a standard deviation of ∼0.07. Here, the trend shows that the diversity factor is ∼0.20 outside occupied hours, with negligible deviations. This gives an reduction outside occupied hour of 50 % compared to the average's peak. A light grey area can be seen outside the range of the standard deviation during occupied hours, supporting that there is electricity consumption during holidays.

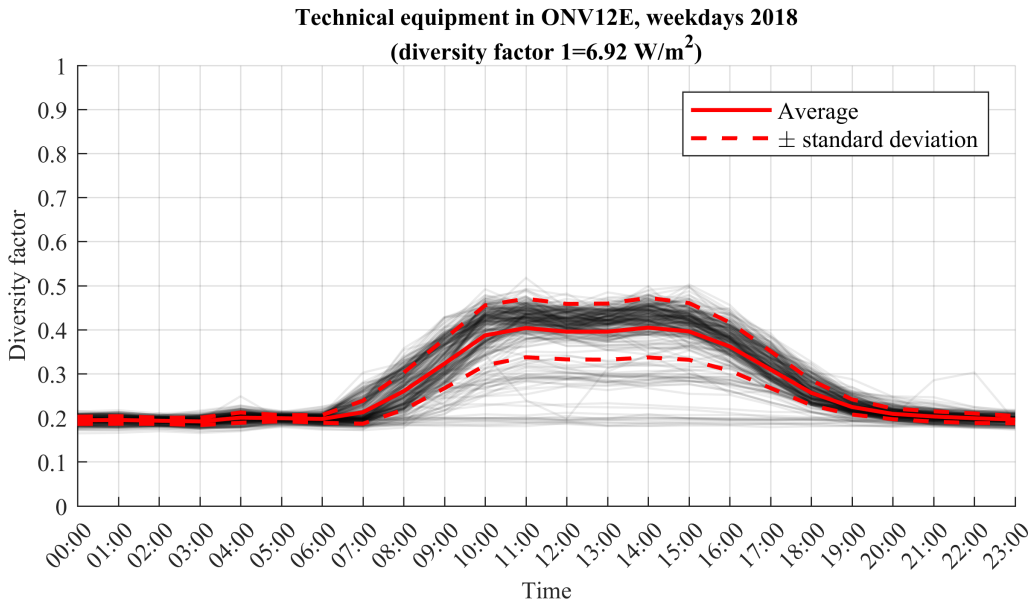

Figure 4.11: Measured electricity consumption for technical equipment in ONV12E during the weekdays of 2018, where a diversity factor of 1 corresponds to 6.92 W/m^2.

Comparing technical equipment in ONV12E to GKBT, see figure 4.12, the diversity factor appears to be ∼0.05 lower for ONV12E overall. The shape is similar, ONV12E shifted one hour forwards with a less prominent lunch break. During most of the occupied hours it should be noticed that GKBT and ONV12E overlaps and are within the range of each other's standard deviation.

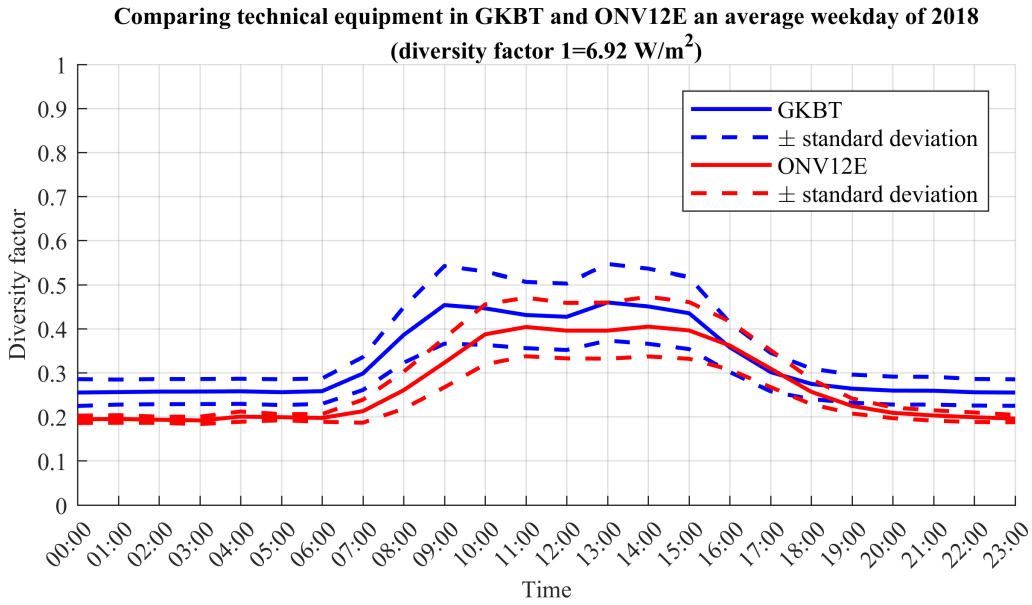

Figure 4.12: Comparison of electricity consumption for lighting in GKBT and ONV, where a diversity factor of 1 corresponds to 6.92 W/m^2.

Comparing measured electricity to technical equipment with other standards and a study, the

measurements are out-powered by the magnitude of the standards, see figure 4.13. Again, GKBT is chosen for comparison due to the quality of the data. All the standards assume zero electricity consumption outside occupied hours, even though this is not what is measured. It is interesting to note that Acker et al. (2012), presented in the literature review, conforms well with GKBT outside occupied hours. At most, TS 3031 peaks at approximately three times higher power than the highest intensity of 6.92 W/m^2 and the lunch break is clearly over-exaggerated. The shape of NS 3031 is somewhat better; more constant during occupied hours, even though the duration hours in TS 3031 seems to be more accurate.

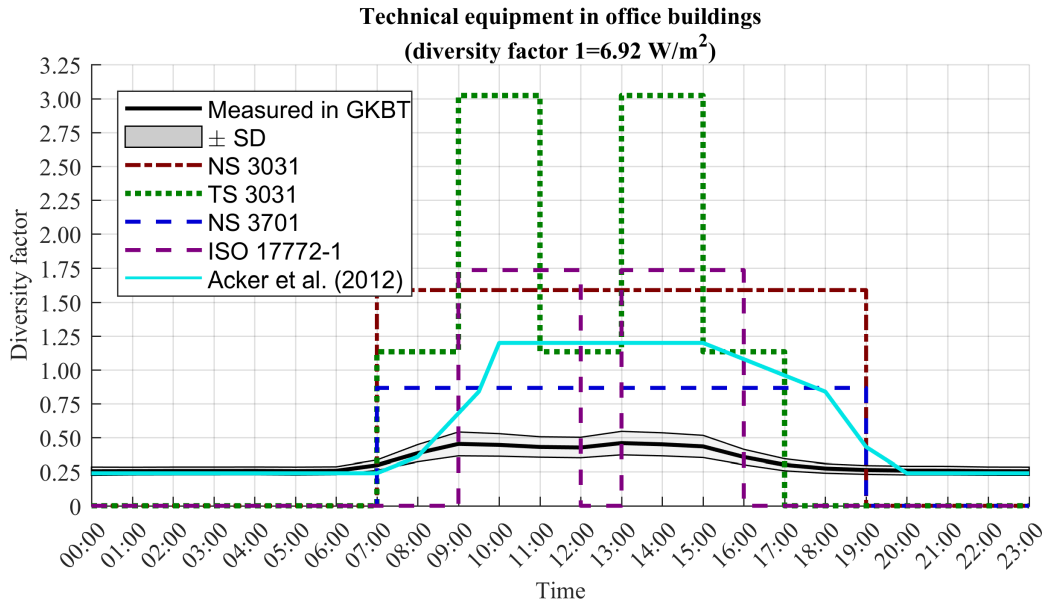

Figure 4.13: Measured electricity consumption for technical equipment in GKBT compared to standards and studies, where a diversity factor of 1 corresponds to 6.92 W/m^2.

Again, the international standard ISO 17772-1 does not fit the measurements. NS 3701 gives a better presentation of the reality, with the lowest peak power. However, the duration is too long. Disregarding the measurements in GKBT, it can be seen that the study of Acker et al. (2012) is somewhere between NS 3031 and NS 3701.

Table 4.3: Summarized findings for technical equipment.

	Measured, GKBT			NS 3031	TS 3031	NS 3701	ISO 17772-1	Acker et al. (2012)
	-SD	Average	+SD					
Min [W/m^2]	1.52	1.73	1.94	0	0	0	0	1.66
Mean [W/m^2]	1.94	2.28	2.56	5.50	5.44	3.00	3.00	4.35
Max [W/m^2]	2.56	3.18	3.53	11.00	20.92	6.00	12.00	8.30

The main findings from figure 4.13 are summarized in table 4.3. Firstly, Regarding the minimum value, Acker et al. (2012) is the only case that do not assume zero consumption outside occupied hours. Thus, Acker et al. (2012) is the only case that is within the range of the standard deviation for the minimum value. Secondly, all cases are outside the measurements regarding the mean values; NS 3701 and ISO 17772-1 being closest to the measured average. Finally, regarding the maximum value, NS 3701 is the best fit being 70 % higher than the maximum upper standard deviation.

4.1.4 Total electricity consumption

Previously, electricity consumption to lighting and technical equipment in GKBT and ONV12E have been studied. In figure 4.14, the total electricity is compared to HENT, as the electricity meters in HENT do not differentiate between technical equipment and lighting.

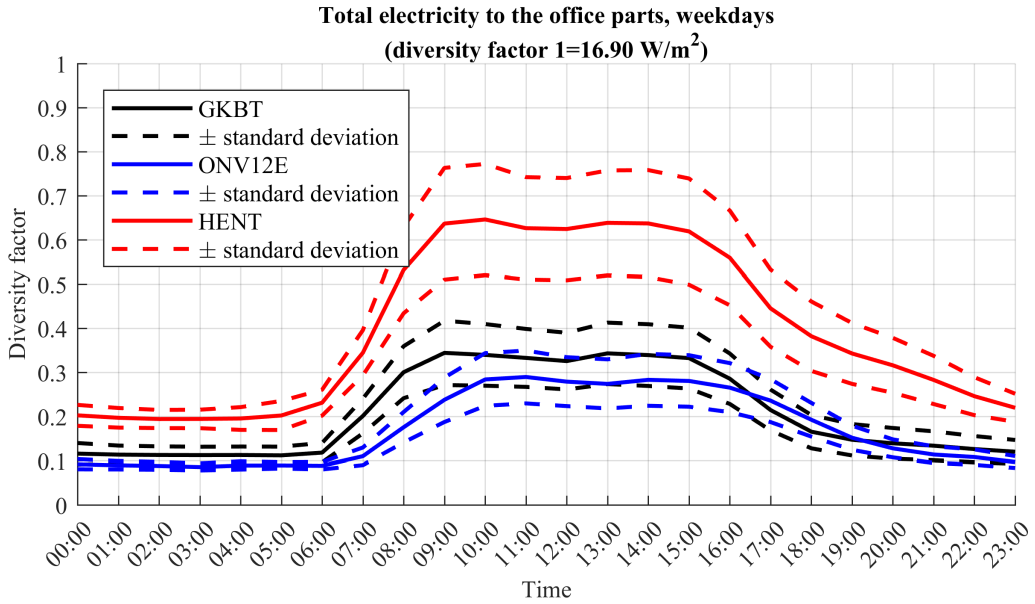

Figure 4.14: Comparison of total electricity consumption to internal gains in the office parts in GKBT, ONV12E, and HENT, where a diversity factor of 1 corresponds to 16.9 W/m^2.

What can be seen in figure 4.14 is mainly that the magnitude of HENT is higher than both GKBT and HENT, with a diversity factor of $\sim$0.66$\pm$ $\sim$0.11. However, the shape conforms well with that of GKBT, while ONV12E is shifted one hour forwards still. It is interesting to see that GKBT and ONV12E conforms well outside occupied hour, while HENT is approximately twice as high.

4.2 Measured power and energy

Heating loads are measured at all the different buildings. The measured heating load consists of heat delivered by heat pump and/or district heating, meaning total heat delivered to the building. The capacities of the heating system are also presented in the figures.

4.2.1 GKBT

In figure 4.15, measurements from GKBT are presented. The measurements are collected for the entire year of 2018. As seen in the figure, the highest amount of heat delivered is 145 kW. The heating capacity of the heat pump is 80 kW, which corresponds to 55 % of the maximum measured heating load during 2018. District heating has a heating capacity of 350 kW, which is 205 kW (141 %) larger than the highest heating load measured. These measurements also include heating of the parking garage, snow melting system, and DHW.

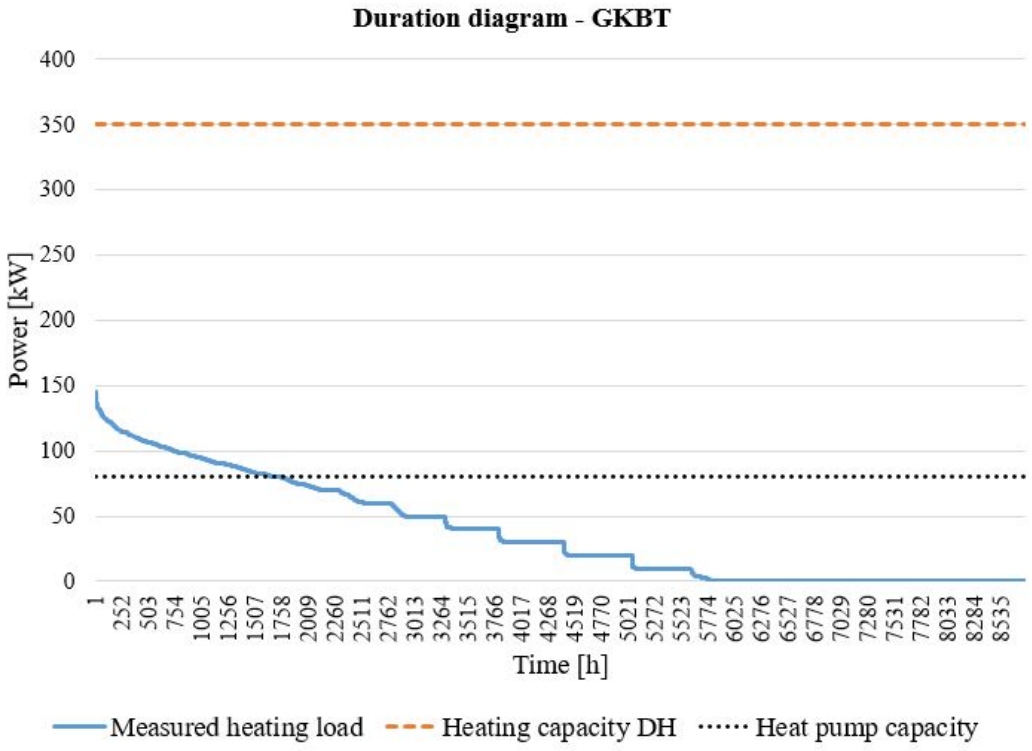

Figure 4.15: Measured heating load from the heating system during 2018 at GKBT.

The peak power occurs in GKBT occurs in the eight hour. In figure 4.16, the heating load for each day of 2018 in the eight hour is plotted with regards to the average outdoor temperature the previous twenty-four hours . The linearization gives that the expected heating load at -19°C should be 141.7 kW. Installed heat pump capacity is as mentioned 80 kW, while the total heating capacity is found to be 350 kW.

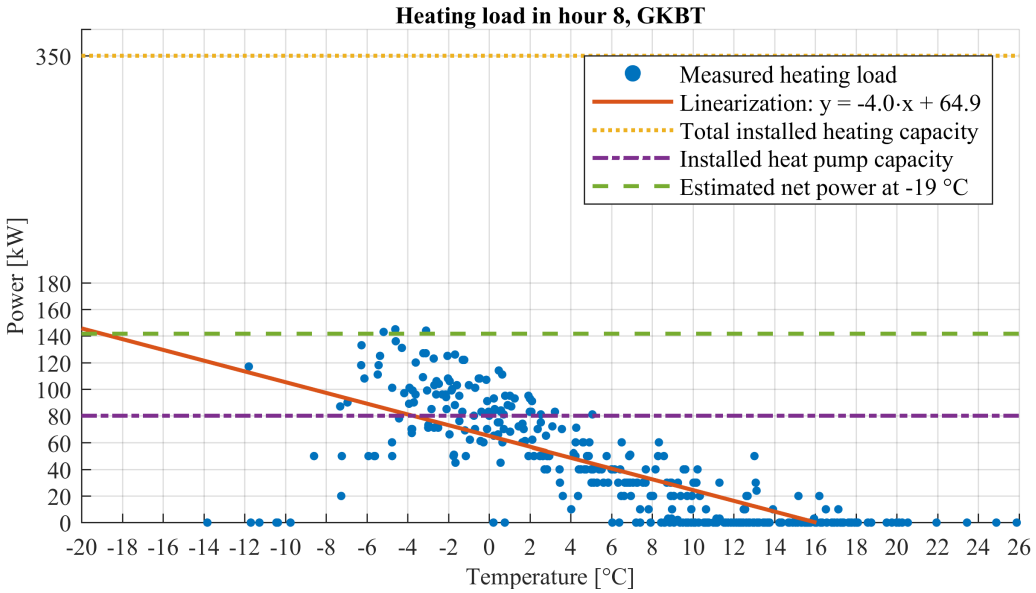

Figure 4.16: Measured space heating load in the 8th hour in GKBT plotted with respect to the average outdoor temperature for the previous 24 hours, compared to installed space heating capacity.

4.2.2 ONV12E

Figure 4.17 presents the duration diagram for ONV12E, based on measurements from 2018. As shown in the figure, the hydronic system in ONV12E is sized for 395 kW, while the heat pump has a heating capacity of 230 kW. The highest amount of heat delivered is 235 kW, which makes the heat pump 5 kW smaller, and the hydronic system 72 % larger than the largest amount of measured heating load during 2018. ONV12E is a part of a ZEN-project, where that surplus heat produced is transferred to ONV12 A-D, and when the heat pump does not deliver enough, heat is transferred from ONV12 A-D to ONV12E. This heat transfer connection is considered in figure 4.17, meaning that the measured heating load shown in the figure is only used at ONV12E. Note that heat delivered to the snow melting system is not considered in these figures (figure 4.17 and 4.18). However, as stated in chapter 3.2.2, the heat pump is sized to cover the total space heating demand and parts of the DHW demand.

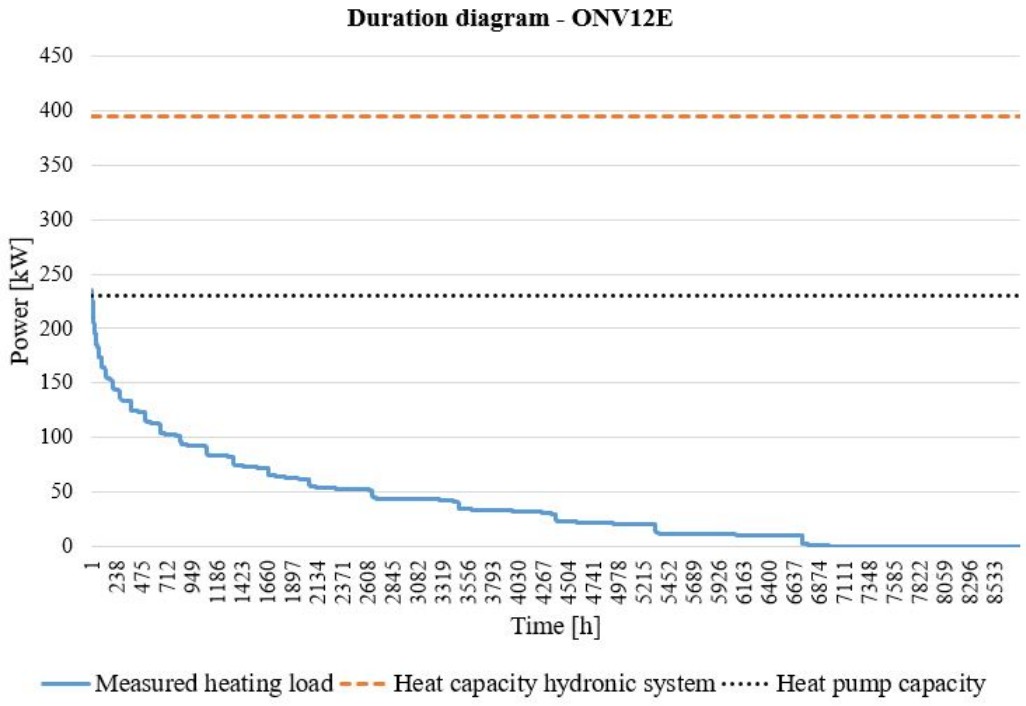

Figure 4.17: Measured heating load from the heating system during 2018 at ONV12E.

The scatter plot in figure 4.18 shows the delivered heating in the ninth hour (the hour in which the peak heating demand occurs). Seemingly, the measurements are more non-linear than for GKBT. The estimated peak heat load at -19 °C is 175.5 kW. However, the figure show that higher heating loads has occured during 2018 than estimated for -19 °C.

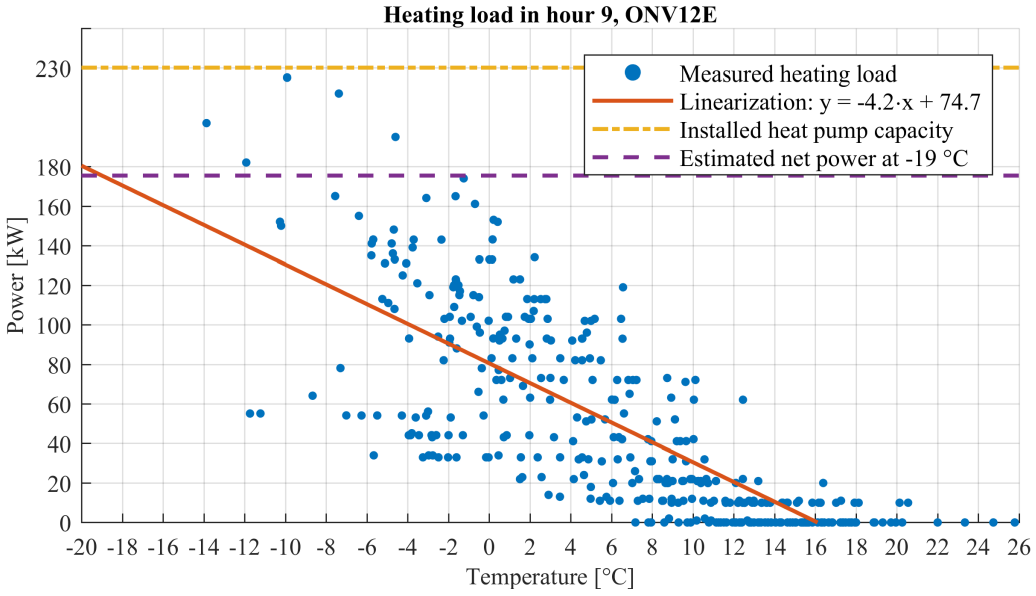

Figure 4.18: Measured space heating load in the 9th hour in ONV12E plotted with respect to the average outdoor temperature for the previous 24 hours, compared to installed space heating capacity.

4.2.3 STG

Figure 4.19 shows the duration diagram from 2018 for STG. Note that the measured heating load in this diagram also include heating of the basement, DHW, and the snow melting system. As seen in the figure, the larges amount of heat delivered is 230 kW, the district heating has a heating capacity of 670 kW, which is 191 % or 440 kW larger than the maximum measured heating load. The heat pump at STG has a heating capacity of 275 kW, which is 20 % larger than the highest amount of heat delivered during 2018.

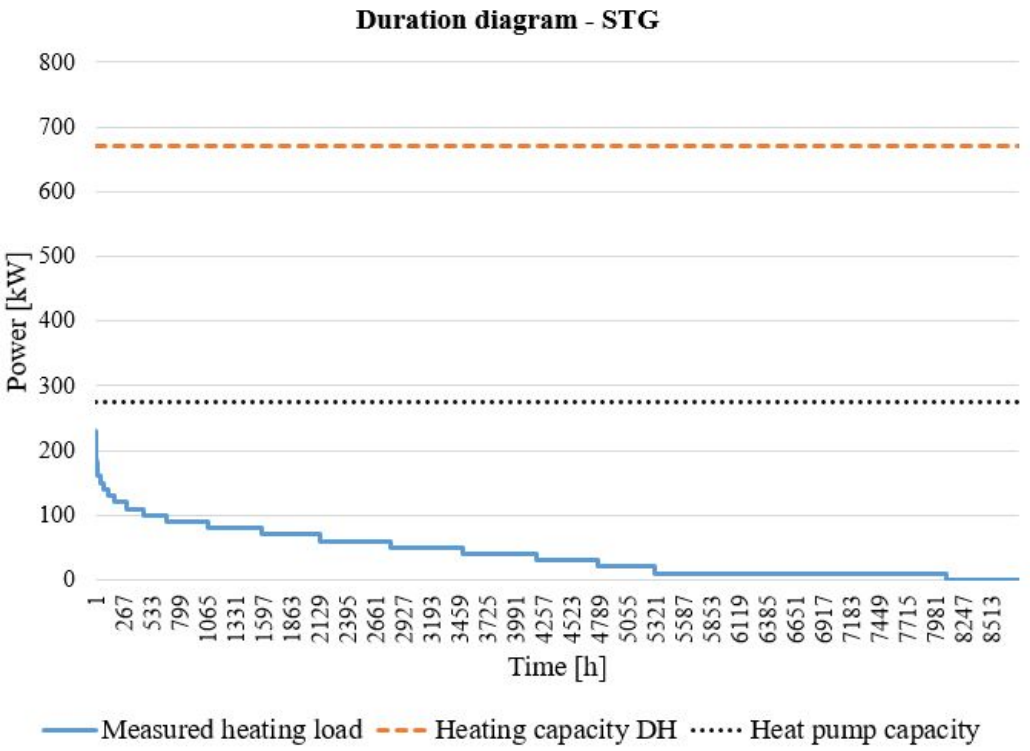

Figure 4.19: Measured heating load from the heating system during 2018 at STG.

The linearized representation of the measured heating load in figure 4.20 yields an estimated space heating load of 141.1 kW at -19°C, being 49 % of the installed heat pump capacity. As for ONV12E, some of the measured heating loads exceed the estimated net peak heat load at -19°C. It can also be noticed that a heating load of 10 kW is measured even for temperatures above 18°C. This can be ascribed to DHW heating.

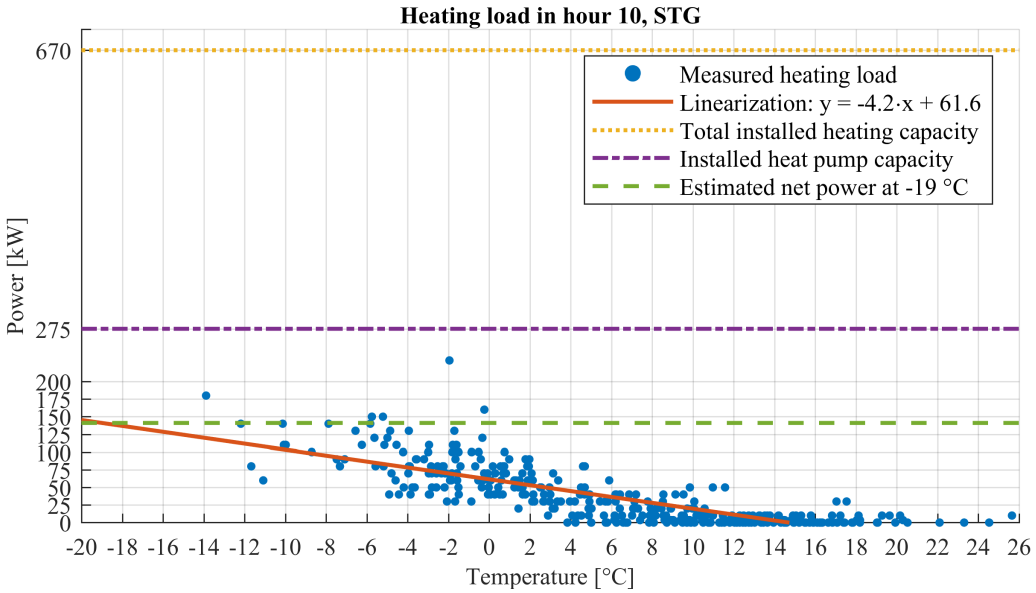

Figure 4.20: Measured space heating load in the 10th hour in STG plotted with respect to the average outdoor temperature for the previous 24 hours, compared to installed space heating capacity.

4.2.4 HENT

Figure 4.21 shows the duration diagram for HENT based on measurements from 2018. The largest amount of heat delivered is 245 kW. The heat pump has a heating capacity of 281 kW, while the district heating provides a space heating capacity of 725 kW and DHW capacity of 250 kW. This makes the heating capacity of the heat pump and district heating 36 kW and 730 kW higher than the measured heating load respectively. Heating of DHW, and the parking garage are included in the measurements.

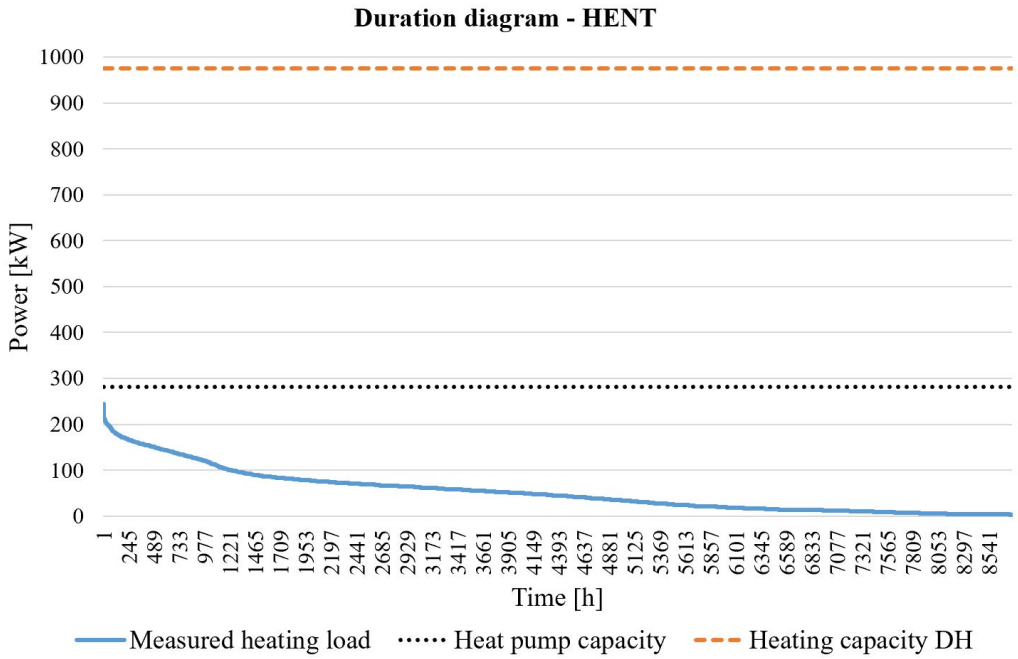

Figure 4.21: Measured heating load from the heating system measured during 2018 at the HENT-building.

The measured heating load has a better linear trend when plotted with regards to temperature for HENT. The linearization yields 203.5 kW at -19 °C. Only one measured point are above this level. As for STG, it is measured heating even for outdoor temperatures above 18 °C, which will contribute to a less steep slope in the linearization. The installed heat pump capacity and the total heating capacity exceed the estimated net power at design conditions by 38 % and 379 % respectively.

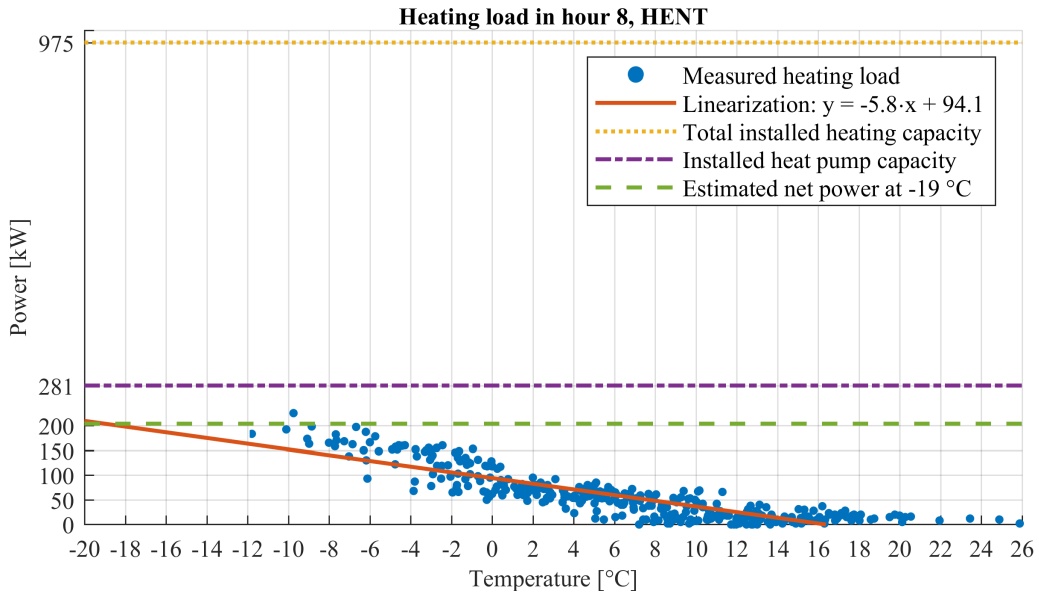

Figure 4.22: Measured space heating load in the 8th hour in HENT plotted with respect to the average outdoor temperature for the previous 24 hours, compared to installed space heating capacity.

4.3 Periodic penetration depth in IDA ICE

In order to validate thermal mass calculations in IDA ICE, as described in the previous chapter, figure 4.23 shows the temperature difference between daily maximum and minimum temperature at different depths in a concrete wall. This figure can be compared to the results in figure 2.16 and table 2.7 to validate how IDA ICE treats periodic penetration depth. Note that both table 2.7 and figure 2.16 concludes that the periodic penetration depth of concrete during a 24 hour period is roughly 15 cm. As shown in the figure, the temperature difference 15 cm in is about 0.7 °C.

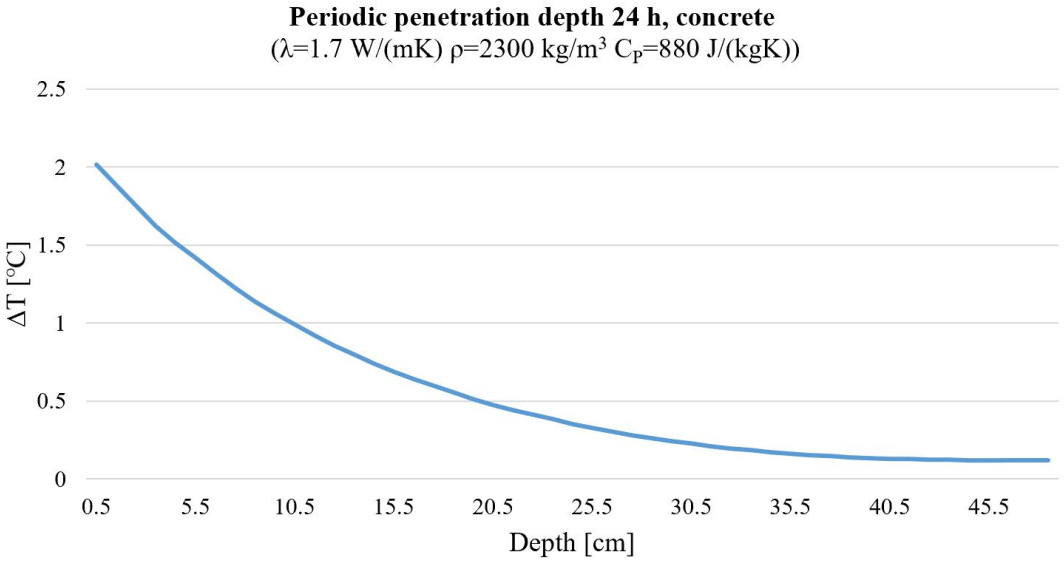

Figure 4.23: Periodic penetration depth for concrete in IDA ICE with the time span of 24 hours.

4.4 Peak heat load calculations based on the building time constant

Table 4.4: Simulated gross space heating load based on the building time constant.

	GKBT	ONV12E	STG	HENT
Worst zone	5th North	4th West	7th North-West	4th South-East
Time constant [days]	6.7	6.7	8.0	6.7
n-day average [°C]	-15.1	-15.1	-13.5	-15.1
Peak heat load DOT at n-day average [kW]	160.8	194.9	273.0	336.7
Peak heat load with DOT of -19 °C [kW]	179.7	219.6	321.7	377.1
Peak heat load reduction [%]	10.5	11.2	15.1	10.7

Table 4.4 presents the different results from τ-based heat load calculations, as described in chapter 3.7. As shown in the table, using this method yields highest reduction in space heating for STG, reduced by

15.1 %, while GKBT achieved the lowest reduction by 10.5 %. The average reduction in calculated peak heat load found by using τ-based n-day average temperature in stead of the commonly used DOT of -19 °C is 11.9 %.

Table 4.5: Minimum temperature and unmet hours for the years 2005-2018 with installed gross power based on the building time constant.

Year	GKBT		ONV12E		STG		HENT	
	T_{min} [°C]	Unmet hours [h]	T_{min} [°C]	Unmet hours [h]	T_{min} [°C]	Unmet hours [h]	T_{min} [°C]	Unmet hours [h]
2005	21.4	0	20.9	0	21.2	0	21.0	0
2006	21.4	0	20.9	0	21.1	0	21.0	0
2007	21.4	0	20.8	0	20.9	0	21.0	0
2008	21.4	0	20.9	0	21.3	0	21.1	0
2009	21.4	0	20.9	0	21.3	0	21.0	0
2010	20.8	0 (17.1)	20.3	6.0	19.9	34.7	20.4	1.8
2011	21.3	0	20.8	0	21.1	0	21.0	0
2012	21.4	0	20.8	0	21.1	0	21.0	0
2013	21.3	0	20.8	0	20.8	0	21.0	0
2014	21.4	0	20.8	0	21.1	0	21.0	0
2015	21.4	0	20.9	0	21.4	0	21.1	0
2016	21.4	0	20.8	0	20.9	0	21.0	0
2017	21.4	0	20.9	0	21.3	0	21.1	0
2018	21.4	0	20.8	0	21.0	0	20.1	0

Table 4.5 shows the number of unmet hours as a consequence of sizing the heating system based on the heating load simulation with τ-based n-day average temperature. As stated previously, the indoor temperature must drop 1 °C below set-point temperature for IDA ICE to count unmet hours. ONV12E, STG, and HENT all experienced unmet hours during 2010, while GKBT had none unmet hours in the primary areas. However it had 17.1 unmet hours in the entrance area. The number of unmet hours occurring during operating hours of the building is not investigated. Table 4.5 also shows that STG achieved the highest amount of unmet hours with 34.7 in addition to the lowest indoor temperature of 19.9 °C. Minimum external temperature for each year, and the external temperature when the minimum indoor temperature occurred, are shown in table A.1 in appendix A.3.

4.5 Dynamic heat load simulations with internal gains from standards

Different amounts of internal gains are tested by dynamic heat load simulations, in order to study how internal gains will affect power need for space heating. The simulation period used is the second half of 2009 and the first half of 2010. The schedule and values for occupancy is taken from TS 3031, while lighting and technical equipment is taken from NS 3701. The method is elaborated in chapter 3.8.

4.5.1 Without solar radiation

Table 4.6: Simulated space heating load with different levels of internal gains (no solar radiation).

Internal gains [%]	Space heating load [kW]			
	GKBT	ONV12E	STG	HENT
0	165.3	242.2	361.5	372.8
25	154.2	226.8	339.7	350.4
50	144.8	210.9	320.3	327.5
75	135.6	197.7	301.6	306.5
100	126.5	184.5	279.9	283.7
Reduction in space heating load (from 0 to 100 %) [%]	23.5	23.8	22.6	23.9

Table 4.6 shows space heating load with different amounts of internal gains, without solar radiation. As shown in the table, STG achieved the lowest reduction in space heating (22.6 %), while HENT achieved the largest reduction (23.9 %). The average reduction in calculated space heating by introducing 100 % internal gains were 23.5 %.

Table 4.7: Time when peak space heating load from table 4.6 occurred.

Internal gains [%]	Time [2010-02-23 XX:XX]			
	GKBT	ONV12E	STG	HENT
0	07:54	07:58	07:44	07:24
25	07:19	07:52	07:18	07:28
50	07:15	07:50	07:19	07:27
75	07:06	07:45	07:16	07:20
100	07:10	07:38	07:18	07:20

Table 4.7 shows the time when the peak space heating load from table 4.6 occurred. As presented in the table, all the peak space heating loads occurred on the same day, within the operating hours for this

building category from the standards. At this day (2010-02-23), the outdoor temperature changes from -23.1 °C at 07:00 to -22.3 °C at 08:00, and is recorded as the coldest day in 50 years in Trondheim.[80]

4.5.2 With solar radiation

Table 4.8: Simulated space heating load with different levels of internal gains (including solar radiation).

Internal gains [%]	Space heating load [kW]			
	GKBT	ONV12E	STG	HENT
0	162.7	240.1	358.0	370.0
25	151.6	224.6	337.6	346.3
50	149.5	210.6	311.9	323.8
75	130.9	195.1	298.1	302.5
100	122.9	180.5	277.6	279.1
Reduction in space heating load (0-100 % internal gains) [%]	24.5	24.8	22.5	24.6

Results from dynamic heat load simulations with internal gains and solar radiation are shown in table 4.8. As shown in the table, STG still achieved the lowest reduction in space heating load (22.5 %), while ONV12E achieved the highest reduction (24.8 %). The average reduction in space heating load by introducing internal gains when solar radiation is accounted for were 24.1 %.

Table 4.9: Time when peak space heating load from table 4.8 occurred.

Internal gains [%]	Time [2010-02-23 XX:XX]			
	GKBT	ONV12E	STG	HENT
0	08:05	07:59	08:14	07:28
25	07:17	07:52	07:22	07:28
50	07:15	07:46	07:20	07:21
75	07:10	07:46	07:18	07:20
100	07:07	07:36	07:16	07:21

As shown in table 4.9, the calculated peak space heating load occurred at the same day and approximately the same time as without solar radiation (see table 4.7).

4.6 Compiled heat load results

Table 4.10: Compilation of measured, installed heat capacities, and simulated space heating load.

	GKBT	ONV12E	STG	HENT
	Measured heat loads			
Maximum measured heating load [kW]	145.0	235.0	230.0	245.0
	Installed capacity			
Total installed heat capacity [kW]	350.0	-	670.0	975.0
Heat pump capacity [kW]	80.0	230.0	275.0	281.0
Estimated installed space heating capacity [kW]	262.0	-	300.0	569.3
	Simulated heat loads			
Peak space heating load (static), DOT = -19 °C [kW]	179.7	219.6	321.7	377.1
Peak space heating load (static), n-day average based on τ [kW]	160.8	194.9	273.0	336.7
Peak space heating load (dynamic), 0 % internal gains [kW]	165.3	242.2	361.5	372.8
Peak space heating load (dynamic), 25 % internal gains [kW]	154.2	226.8	339.7	350.4
Peak space heating load (dynamic), 50 % internal gains [kW]	144.8	210.9	320.3	327.5
Peak space heating load (dynamic), 75 % internal gains [kW]	135.6	197.7	301.6	306.5
Peak space heating load (dynamic), 100 % internal gains [kW]	126.5	184.5	279.9	283.7
Peak space heating load (dynamic), solar radiation, 0 % internal gains [kW]	162.7	240.1	358.0	370.0
Peak space heating load (dynamic), solar radiation, 25 % internal gains [kW]	151.6	224.6	337.6	346.3
Peak space heating load (dynamic), solar radiation, 50 % internal gains [kW]	139.5	210.6	311.9	323.8
Peak space heating load (dynamic), solar radiation, 75 % internal gains [kW]	130.9	195.1	298.1	302.5
Peak space heating load (dynamic), solar radiation, 100 % internal gains [kW]	122.9	180.5	277.6	279.1

Table 4.10 shows a compilation of the simulated space heating loads both static and dynamic, based on the previously presented results. Heating capacities for each building are also presented. Note that the static simulations are gross space heating load, meaning that internal gains and solar radiation are not considered. However, the dynamic simulations gives a net heating load for different amounts of internal gains included. Solar radiation is excluded in the fist five dynamic simulations, while it is included in the last five.

As shown in table 4.10, GKBT, STG, and HENT all needed less heat than available in their respective heating supply systems. Both STG and HENT have higher heating capacity in their heat pumps than the maximum measured heating load during 2018. STG's heat pump has a capacity that is 19.6 % higher than maximum measured heating load, while HENT's heat pump is 14.7 % higher. Note that results from simulation and measurements should not be compared directly in this table, as the measurement and simulation neither represent the same case nor have the same boundary conditions.

It is worth noticing that ONV12E's dynamic heating load simulation with 0 and 25 % internal gains, both with and without solar radiation, resulted in higher space heating loads than the static simulation with DOT = -19 °C, while GKBT and HENT achieved lower space heating load with dynamic simulation whether or not internal gains and solar radiation are included. However, by introducing more internal gains, the dynamic simulations for ONV12E also achieved lower space heating load than the static heat load simulations with DOT = -19 °C and n-day average temperature. On the other hand, the lowest resulting space heating loads for STG appeared for the static simulation and the τ-based n-day average temperature.

4.7 Dynamic heat load simulation with measured internal gains

Table 4.11: Comparison of measured and simulated space heating load

	Space heating load
Measured [kW]	106.0
Simulated [kW]	119.0
Deviation [%]	10.9

Table 4.11 presents a comparison between measured space heating from 2018 and simulated space heating load in GKBT with measured internal gains and AMY weather file from 2018. As presented, the highest measured space heating load were found to be 106.0 kW, while simulated space hating load was 119.0 kW. Thus, the deviation between measured and simulated space heating load were found to be 10.9 %.

Chapter 5

Discussion

5.1 Measured internal gains in GKBT

5.1.1 Occupancy

When studying total occupancy in GKBT and HENT, there are uncertainties in the results regarding the fact that it is achieved little knowledge about what is included. In practice, every air diffuser that is equipped with motion sensors are included. However the total number of diffusers are unknown. In areas where several occupants stay at the same time, the diffusers give a poor estimation of the total number of occupants. As previously mentioned, each sensor has an angle of coverage of 51.3°. With a room height of 2.7 m in GKBT, each sensor could in theory cover up to 36 m^2. With 5 m^2 per person (NS 3701) each sensor could in theory count seven persons as one. On the other hand, in singe cell offices and other spaces not meant for more than one persons, the representation will be accurate.

The measured data sets for both buildings can be said to be of high quality. For both buildings there are less than 30 time steps in total where the occupancy has not been logged. This is acceptable as there are 144 and 96 time steps daily for GKBT and HENT respectively. The missing time steps are seemingly randomly distributed throughout the year and appears mostly outside occupied hours.

GKBT consists mostly of cell offices, but also have some open landscape areas as well as meeting rooms and break rooms. The fact that GKBT consists mostly of cell offices can be one of the reasons why small differences is found between total occupancy and occupancy in cell offices. It is also interesting to consider the occupants movements. For instance, in the break rooms, the motion sensors can be triggered by one person. If a group of occupants are having a break, and one person leaves for his cell office, the level of occupancy will be unchanged in the break room and increase for the cell offices. This behaviour of the motion sensors can explain why the measured occupancy is slightly higher in the cell offices than

for the total occupancy.

When studying the occupancy in the meeting rooms in GKBT, the results are much less reliable. These results are based on mass balance calculations for the rooms. Here, several assumptions are made. It is assumed fully mixed ventilation and no air flowing in through the door (meaning that the door is assumed to be always closed). Further, it is assumed balanced ventilation, constant CO_2 concentration in the supply air, and constant CO_2 generation rate from the occupants. In reality, the pollutants in the rooms will not be fully mixed. Whereas the door can be assumed to be closed during meetings, opening of the door and movement of air due to occupants leaving or arriving will affect the mass balance. Assuming constant CO_2 concentration in the supply air is a rather crude assumption, as the outdoor CO_2 concentration is dependent on for example weather conditions, and traffic.

Nevertheless, the numerous assumptions are considered and it is assumed that the calculations will yield an acceptable estimation to indicate something about the occupancy pattern in the meeting rooms. As mentioned in the previous chapter, the occupancy pattern in the meeting rooms are much less predictable than the total occupancy or the occupancy in the cell offices. However, this is as expected as meetings vary in length and frequency. As previously mentioned, the calculations yielded 1 occupant in average during the night. This emphasize the weakness of the mass balance requiring several assumptions. This can probably be ascribed to the assumption of constant outdoor CO_2 concentration which is estimated by the lowest measured concentration in each room (as described in chapter 3). When the external CO_2 concentration is slightly elevated above the assumed constant value, this will be considered as CO_2 generation from occupants in the mathematical model.

In the literature review, it was found that Halvarsson (2012) stated an average occupancy of 0.4, varying from 0.2 to 0.6 on workdays between 08:00 and 17:00. Thus, the measurements of total occupancy for GKBT and HENT are both supporting the findings in Halvarson (2012), except that the measured diversity factor become lower than 0.2 around 16:00. For the cell offices, an average diversity factor of approximately 0.45 ± 0.12 is found during occupied hours, excluding the lunch break. Thus, the upper limit for the standard deviation is just slightly lower than the given absence factor, 0.4 (corresponding to an occupancy of 0.6) given in NS-EN 15193-1.

The holidays seems to be more distinct in HENT than in GKBT. However, for both buildings the holidays can be said to be significant, as the average occupancy is bellow the darkest trend areas in the figures. This finding conforms with Duarte et al. (2013), that the occupancy varies between different days/months. Therefore, it can be argued that the weekdays and holidays should be separated and plotted individually. In this way, the average value would better represent the day-to-day occupancy and the standard deviation would be smaller.

For HENT, there is a trend that shows a somewhat higher total occupancy after 16:00 for some days. It is speculated that this can be due to the fact that there are several different activities taking place in HENT,

such as a shop. It is not possible to exclude parts of the building when studying the total occupancy directly in the building management system. If the shop has expanded opening hours for some days of the week, this can explain the trend in question. However, this is not further investigated.

When comparing the measured occupancy to the different standards and studies from the literature review, mainly two things must be considered. Firstly, the values from the standards are not meant for sizing the HVAC system (except ISO 17772-1). Even though the measured occupancy in GKBT and HENT should give a representation of occupancy patterns in office buildings, the measurements from these two buildings do not provide a sufficient basis to determine the occupancy pattern in a third building exactly. However, it can be used as a basis to make an educated guess. Secondly, the occupancy given in the standards should be used for the whole building, both primary and secondary area. If this is compared to measurements from cell offices or meeting rooms (primary areas), it is not the same basis for comparison. Therefore, the measured total occupancy are used for comparison to account for the different types of primary and secondary areas. This does not apply for ISO 17772-1, which gives different diversity factors for different areas. As discussed, the measured total occupancy is likely to be lower than the actual occupancy, giving no reason to conclude a clear discrepancy between measured occupancy and the standard TS 3031.

5.1.2 Lighting and technical equipment

In both GKBT and ONV12E, electricity meters dedicated to measure electricity to lighting and technical equipment are distributed throughout the buildings: one per floor (3 floors) for GKBT and two per floor (3 floors) for ONV12E. The measurements are presented as area weighted averages to give the power intensity, W/m^2. As the project files for ONV12E are not provided, the area is read from the BEM provided by previous Master students working with the same buildings. Therefore, there are uncertainties in the accuracy of exact values when the results for ONV12E are presented as area weighted averages. This uncertainty will mainly affect the magnitude of the plotted diversity factor, but will not affect the schedule/shape.

As mentioned, there are more electricity meters installed in ONV12E than in GKBT. This is the main reason why the plotted electricity appears to be smoother from hour to hour in ONV12E. It is relevant to discuss the fact that the power consumption is logged as the electricity consumption (kWh) in the previous hour. This means that plotting the power consumption as continuous graphs will give a somewhat inaccurate presentation of the results. The results should be interpreted in the same way as a step function: the level of power consumption as a constant for each hour. This would make the trend lines more difficult to interpret, but the reader should be aware that this is how the results should be interpreted.

Overall, this study do not include measurements from a high number of electricity meters, or a very

large floor area in total. This means that the measurements will give poor statistical significance when studying a small time period. However, as an entire year of measurements are included in the study, the results will show trends that assumably would be representative for the actual electricity consumption in the buildings.

In ONV12E there were some issues regarding the measurements, as it was identified that the electricity meters were connected wrongly to the motherboard. This error made the data provided by the building management system faulty as some of the Modbus addresses for lighting and technical equipment where switched. However, the erroneous connections were explained by Småøyen, which made it possible to take this into consideration when processing the data. Nevertheless, such complications will introduce uncertainties in the results.

A question that rises when discussing internal gains, is whether or not the gains vary on a day-to-day basis or if the gains are dependent on the time of year. With short, dark winter days and long, light summer days, this could influence the electricity consumption. In fact, this will depend on the lighting control strategy. If the light is motion controlled, the lighting can depend strictly on the occupancy pattern. The occupancy pattern is not found to vary for different times of the year, neither for GKBT nor HENT. However, if the light is controlled by daylight, differences between summer and winter are to be expected. For GKBT, the lighting seems to be varying by 0.1, while it varies by 0.4 (cf. figure 4.6 and 4.7) from day to day during occupied hours. As ONV12E aims for a better energy label (BREEAM Excellent), it could be that it is invested in a smarter light control system which will make the light consumption vary more on a day-to-day basis. However, this is just an hypothesis and there is not a strong enough basis to draw a conclusion that electricity consumption to lighting varies dependent on the time of the year.

The way the electricity is measured makes it possible to compare the measurements to the standards directly, as it is not differentiated between primary and secondary area. Even though GKBT and ONV12E do not provide a sufficient basis to determine the diversity factors alone, it is clear that the standard values are mostly overestimated compared to what is measured. It is also clear that the assumption of zero electricity to technical equipment outside occupied hours is wrong, based on the measurements. This will in turn give discrepancies between simulated peak power and energy use compared to what will actually be the case in the building, as the standards state that 100 % of the electricity is converted to heat. For energy, it would mean that delivered energy from the heating system is underestimated, because it is assumed more heat from internal gains. This should also be the case for estimated power. However, in the following chapter it is discussed that estimated power is experienced to be higher than what is measured. This can be explained by the fact that internal gains are commonly excluded in standard HVAC design procedures, meaning that it is assumed 0 kW internal gains in the design calculations. Again, it is relevant to stress that the standards in question, ISO 17772-1 excluded, do not give values for internal gains meant for HVAC sizing.

In chapter 4.1.4, it is shown that GKBT, ONV12E and HENT have somewhat different diversity factors regarding total electricity consumption to lighting and technical equipment. It should be considered that the range of the standard deviation overlaps for certain periods of the day. Nevertheless, T-testing the measurements suggests that there is a significant difference between the measurements ($p<0.05$). This can be explained by the fact that there are different tenants and companies in the different buildings, and that the different companies can have different user patterns, equipment, and routines. This is consistent with the findings in Menezes et al. (2012) as described in the literature review.

5.2 Measured power and energy

5.2.1 GKBT

The maximum measured heating load in GKBT was 145 kW (figure 4.15). The heat pump is sized to 80 kW, which is 55 % of the maximum measured heating load. Thus, the power coverage factor for the heat pump is 55 %. As stated in chapter 2.5.3, typical power coverage factors for heat pumps is normally between 40 and 70 % at DOT. This suggests that the heat pump installed in GKBT is sized correctly, although GKBT's heat pump coverage factor would be somewhat lower at DOT, as higher heating load is expected at colder temperatures.

The heating capacity of the district heating is 350 kW, which is 241 % higher than the maximum measured heating load, suggesting an oversized peak load system. However, oversized district heating peak load systems do not affect investment cost to a large extent, but can result in regulatory problems for the hydronic system as too large valves leads to poor regulation at small valve openings. In the literature study it is stated that the life time of oversized systems is known to decrease as it does not operate within its intended working area. Another disadvantage of oversized systems is that the operation costs increases due to poor part load efficiencies.

The scatter plot for GKBT is shown in figure 4.16. As shown in the figure, it is estimated a net heat load at -19 °C of 141.7 kW, which would result in a power coverage factor of 56 % with the installed heat pump capacity. This is within the typical range, although slightly higher than the power coverage factor based on the measured 145 kW. As seen in the figure, the scatter plot estimated a lower heating load than the highest measured heating load. This suggests that the estimated heating load from the linearization is inaccurate. One factor that impacts the linearization is heating of DHW. DHW-heating should be considered to be temperature independent and should be excluded from the linearization as DHW will count as delivered heat even when the outdoor temperature is high. This results in a less steep slope for the linearization and underestimation of peak heat load at DOT. This argumentation is valid for the scatter plots for all the buildings. Also, in the data-set there is several measurements of zero power consumption at low outdoor temperatures, reducing the estimated heating load even further. It could be

discussed if scatter plots should only be used with temperature dependant loads, such as space heating and ventilation heating.

The measurements extracted from the building managements system were not missing any values nor had any extreme values, suggesting high quality measurements. However, as shown in the scatter plot (figure 4.16), there somewhat weak correlation between the outdoor temperature and measured heating load, as the highest measured heat load occurred at approximately -5 °C outdoor temperature. This lack of correlation could suggest poor regulation of the heating system, as expect peak loads are expected to occur at lower outdoor temperatures. However, as the correlation between outdoor temperature and measurements is quite sensitive, the estimations must be evaluated with care.

5.2.2 ONV12E

As shown in figure 4.17, the highest measured heating load during 2018 was 235 kW. The heat pump has a heat capacity of 230 kW, yielding a power coverage factor of 97.9 % during 2018. This coverage factor is outside the typical range and could at first sight suggest an oversized heat pump. However, the heat pump is sized to cover the entire space heating demand and parts of the DHW use, suggesting a quite fitting heating capacity. However, as 2018 is not a design year, the heat pump's heating capacity is slightly too low to cover heating loads that would occur at lower outdoor temperatures. Nevertheless, ONV12E is indirectly connected to the district heating grid through ONV12 A-D working as a peak load system, and could then be used when the heat pump is not able to cover the heating demand.

The scatter plot in figure 4.18 suggests a lower net heat load at -19 °C than what is delivered during 2018. In the figure, the estimated net heat load at -19 °C is 175.5 kW, while the installed capacity is 230 kW resulting in a power coverage factor of 131 %. However, there seems to be poor correlation between the outdoor temperature and measured heating load, resulting in erroneous estimation of net heat load. This can possibly come from heating of DHW, or the connection with ONV12 A-D.

Measurements extracted from ONV12E had little to none missing values or extremes. However, as there are little correlation between outdoor temperature and measured heat load, it could be suggested incorrect metering or poor regulation.

5.2.3 STG

The highest measured heating load for STG was 230 kW (figure 4.19). The heat pump is sized for 275 kW, resulting in a power coverage factor for the heat pump of 120 % during 2018, suggesting that the heat pump at STG is oversized. Since 2018 was not as cold as the design period for heating in Trondheim, the power coverage factor will be lower when comparing the heat pump's heating capacity to larger net heat loads that are expected to occur at lower temperatures.

For the purpose of getting insight about the economic consequences of oversizing, it is assumed that the heat pump should have a power coverage factor of 70 % of the maximum measured heating load during 2018, i.e. a heating capacity of 161 kW. A heat pump of this size would save 513 000 NOK in investment costs compared to the heat pump installed at STG today, assuming 4500 NOK/kW (see chapter 2.5.3). However, this is an example based on measurements, which are not available in the design phase of the project.

The district heating has a heating capacity of 670 kW, comprising of 300 kW for DHW and 370 kW for space heating (see table 3.2). The district heating must be able to cover the total heating demand at design conditions, as the heat pump stops working when the outdoor temperature drops below -10 °C (R410a working fluid). The peak load system had in 2018 a power coverage factor of 291 %, suggesting an oversized peak load system. However, as discussed previously, an oversized district heating peak load system do not affect the investment cost substantially, but it can affect regulation of the hydronic system, lifetime of the components, and operation costs.

As shown in the scatter plot for STG (figure 4.20), it is estimated a net heat load at -19 °C of 141.1 kW. Thus, the heat pump's has a power coverage factor of 195 % based on estimated design conditions, which is higher than the power coverage factor based on measurements. The estimated heat load found by the linearization is lower than the highest measured heating load of 2018. There are several reasons for a low estimated heat, as previously discussed for GKBT and ONV12E. The highest measured heat load occurred when the outdoor temperature was -2 °C, which could suggest poor regulation or incorrect metering.

The measurements extracted from STG had several weaknesses. Firstly, there were several measured heating loads higher than the total installed heating capacity (up to 3000 kW), these extremities were removed and the missing values were filled in with the same value as the previous hour. This will affect the quality of the measurements, and could potentially result in erroneous measured heating load. Secondly, measurements during summer were missing as stated before. To fill in the missing values for heating during summer, the data was linear interpolated. This will not give an accurate representation of the heating during summer, consisting mostly of DHW heating. However, as this period is not the most important when studying peak heat loads, the interpolation was considered to be satisfactory. Note that interpolated values are only used when measurements were missing.

5.2.4 HENT

The maximum measured heating load during 2018 was 245 kW (figure 4.21), while the heat pump has an heating capacity of 281 kW. This results in a power coverage factor of 114.7 % for the heat pump during 2018, suggesting an oversized heat pump. As previously discussed, this is based on the typical power coverage factor of 40-70 % at DOT. In the literature review, it was found that an oversized heat

pump will lead to increased investment costs, reduced part load efficiency, and decreased lifetime.

The district heating has a total installed heating capacity of 975 kW. Comparing the district heating's heating capacity to the maximum measured heat load results in a power coverage factor of 398 %. In terms of investments, oversized capacity of district heating have little effect on the costs. However, as the component will be very large they will cost more than smaller sized components. Large components might also become a problem for regulation, as discussed for the other buildings.

As shown in the scatter plot for HENT (figure 4.22), the estimated net power at -19 °C is 188.7 kW. This estimated net heat load can be used to suggest a more accurate heat pump size, based on measurements from the building in question. The estimated net heat load of 188.7 kW suggests a heat pump capacity of 75.5-132.1 kW based on the typical 40-70 % power coverage factor. With an investment cost of 4500 NOK/kW, the investment cost for the heat pump could be decreased by 670 500 - 927 000 NOK. However these numbers are based on measurements, meaning that the building must be constructed and used for some time before the net heat load can be estimated using this method. As for the other buildings, the estimated net heat load at DOT is lower than the maximum measured heat load during 2018.

The measurements extracted from HENT were without extremes and missing values, which indicates high quality. As seen in the scatter plot, HENT achieve the best correlation between outdoor temperature and measured heat load. On the other hand, the estimated net heat load is lower than the maximum measured heat load, suggesting some weaknesses in the measurement and/or the method for estimating net heat load.

5.3 Periodic penetration depth in IDA ICE

Periodic penetration depth was important to validate as it decides the amount of thermal mass that should be considered when performing the step response. The time period, and thereby the thickness of thermal layers, can be chosen based on the time when the thermal mass is assumed to be active in the heating of the building. As stated in the literature review (chapter 2.4.5), the periodic penetration depth for a 24 hour period for concrete should be about 15 cm. Figure 4.23 showed that the temperature difference between daily maximum and minimum at 15 cm was roughly 0.7 °C in IDA ICE. Figure 2.16 in the literature review shows the same temperature difference as found in IDA ICE, thus it can be assumed that the periodic penetration depth is considered correctly in IDA ICE.

However, there might be some differences between the two cases. The study in the literature review used Newton boundary condition on the surface, while in IDA ICE a mathematical object for envelope surface was used. This is not studied further. Thus, the differences in the two methods are not known and could potentially affect the amount of thermal mass and the thickness used in the step response. On the other hand, most of the buildings investigated in this thesis were assumed to have hollow core concrete slabs,

where most of the concrete was assumed to be close to the surface, and thereby being active during the chosen time period. Based on this assumption, the thickness for hollow core concrete slabs were not limited, which can lead to more thermal mass considered in the step response than what is active during the chosen time period, resulting in a longer time constant.

5.4 Simulations

5.4.1 Building energy model

When constructing a model in IDA ICE, several assumptions and simplifications are done to ease the computations and deal with aspects that are unknown or uncertain. For ONV12E, the large number of assumption gives large uncertainties in the results. This BEM is provided by other students, and the numerous assumptions connected to the construction of this BEM are not clarified, thus the validity of the model is low. The BEM provided of ONV12E was also very detailed and did not suit the purpose of this thesis. Therefore, the model was simplified even further to make the simulations run smoothly. A down-side of using this model is that it should not been drawn any definite conclusions when comparing measurements to the simulated results. However, the up-side is that the model is sufficiently accurate to study changes between different modelling approaches.

For all the buildings, several simplifications are made to reduce the computational time. It is important to find the balance between simplifications and accuracy fitting the problem at hand and enabling the possibility to run numerous tests in an acceptable time perspective. The first issue, is the zoning of the model. For example, cell offices, meeting rooms, open landscape areas, cafeterias and toilets will have different load profiles. The orientation of the buildings will yield different solar gains. For each building, the zones are chosen in the same way as the air handling units are distributed, which is mainly based on the orientation of the buildings. However, this means that the different types of areas are not accounted for, which will introduce inaccuracies. Nevertheless, the standards mostly give values for primary and secondary areas combined. If the results are compared to measurements with each single zone as boundary conditions, discrepancies are to be expected. When studying peak power on a building level, it is assumed that the assumptions and simplifications for each zone are evened out, giving sufficiently accurate results.

Several other simplifications and assumptions are made. Firstly, all windows with similar properties on the same walls connected to the same zone are merged. This results in a smaller total window circumference, which can give reduced energy loss through the windows. However, the U-value given for the windows used in the model includes frames. Therefore, it can be difficult to say how the window frames contributes to energy loss, and the simplification will probably give acceptable results as there is a lack of more details about the windows. Secondly, CAV is used in the IDA ICE model. As the

buildings mostly have VAV and DCV, assuming CAV can increase both energy and power demand for the ventilation system. Therefore it is used a correction factor of 0.8 as described in chapter 6.1.1.1.4 in NS 3031 in some of the simulations (see chapter 3.7 - 3.9). The efficiency of the heat exchanger in IDA ICE is constant, while in reality it changes over time. This can introduce deviations between simulations and reality. Finally, the walls in the IDA ICE model are uniform, with the same construction for every wall towards exterior. In reality, there are different types of wall constructions used in the buildings. The U-values has been area weighted, while the thermal mass of load bearing systems in the walls are neglected. This simplification is based on the fact that the floor slabs have significantly more thermal mass than the load bearing system in the walls, which makes it negligible.

Underground parkings and technical rooms placed on the roof are excluded from the BEMs for all the buildings. The technical room have high internal loads, which can reduce the heat loss through the roof. However, the buildings are insulated to meet modern insulation requirements, so the reduced heat loss due to the technical room is assumed to be minimal. Underground parkings are considered in the BEMs by connecting adjacent surfaces to a fixed temperature of 5 °C.

5.4.2 Weather data

Weather files for IDA ICE were created based on data from Copernicus and eKlima (AMY weather files). These files comprises of six columns, one for each variable, that each consists of 8760 values, resulting in 52 560 values for each year. In total, it were created 14 weather files. However, some of the extracted values were missing; roughly 2500 values. The missing values were filled in with the same value as the same hour from the previous day, as IDA ICE needs a complete year to run a simulation. This will result in inaccuracies that could potentially lead to erroneous simulation results. Nevertheless, as there were missing less than 0.5 % of the total values, it is assumed that the weather files would give sufficiently accurate results for this thesis.

The most important period for this thesis is the start of 2010 as this includes the design period for Trondheim, and is therefore of great interest when investigating peak heat loads in the buildings. This period do not lack any values, which increases the reliability for this period. However, it is important to keep in mind that these weather files will not give a perfect representation of the weather in the studied periods, but can give a good indication of how the buildings would behave.

5.5 Peak heat load calculations based on the building time constant

Results from static space heating load simulations are shown in table 4.4 both for n-day average temperature and DOT of -19 °C. It is shown a reduction in gross space heating load for all of the case buildings. This reduction is expected as the outdoor temperature used in the steady-state simulations is higher than the more commonly used 3-day average temperature of -19 °C. The average reduction in gross space heating load was 11.9 %, which may lead to a better operating heating system, as components in the heating system can be more fitting and would have a more suitable working areas for the actual heat demand of the buildings.

The time constant is relatively similar for all of the BEMs. STG has the longest τ of 8 days. Although STG achieved the longest time constant, the time constants did not differ much. This may be a result of, among other factors, similar amounts of thermal mass. The thermal mass is mainly based on the concrete slabs which are quite similar for all of the case buildings. Three out of four buildings are assumed to have hollow core concrete slabs of more or less equal dimensions. STG is assumed to have solid concrete slabs of a smaller dimension. Nevertheless, these will contain more thermal mass than the hollow core slabs.

All the BEMs have approximately equal ventilation rates and efficiencies, making the ventilation losses quite similar. Transmission losses will also be relatively similar, as all of the BEMs have low and approximately equal U-values. STG has the lowest U-value, resulting in lower transmission losses compared to the other BEMs. Additionally, the infiltration losses are more or less equal as all of the BEMs have pressure coefficients for semi-exposed buildings and low infiltration rates. These similarities would result in similar heat loss coefficients, which lead to similar time constants, according to equation 2.11.

The building time constant is determined by finding the lowest primary zone time constant. However, during the calculations, it was noticed that large open zones, like the entrance area, could have a shorter time constant than the chosen zone. Nevertheless, it was chosen to use the shortest time constant from the primary area where it is expected that occupants stay over longer time. Choosing this time constant could potentially result in an undersized heating system in the entrance area. Nevertheless, as the entrance areas are considered as secondary areas, with no substantial occupancy, it is assumed that a small drop in temperature is acceptable, and not causing too much dissatisfaction. However, if the entrance area have a manned reception or other work stations, it is important to ensure thermal comfort for the occupants.

Dynamic simulations without internal gains were conducted to investigate how the heating system would preform without any additional heat gain. All the buildings except GKBT experience unmet hours in 2010. It was not unexpected that the buildings experienced unmet hours in 2010, as this year contains the design period for heating. Even tough GKBT did not experience any unmet hours in the primary areas, it experienced 17.1 unmet hours in the entrance area. This is a result of sizing the heating system

after the shortest time constant in the primary areas. It could be suggested that the the heating system at GKBT could be sized even smaller, as no unmet hours occurred in the primary areas. Additionally, as internal gains are not included in these simulations, it could be argued that the unmet hours would be reduced or eliminated in all of the buildings due to the extra heat emitted by occupants, lighting, and technical equipment. Another important aspect when considering how thermal mass influences buildings, as stated by Karlsson et al. (2013), is that the temperature has to drop in order for the thermal mass to emit excess heat. The fact that the temperature has to drop is important to keep in mind as it may not be possible to accept a reduction in temperature in all buildings.

Steady-state calculations are often used for calculating the heat load, as in NS 12831. However, dynamic calculations has to be used in order to include thermal mass. Although steady-state calculations do not take thermal mass into account, there are several other methods for adjusting the heat load based on thermal mass. In this thesis it has been suggested to adjust the DOT based on the building time constant. Another method is presented in ISO 13612-1, where a correction factor ranging from 1 to 0.9 is multiplied with the heat load to account for the amount of thermal mass in the building (see chapter 2.5.3).

5.6 Dynamic heat load simulations with internal gains from standards

The calculated space heating load is reduced when introducing internal gains (table 4.6 and 4.8). This is expected as including internal gains results in extra heat gains emitted into the building from occupants, lighting, and technical equipment. Internal gains for lighting and technical equipment are taken from NS 3701, as previously mentioned, results showed that these are the closest to what is measured in GKBT. Occupancy is taken from TS 3031. Another reason to choose these standards for internal gains is that they are available for most people working in the building industry. However, it should be stressed that the standards state that these internal gains are not to be used for sizing as they are only meant for control calculation against the building regulations.

By including internal gains, it was identified a decrease in the calculated heat load. This suggests that it would be wise to include internal gains when designing equipment sensitive to the boundary conditions, as for example heat pumps. This supports the findings in the literature view; that net heat load should be used when designing the base load system. When sizing the peak load system it is important that the system has sufficiently high capacity. As the aforementioned standards not are meant for sizing, and the measured internal gains in the different buildings vary, it should be conducted further studies before internal gains are included in the design of the peak load systems.

Including solar gains

The space heating load is further reduced by introducing solar radiation, but it did not have a large impact. The peak space heating load occurred in February, with very limited solar radiation, explaining the small impact on the space heating load. It can be discussed if solar radiation is worth including in the simulation as peak heat loads often occur in periods with little to no solar radiation. Also, by excluding solar radiation is one more uncertainty removed from the simulation. Nevertheless, the sky is often clear when the coldest days occur.

5.7 Compiled heat load results

Table 4.10 presents the compiled space heating results from static and dynamic simulations, with and without internal gains and solar radiation, as well as measured and installed capacities. It is important to keep in mind that the results from the simulations are based on weather data from 2009/2010 and are therefore not suitable for direct comparison to the measurements from 2018. In addition, the maximum measured heating load includes heating of DHW, snow melting systems, and technical rooms, while these extra heating loads are not simulated in IDA ICE. Preferably, power consumption for DHW, snow melting systems and technical rooms should be measured separately to get a better understanding of the space heating capacity. Unfortunately, this is only available for GKBT. However, estimated installed space heating capacity can to some degree be compared to simulations, as these often are based on the design heating period, which occurred in 2010.

All the BEMs, except STG, simulated lower space heating load at -19 °C than estimated installed space heating capacity. There are several possible explanations for these deviations. One reason could be that safety factors are used. Another reason could be different input values used in the simulations, which deviate from what is used by the consultants working on the design. Unfortunately, the actual design calculations were not available during this work.

Steady-state heat load simulation with n-day average temperature yielded lower simulated space heating load compared to estimated installed space heating capacity for all the buildings. As discussed before, this reduction is expected and could potentially lead to a better operating heating system.

The BEM for ONV12E achieved lower space heating load in all simulations compared to the maximum measured heating load and the heat pump's heating capacity. As the estimated space heating load is unknown, it is difficult to draw conclusions about the simulated results. Although the estimated space heating capacity is unknown, the heat pump at ONV12E is designed to cover the total space heating demand and parts of the DHW demand, making the heat pump's capacity a good indicator on the installed space heating capacity. Thus, it would be reasonable to estimate the net space heating somewhere

between the heat pump's capacity and the simulated space heating load. Since the BEM of ONV12E is based on another Master's thesis not giving detailed information about the modelling assumptions, it is not possible to say exactly why the deviations occur.

5.8 Dynamic heat load simulations with measured internal gains

By excluding the heat supplied to DHW, snow melting system, and technical rooms for GKBT, the measurements can be compared to simulated space heating load directly. It was found a deviation of 10.9 % between measured and simulated space heating load (table 4.11). As this deviation is relatively small, it could be suggested that a simple BEM can yield good estimations of net space heating loads.

The deviation between simulation and measurements could possibly be explained by the fact that a very simple BEM is used, where the cafeteria and industrial purposes of the ground floor is neglected. Further calibration of the model would most likely help reducing the building performance gap. However, calibration requires a lot of information and measurements from the building, meaning that the building has to be built in order to have enough information for calibration. The BEM for GKBT is mostly based on information available in the project and design phase of the building, suggesting that one can make fairly good estimations of space heating loads with information that is available before the building is raised. Another reason for this deviation might be that IDA ICE gives peak heat loads as an average over 15 minutes, while the measurements are averaged over an hour. This means that short-lived, high peaks will be more evened out by the measurements than in the simulations, resulting in higher simulated loads than measured loads.

Chapter 6

Conclusion

Measured occupancy do not give any new insights in occupancy patterns, but supports the findings in Halvarson (2012) and Duarte et al. (2013), as well as the absence factor in table B.6 in NS-EN 15193-1. The main difference is that the measurements suggest one hour shorter workday and different behavior for different tenants in the same building category. If detailed simulation results are required, different rooms' loads such as cell offices and meeting rooms should be separated. However, for overall heat load calculations it is assumed sufficient to consider primary and secondary areas as one.

For lighting, it was found that the standards investigated in this thesis exaggerate the intensity (W/m^2) and duration compared to measurements, even though the intensity given NS 3701 and the duration given in TS 3031 corresponds well to the measurements separately. Electrical consumption to lighting outside occupied hours could be included, due to emergency lighting. However, further studies are needed as the measurements' lower standard deviation shows zero intensity, while the average value is above zero.

The electricity intensity for technical equipment in the standards are found to be substantially higher than what is measured. The measurements showed that a considerable amount of electricity was consumed by technical equipment outside occupied hours, while non of the standards report the same. Including this finding in calculations should give a substantial amount of heat supplied to the office buildings from internal gains. However, the measurements were found to differ between the case buildings, meaning that further studies are needed in order to give a better understanding of these dynamic heat gains.

Strictly based on power coverage factor, it could be suggested that three out of the four case buildings have oversized peak load systems, while two out of four have oversized heat pumps. This can result in large investment cost, poor regulation, reduced lifetime, and increased operation costs. It is shown that utilizing n-day average temperature based on the building time constant can reduce the calculated peak space heating load compared to using DOT of -19 °C. It should be noted that this method requires the possibility to lower the indoor air temperature during design periods, such as the winter of 2010.

However, reducing the capacity of the heating system could give better regulation, lower investment costs, increased lifetime, and lower operating costs.

Internal gains should be included in heat load calculations used for sizing of heat pumps. This will reduce the chance of oversizing, which reduces investment costs and increases the efficiency of the heat pump. However, it is required further studies of internal gains before it can be used to size the peak load system, especially in highly insulated buildings where internal gains are a large contributor. Internal gains can vary from building to building, and using wrong input values for internal gains could lead to an undersized peak load system.

The comparison between measured and simulated space heating at GKBT, with measured internal gains and actual weather data suggested that simulations can be quite accurate even for simplified BEMs.

Chapter 7

Further work

There are several aspects that can be further investigated to increase the accuracy of heat load calculations. Here, some suggestions are made.

It is not common practice to include internal gains in heat load calculations in Norway. NS-EN 12831 states that internal gains can be included in heat load calculations if national regulation allows it. It would be interesting to investigate which countries include internal gains in their calculations and what they experience using this method.

It would be interesting to further compare standards and measurements for occupancy, lighting, and technical equipment. This will give a better understanding of net heat loads in buildings, which in return can be used for better HVAC system design. When studies on occupancy in office buildings are conducted, one should also study meeting rooms and and secondary areas. These areas lack investigation as it is hard to get accurate measurements with the equipment that is commonly installed in buildings today. This calls for more advanced measuring in such areas. Another interesting aspect regarding occupancy is the correlation between occupancy in cell offices and open landscape areas. It could be assume that there should not be large differences between these two room types, but further studies are required to draw any conclusions. Several companies manage large databases consisting of measurements from the BMS for a large number of buildings. This can be powerful data to be used in further studies of internal gains.

The suggested method of basing the DOT on the building time constant could be further analyzed. This is done for four building in this thesis, but continuing to evaluate, test, and improve the method will determine if this should be developed to be a part of the standard design procedure in Norway as well as other countries.

Night-time setback is not investigated in this thesis. However, this strategy is often used to save energy.

It could be interesting to investigate how a heating system designed for night-time setback performs compared to a heating system that is not designed for night-time setback.

IDA ICE offers the possibility to specify the building time constant in *System parameters - Post processing*, where it is stated *"... determining "memory" for when a casual gain or loss is useful or harmful"*. It would be interesting to know more about how this is treated and implemented in the software.

Bibliography

[1] E. Oskarson. FN's bærekraftsmål. *FN-sambandet*, 2018.

[2] E. Oskarson. Parisavtalen. *FN-sambandet*, 2018.

[3] V. V. H. Bloch and J. Bjørke. Building stock. *Statistics Norway*, 2018.

[4] J. Skree and J.-D. Vatndal. Energibruk i bygg – RAMMER, KRAV OG MULIGHETER. *Norsk Teknologi*, 2008.

[5] J. Stene and O. Ø. Smedegård. Hensiktsmessige varme- og kjøleløsninger i bygninger. Technical report, COWI, 2013.

[6] J. A. Clarke. *Energy Simulation in Building Design*. Butterworth-Heinemann, 2001.

[7] A. C. Menezes, A. Cripps, D. Bouchlaghem, and R. Buswell. Predicted vs. actual energy performance of non-domestic buildings: Using post-occupancy evaluation data to reduce the performance gap. *Applied Energy*, 97, 2012.

[8] C. J. Hopfe and J. L. M. Hensen. Uncertanty analysis in building performance simulation for desingn support. *Energy and Buildings*, 2011.

[9] THEMA Consulting Group. Energibruk i kontorbygg. Technical report, Norges vassdrags- og energidirektorat, 2013.

[10] Norwegian water resources and energy directorate (NVE). Smart metering (AMS), 2018. https://www.nve.no/energy-market-and-regulation/retail-market/smart-metering-ams/ [Accessed: 2018-12-13].

[11] T. H. Dokka, A. Svensson, T. Wigestad, I. Andresen, I. Simonsen, and T. F. Berg. Energibruk i bygninger - Nasjonal database og sammenligning av beregnet og målt energibruk. *SINTEF Byggforsk Prosjektrapport*, 76, 2011.

[12] P. G. Schild, M. K., and C. Grini. Comparison and analysis of energy performance requirements in buildings in the Nordic countries and Europe. *SINTEF Byggforsk Prosjektrapport*, 55, 2010.

[13] Standard Norge. NS 3031:2014 Calculation of energy performance of buildings - Method and data, 2014.

[14] Standard Norge. SN/TS 3031 Energy performance of buildings - Calculations of energy needs and energy supply, 2016.

[15] Standard Norge. NS 3701:2012 Criteria for passive houses and low energy buildings, non-residential buildings, 2012.

[16] Standard Norge. NS-EN 12831-1:2017 Energy performance of buildings - method for calculation of the design heat load, part 1: Space heating load, module m3-3, 2017.

[17] International Organization of Standardization. ISO 17772-1 Energy performance of buildings - Indoor environmental quality - Part 1: Indoor environmental input parameters for the design and assessment of energy performance of buildings, jun 2017.

[18] International Organization of Standardization. ISO 7730:2015 Ergonomi i termisk miljø Analytisk bestemmelse og tolkning av termisk velbefinnende ved kalkulering av PMV- og PPD-indeks og lokal termisk komfort, 2015.

[19] European Standard. EN 15251:2007 Indoor environmental input parameters for design and assessment of energy performance of buildings addressing indoor air quality, thermal environment, lighting and acoustics, 2007.

[20] Standard Norge. NS-EN 15193-1:2017 Energy performance of buildings Energy requirements for lighting, 2017.

[21] International Organization of Standardization. ISO 13612-1:2014 Heating and cooling system in buildings - Method for caluculation of the system performance and system design for heat pump system - Design and dimensioning, 2014.

[22] C. Duarte, K. V. D. Wymelenberg, and C. Reiger. Revealing occupancy patterns in an office building through the use of occupancy data. *Energy and Buildings*, 67, 2013.

[23] J. Halvarsson. *Occupancy pattern in office buildings*. PhD thesis, Norwegian University of Science and Technology, 2012.

[24] SINTEF Byggforsk. Krav til lys og belysning [421.610], 1997.

[25] Å. Blomsterberg, C. Dalman, J. Gräslund, K.-Å. Henriksson, B. Jansson, R. Jansson, J. Kellner, P. Levin, and J.-U. Sjögren. Brukarindata kontor - Version 1.1, 2013.

[26] L. Martirano. A smart lighting control to save energy. In *Proceedings of the 6th IEEE International Conference on Intelligent Data Acquisition and Advanced Computing Systems*, pages 132–138, 2011.

[27] B. Acker, C. Duarte, and K. V. D. Wymelenberg. Office space plug load profiles and energy saving interventions. *ACEEE Summer Study on Energy Efficiency in Buildings Proceedings*, 2012.

[28] UK NCM. Uk's national calculation method for non domestic buildings. http://www.uk-ncm.org.uk/ [Accessed: 2019-01-30].

[29] T. Dwyer. Continuous flow direct water heating for potable hot water. *CIBSE Journal*, 2013.

[30] SINTEF Byggforsk. About VarmtVann2030, 2017. https://www.sintef.no/varmtvann [Accessed: 2018-10-18].

[31] L. Lan, P. Wargocki, and Z. Lian. Optimal thermal environment improves performance of office work. *REHVA Journal*, 2012.

[32] Z. S. Li, G. Q. Zhang, and J. L. Liu. IMPACT OF INDOOR ENVIRONMENT ON COMFORT AND PRODUCTIVITY IN INTELLIGENT BUILDING. *Indoor Air*, 2005.

[33] J. Schnieders. Adaptive versus Heat Balance Comfort Models. *The Passive House Resource*, 2015.

[34] L. Yang, H. Yan, and J. C. Lam. Thermal comfort and building energy consumption implications – A review. *Applied Energy*, 2013.

[35] GreenSpec. Thermal mass. http://www.greenspec.co.uk/building-design/thermal-mass/ [Accessed: 2019-01-28].

[36] S. Verbeke and A. Audenaert. Thermal inertia in buildings: A review of impacts across climate and building use. *Renewable and sustainable energy reviews*, 82:2300–2318, 2018.

[37] V. Novakovic, S. O. Hanssen, J. V. Thue, I. Wangensteen, and F. O. Gjerstad. *Energy Efficiency in Buildings – sustainable energy use*. Gyldendal Undervisning, 2007.

[38] J. Karlsson, L. Wadsö, and M. Öberg. A conceptual model that simulates the influence of thermal inertia in building structures. *Energy Build*, 2013.

[39] A. Reilly and O. Kinnane. The impact of thermal mass on building energy consumption. *Applied Energy*, 2017.

[40] B. Slee, T. Parkinson, and R.Hyde. CAN YOU HAVE TOO MUCH THERMAL MASS? In *Cutting Edge: 47th International Conference of the Architectural Science Association*, 2013.

[41] K.W. Childs, G.E. Courville, and E.L. Bales. Thermal mass assessment: an explanation of the mechanisms by which building mass influences heating and cooling energy requirements. *U.S. Department of Energy Office of Scientific and Technical Information*, 1983.

[42] A. J. Khalifa and E. Abbas. The optimum thickness of some thermal storage materials used for solar space heating. In *4th SRO Conference*, 2006.

[43] International Organization of Standardization. ISO 13786:2017 Thermal performance of building components - Dynamic thermal characteristics - Calculation methods, 2017.

[44] J. Babiak, M. Minárová, and B. W. Olesen. What is the effective thickness of thermally activated concrete slab?, 2007.

[45] J. Karlsson, L. Wadsö, and M. Öberg. A conceptual model that simulates the influence of thermal inertia in building structures. *Energy and Buildings*, 60:146–151, 2013.

[46] Sveriges centrum för nollenergihus. *Kravspecifikation för nollenergihus, passivhus och minienergihus, FEBY12*, 2012. https://www.feby.se/images/Rapporter/KravspecifikationFEBY12-lokalersept.pdf [Accessed: 2018-12-13].

[47] SINTEF Byggforsk. Klimadata for termisk dimensjonering og frostsikring [451.021], 2012.

[48] FEBY Forum för Energieffektivt Byggande. Förändringar i FEBY18 relativt FEBY12, 2018. https://www.feby.se/kriterier [Accessed: 2018-09-10].

[49] Standard Norge. NS-EN ISO 15927-5 Hygrothermal performance of buildings - Calculation and presentation of climatic data - Part 5: Data for design heat load for space heating, 2005.

[50] ASHRAE International. IWEC2 Weather files for energy calculations, 2012. https://www.ashrae.org/technical-resources/bookstore/ashrae-international-weather-files-for-energy-calculations-2-0-iwec2 [Accessed: 2018-12-02].

[51] M. S. Doggett. Climate Data for Building Simulations. *The Building Enclosure*, 2014.

[52] T. Ericson, A. Fidje, J. E. Fonneløpand, B. Langseth, I. H. Magnussena, W. W. Rode, and B. Saugen. Varmepumper i energisystemet. *NVE Rapport*, 60, 2016.

[53] J. Stene. *Varmepumper : grunnleggende varmepumpeteknikk*, volume STF84 A97302 of *SINTEF Rapport*. SINTEF Energi, Klima- og kuldeteknikk, Trondheim, 4 edition, 1997.

[54] J. Stene. Thermodynamics for The Heat Pump Cycle. In *TEP4260*, 2018.

[55] J. Stene. Components for Heat Pump Units. In *TEP4260*, 2018.

[56] J. Stene. Varmepumper for oppvarming og kjøling av bygninger. *SINTEF Energiforskning AS*, 2000.

[57] J. Stene. Dimensioning of Heat Pumps for Heating and Cooling. In *TEP4260*, 2018.

[58] J. Stene. Personal communication, May 2019.

[59] Statskraft varme. Energy calculator. https://www.statkraftvarme.no/utbygging/valg-av-energilosning/energikalkulator/ [Accessed: 2019-05-08].

[60] J. Stene. Personal communication, Feb. 2019.

[61] E. Djunaedy, K. Wymelenberg, B. Acker, and H. Thimmana. Oversizing of hvac system: Signatures and penalties. *Energy and Buildings*, 43:468–475, 2011.

[62] P. C. Thomas and S. K. Moller. HVAC system size - Getting it right. *CRC Construction Innovation*, 2006.

[63] J. L. Gorter. HVAC Equipment Right-sizing: Occupant Comfort and Energy Savings Potential. *Energy Engineering*, 109, 2011.

[64] T. Kalamees. IDA ICE: the simulation tool for making the whole building energy- and HAM analysis. *Tallinn Technical University*, 2004.

[65] EQUA. Validations & certifications, 2018. https://www.equa.se/en/ida-ice/validation-certifications [Accessed: 2018-12-16].

[66] L. Alfstad. Analysis of the thermal energy system at otto nielsens vei 12e. Master's thesis, NTNU, 2018.

[67] Florent Dulac. Investigation of the detailed design of a multifunctional heat pump system. Master's thesis, NTNU Norwegian University of Sciense and Technology, 2018.

[68] Kjeldsberg. Staalgaarden nord. https://www.kjeldsberg.no/?eiendomsutvikling=stalgarden-nord [Accessed: 2019-02-07].

[69] P. Severinsen. Personal communication, Feb. 2019.

[70] Voll Arkitekter. Vestre rosten 69. http://vollark.no/portfolio_page/vr69/ [Accessed: 2019-04-03].

[71] GK. Vestre rosten 69. https://www.gk.no/artikler/2016/8/8/vestre-rosten-69/ [Accessed: 2019-04-03].

[72] Lindinvent. *XPIR – External occupancy sensor*. https://www.lindinvent.com/media/56324/xpir_pb22_eng.pdf. [Accessed: 2019-04-29].

[73] Engineering ToolBox. Met - Metabolic Rate, 2004. https://www.engineeringtoolbox.com/met-metabolic-rate-d_733.html [Accessed: 2019-04-09].

[74] G. Ansanay-Alex. Estimating Occupancy Using Indoor Carbon Dioxide Concentrations Only in an Office Building: a Method and Qualitative Assessment. In *11th REHVA World Congress "Energy efficient, smart and healthy buildings"*, 2013.

[75] G. Cao. Indoor air quality and ventilation requirements. In *TEP4315 Indoor Environment*, 2018.

[76] A. Persily and L. de Jonge. Carbon dioxide generation rates for building occupants. *Indoor Air*, 2017.

[77] K. B. Lindberg. *Impact of Zero Energy Buildings on the Power System*. PhD thesis, NTNU, 2017.

[78] Norwegian Meteorological Institute. Eklima weather observations. http://sharki.oslo.dnmi.no/portal/page?_pageid=73,39035,73_39101&_dad=portal&_schema=PORTAL [Accessed: 2019-05-10].

[79] L. Lundström. Personal communication, Feb. 2019. Ph.D Candidate, Mälaradalen University.

[80] NRK. Trondheim kaldeste på 50 år, 2010. https://www.nrk.no/trondelag/trondheim-kaldest-pa-50-ar-1.7008066 [Accessed: 2019-05-02].

Appendix A

A.1 Adjusting the design outdoor temperature

$$\theta_e = \theta_{e,0} + \Delta\theta_{e,\tau} \tag{A.1}$$

$$\theta_{e,0} = \theta_{e,Ref} + G_{\theta,Ref} \cdot (h_{build} - h_{Ref}) \tag{A.2}$$

$$\Delta\theta_{e,\tau} = max\langle min\langle k_\tau \cdot \tau + \Delta\theta_{e,\tau,0}; \Delta\theta_{e,\tau,max}\rangle; \Delta\theta_{e,\tau,min}\rangle \tag{A.3}$$

Where

θ_e	=	adjusted DOT,
$\theta_{e,0}$	=	DOT adjusted for height,
$\Delta\theta_{e,\tau}$	=	DOT adjusted for thermal capacity,
$\theta_{e,Ref}$	=	DOT at designated reference site,
$G_{\theta,Ref}$	=	temperature gradient for the designated reference site,
h_{build}	=	mean height of the building above sea level,
h_{Ref}	=	height of the reference site above sea level,
k_τ	=	slope,
τ	=	time constant,
$\Delta\theta_{e,\tau,0}$	=	basic value,
$\Delta\theta_{e,\tau,max}$	=	upper limit,
$\Delta\theta_{e,\tau,min}$	=	lower limit.

A.2 Diversity factors from ISO 17772-1

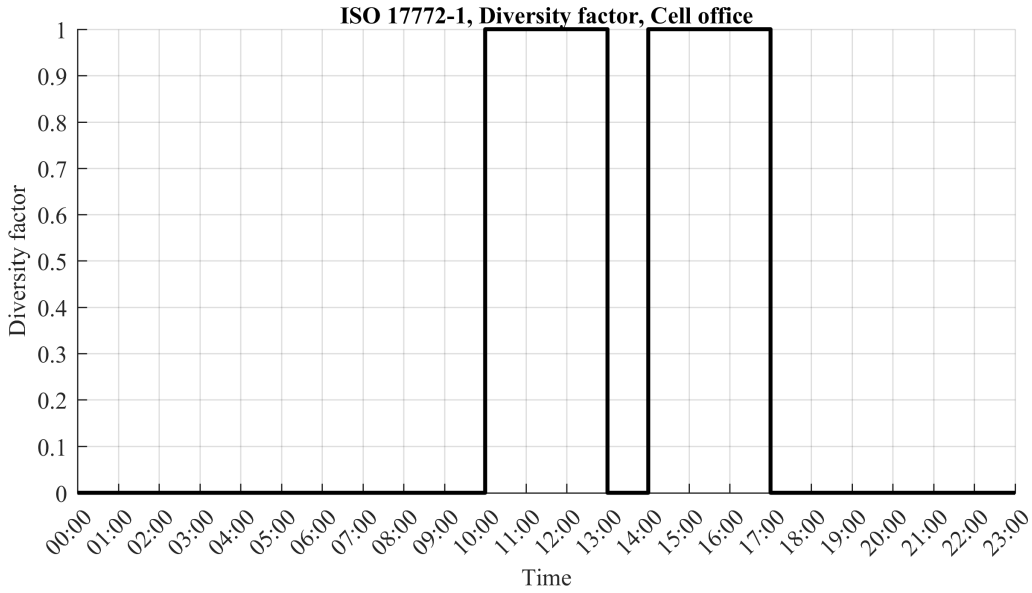

Figure A.1: Schedule for cell offices from ISO 17772-1:2017, used for occupancy, lighting, and technical equipment.

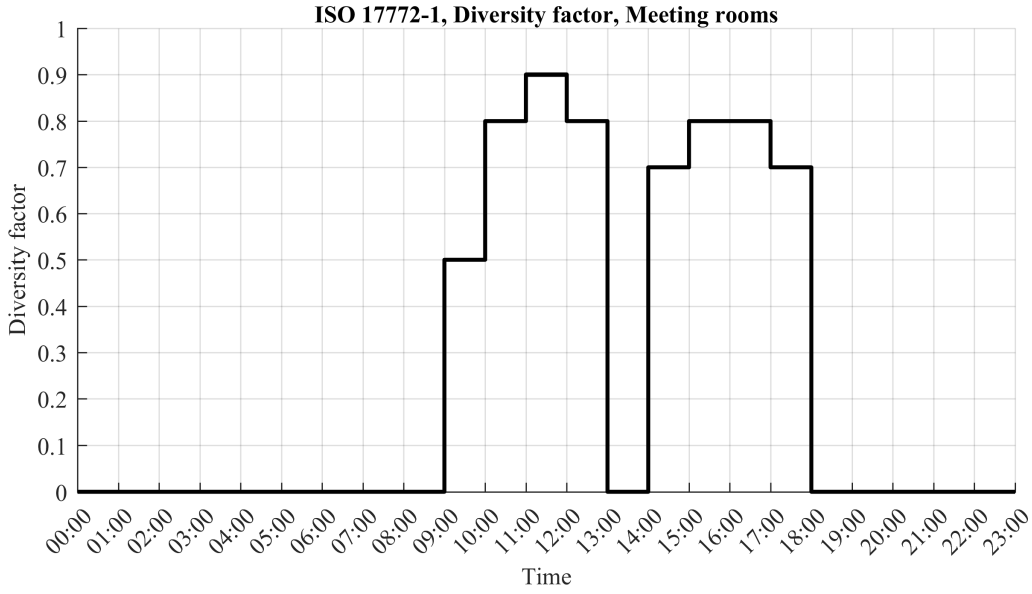

Figure A.2: Schedule for meeting room from ISO 17772-1:2017, used for occupancy, lighting, and technical equipment.

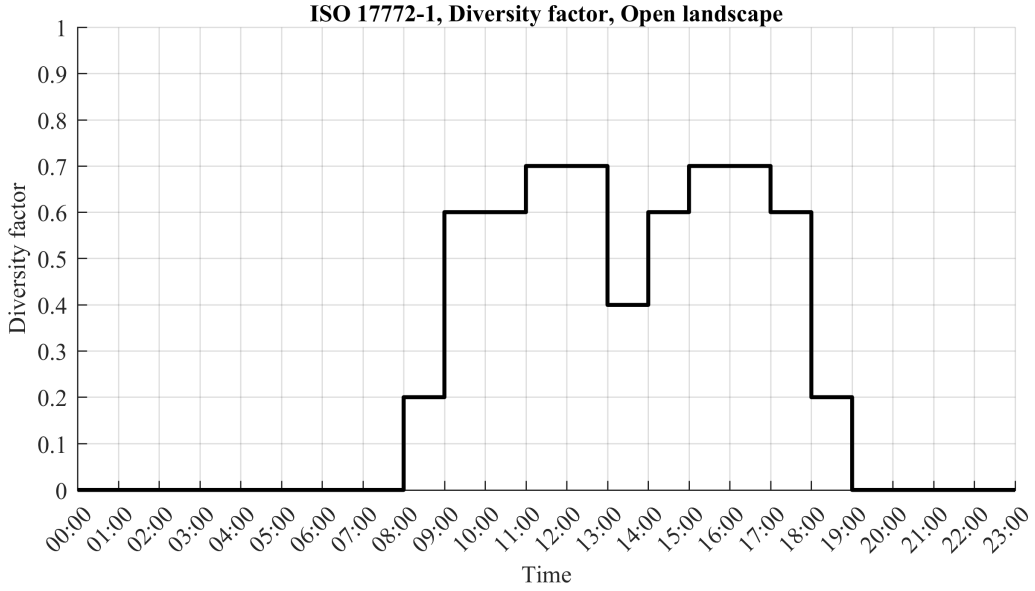

Figure A.3: Schedule for landscape offices from ISO 17772-1:2017, used for occupancy, lighting, and technical equipment.

A.3 Time constant based heating capacity test

Table A.1: Minimum external temperature for each year, and the external temperature when the minimum indoor temperature from table 4.5 occurs for each building.

Year	T_{min}	GKBT		ONV12E		STG		HENT	
		T_e [°C]	Time [h]	T_e [°C]	Time [h]	T_e [°C]	Time [h]	T_e [°C]	Time [h]
2005	-15.9	-13.9	1447	-10.8	1855	-10.7	8647	-11.1	1423
2006	-17.2	-14.7	1663	-14.7	1663	-14.7	1663	-13.4	1543
2007	-18.6	-14.0	1231	-16.8	919	-16.8	919	-16.8	919
2008	-14.3	-14.3	1951	-9.7	2023	-9.7	2023	-10.2	8287
2009	-14.1	-12.1	343	-12.1	343	-13.1	79	-13.1	79
2010	-23.3	-23.0	1280	-21.5	1258	-21.2	1259	-19.3	179
2011	-16.6	-13.9	1015	-16.6	1039	-16.6	1039	-16.6	1039
2012	-15.9	-15.5	8143	-15.5	8143	-15.5	8143	-13.1	751
2013	-18.7	-16.5	943	-15.9	1711	-15.9	1711	-15.9	1711
2014	-16.3	-15.6	8599	-15.6	8599	-15.6	8599	-15.6	8599
2015	-11.4	-10.4	535	-10.4	535	-10.4	535	-10.4	535
2016	-17.1	-16.1	175	-16.1	175	-16.1	175	-16.1	175
2017	-13.5	-11.0	7783	-11.0	7783	-11.0	7783	-11.0	7783
2018	-17.1	-16.2	1399	-16.2	1399	-16.2	1399	-16.2	1399

Table A.1 shows the minimum external temperature, T_{min}, for each year and the external temperature, T_e, when the minimum indoor temperature from table 4.5 occurs for each building. As shown in table A.1, the lowest minimum indoor temperature do not always occurs when the lowest external temperature occurs.

Marius Aaslund Berge & Ola Eriksen

Power Sizing Procedures for Highly-Insulated Office Buildings

NTNU
Kunnskap for en bedre verden